

# Moored Current and Hydrographic Measurements near the Halifax Line across the Scotian Slope, 2000 to 2008

John W. Loder and Yuri Geshelin

Ocean and Ecosystem Sciences Division  
Fisheries and Oceans Canada  
Bedford Institute of Oceanography  
1 Challenger Drive, Dartmouth, Nova Scotia  
Canada B2Y 4A2

2025

Canadian Technical Report of  
Hydrography and Ocean Sciences 399



Fisheries and Oceans  
Canada

Pêches et Océans  
Canada

Canada

## **Canadian Technical Report of Hydrography and Ocean Sciences**

Technical reports contain scientific and technical information of a type that represents a contribution to existing knowledge but which is not normally found in the primary literature. The subject matter is generally related to programs and interests of the Oceans and Science sectors of Fisheries and Oceans Canada.

Technical reports may be cited as full publications. The correct citation appears above the abstract of each report. Each report is abstracted in the data base *Aquatic Sciences and Fisheries Abstracts*.

Technical reports are produced regionally but are numbered nationally. Requests for individual reports will be filled by the issuing establishment listed on the front cover and title page.

Regional and headquarters establishments of Ocean Science and Surveys ceased publication of their various report series as of December 1981. A complete listing of these publications and the last number issued under each title are published in the *Canadian Journal of Fisheries and Aquatic Sciences*, Volume 38: Index to Publications 1981. The current series began with Report Number 1 in January 1982.

## **Rapport technique canadien sur l'hydrographie et les sciences océaniques**

Les rapports techniques contiennent des renseignements scientifiques et techniques qui constituent une contribution aux connaissances actuelles mais que l'on ne trouve pas normalement dans les revues scientifiques. Le sujet est généralement rattaché aux programmes et intérêts des secteurs des Océans et des Sciences de Pêches et Océans Canada.

Les rapports techniques peuvent être cités comme des publications à part entière. Le titre exact figure au-dessus du résumé de chaque rapport. Les rapports techniques sont résumés dans la base de données *Résumés des sciences aquatiques et halieutiques*.

Les rapports techniques sont produits à l'échelon régional, mais numérotés à l'échelon national. Les demandes de rapports seront satisfaites par l'établissement auteur dont le nom figure sur la couverture et la page de titre.

Les établissements de l'ancien secteur des Sciences et Levés océaniques dans les régions et à l'administration centrale ont cessé de publier leurs diverses séries de rapports en décembre 1981. Vous trouverez dans l'index des publications du volume 38 du *Journal canadien des sciences halieutiques et aquatiques*, la liste de ces publications ainsi que le dernier numéro paru dans chaque catégorie. La nouvelle série a commencé avec la publication du rapport numéro 1 en janvier 1982.

Canadian Technical Report of  
Hydrography and Ocean Sciences 399

2025

Moored Current and Hydrographic Measurements near the Halifax Line across the  
Scotian Slope, 2000 to 2008

by

John W. Loder and Yuri Geshelin

Ocean and Ecosystem Sciences Division  
Maritimes Region  
Fisheries and Oceans Canada

Bedford Institute of Oceanography  
P. O. Box 1006  
Dartmouth, Nova Scotia  
Canada B2Y 4A2

© His Majesty the King in Right of Canada,  
as represented by the Minister of the Department of Fisheries and Oceans, 2025

Cat. No. Fs 97-18/399E-PDF      ISBN 978-0-660-77797-9      ISSN 1488-5417

Correct citation for this publication:

Loder, J.W., and Geshelin, Y. 2025. Moored current and hydrographic measurements near the Halifax Line across the Scotian Slope, 2000 to 2008. *Can. Tech. Rep. Hydrogr. Ocean Sci.* 399: x + 87 p.

## TABLE OF CONTENTS

<b>List of Figures</b>	iv
<b>List of Tables</b>	vi
<b>Abstract</b>	vii
<b>Résumé</b>	viii
<b>1. Introduction</b>	1
<b>2. Background and Program Summary</b>	4
2.1 Oceanographic Setting	4
2.2 Overview of the 2000-04 and 2004-08 Moored Measurement Programs	7
2.2.1 2000-04 DFO-PERD-Industry Program	8
2.2.2 2004-08 DFO-PERD and RAPID WAVE Programs	9
2.3 Program Chronologies	12
2.3.1 2000-04 DFO-PERD-Industry Program	12
2.3.2 2004-08 DFO-PERD-RAPID Program	15
2.4 Complementary Datasets	16
2.4.1 CTD Sections from AZMP, AZOMP and Other	16
2.4.2 Sea Surface Temperature from Satellite Imagery	18
2.4.3 Sea Surface Elevation from Satellite Altimetry	18
<b>3. Instrumentation, Data Return, Quality Control and Data Features</b>	19
3.1 Aanderaa Current Meters	19
3.1.1 Overall Summary	19
3.1.2 Example RCM Data Displays	24
3.2 Acoustic Doppler Current Profilers	38
3.2.1 Overall Summary	38
3.2.2 Example ADCP Data Displays	40
3.3 Electromagnetic Current Meters	50
3.4 MicroCAT Temperature, Conductivity and Pressure Recorders	52
3.4.1 Overall Summary	52
3.4.2 Example MC Data Displays	54
3.5 Minilog Temperature Recorders	59
3.6 Water Level Recorders	60
<b>4. Multi-Site and Multi-Year Time Series</b>	61
4.1 Time Series involving Multiple Sites during 2000-04	61
4.2 Concatenated (Merged) Time Series from the 2000-04 Program	62
4.3 Time Series of Seasonal Means, 2000-04	69
4.4 Transport Time Series, 2000-04	71
4.5 Multi-Year Time Series from the 2004-08 Program	72
<b>7. Concluding Remarks</b>	73
<b>8. Acknowledgements</b>	75
<b>9. References</b>	75
<b>Appendix. Mooring Diagrams</b>	80

## LIST OF FIGURES

- Figure 1.** Lines of regular (typical tri-seasonal) oceanographic profile sampling in the Scotian Shelf and adjacent regions in DFO's Atlantic Zone Monitoring Program.
- Figure 2.** Locations of regular oceanographic profile sampling on the Halifax Line in DFO's AZMP and on the eXtended Halifax Line in DFO's AZOMP. Also shown are the sites of moored measurements of more than a year in duration.
- Figure 3.** A map downloaded ca 2001 from the website of the then Canada Nova Scotia Offshore Petroleum Board showing blocks of "land" with Exploration and Production Licenses, and new blocks that were up for bids.
- Figure 4.** Location of mooring sites SS-A, SS-B and SS-C in relation to major topographic features on the outer Scotian Shelf and Slope.
- Figure 5.** (a) Annual-mean ocean temperature at 100m, and (b) a schematic of the primary branches of the upper-ocean circulation in the Northwest Atlantic off Nova Scotia.
- Figure 6.** Sea surface temperature (SST) in the Northwest Atlantic south of Nova Scotia from a composite of AVHRR satellite images during 1-3 April 2002.
- Figure 7.** (a) Schematic of the typical extent of Slope Water. (b) Location of the boundary between the Gulf Stream and Slope Water at 200m below the surface based on the Gulf Stream '60 temperature-salinity survey. (c) Schematic of the circulation and water mass boundaries in the Slope Water region and over the Atlantic Canadian Shelf to its north, based on the Gulf Stream '60 survey and Gatién's analysis.
- Figure 8.** Schematic of the cross-slope vertical distribution of water masses over the Scotian Slope and Rise south of Nova Scotia (from Gatién 1976), based on the Gulf Stream '60 survey, and in particular on its Section III which extends south from the western Scotian Shelf.
- Figure 9.** Seasonal-mean flow across the HL over the outer Scotian Shelf and upper Scotian Slope from the numerical model solutions of Hannah et al. (2001).
- Figure 10.** Schematic of the nominal design of the primary mooring array in the 2000-04 program, with upward-looking ADCP for the near-surface region and RCMs and MCs below.
- Figure 11.** (a) Bathymetric map of the Western North Atlantic with the lines with moored measurements during 2000-2004 for investigating multi-year variability in the AMOC. (b) Schematic of moorings planned by POL/NOC at 6 sites on Line B involving BPRs and MCs, with the 2 DFO PERD moorings at sites SS-D and SS-E included.
- Figure 12.** (a) Potential Temperature ( $\theta$ ), (b) Salinity, (c) Potential Density ( $\sigma_\theta$ ) and (d) Dissolved Oxygen (DO) in the upper 1000m over the Scotian Shelf edge and Slope, from the Hud02-032 survey in July 2002.
- Figure 13.** (a)  $\theta$ , (b) S and (c) DO over the full water depth from the Hud02-032 survey in July 2002.
- Figure 14.** (a)  $\theta$ , (b) S and (c)  $\sigma_\theta$  over the full water depth along Line B from the Hud05-055 survey in October-November 2005.
- Figure 15.** Composites of SST for four semi-monthly periods in the springs of 2001 and 2002 showing the complex structure of Gulf Stream meanders, rings and related features in the Scotian Shelf and Slope Water region.

- Figure 16.** Time series of the along-slope surface current between (a) the 200- and 1000-m isobaths, and (b) the 1000-and 2000-m isobaths on Track 050 of the TOPEX/POSEIDON altimetry satellite to the west of the HL.
- Figure 17.** Time series of (a) Rate from the 8 RCMs, (b, c, d) Direction, and the eastward (U) and northward (N) components of velocity from 4 of the RCMs, (e) T from all 8 RCMs, and (f) S from the upper 6 RCMs, on M1352 at SS-A1 during June-November 2000.
- Figure 18.** Time series of U and T from the upper two RCM8s on M1352 at SS-A1 in October-November 2000, and of the approximate eastward component of velocity on the nearest TOPEX/Poseidon altimetry tracks to the east and west of the mooring line
- Figure 19.** Progressive vector diagrams (PVDs) for velocity from the 5 RCM8s with full record lengths on M1352 at SS-A1 during June-November 2000.
- Figure 20.** Time series of (a) R and (b) T from the 5 RCM8s on M1388 deployed at SS-B1 from May to October 2001.
- Figure 21.** PVDs for hourly velocity from the 5 RCM8s on M1388 deployed at SS-B1 from May to October 2001.
- Figure 22.** Time series of (a) R from 5 RCM8s, (b) D from 3 of the RCMs, (c) U and (d) V from 2 of the RCMs, and (e) T from 5 of the RCMs, on M1412 deployed at SS-B2 from October 2001 to June 2002
- Figure 23.** PVDs for hourly velocity from 3 of the RCM8s on M1412 deployed at SS-B2 from October 2001 to June 2002.
- Figure 24.** Time series of T, D and R from the RCM11 at 791 mbs and RCM8 at 792 mbs on M1479 at SS-B5 from April 2023 to May 2024.
- Figure 25.** Scatterplots of T, D and R from the RCM8 at 792m versus those from the RCM11 at 791m on M1479 at SS-B5 from April 2023 to May 2024.
- Figure 26.** Time series of (a) R, (b) D, (c) U and (d) V from the RCM8s at different depths on M1414 and M1413 at SS-C1, from October 2001 to May 2002.
- Figure 27.** Time series of (a) T, (b) S, and (c) P from the RCM8s at different depths on M1414 and M1413 at SS-C1, from October 2001 to May 2002.
- Figure 28.** PVDs for hourly velocity from the 4 RCM8s on M1414 and the RCM8 on M1413 deployed at SS-C1 from October 2001 to June 2002.
- Figure 29.** Time series of T, R, D, and U and V from the RCM8 at 3345 mbs on M1624 at SS-E2, from October 2006 to October 2007.
- Figure 30.** Time series of T, R, D, and U and V from the RCM8 at 3345 mbs on M1624 at SS-E2, from October 2006 to October 2007.
- Figure 31.** Time series of T, R, D, and U and V from the RCM11 at 3414 mbs on M1667 at SS-E4, from October 2007 to October 2008.
- Figure 32.** Time series of %GP in the bins at 188 and 228 mbs from the ADCP on M1378 at SS-A2, and T from that same ADCP and from the RCM8 at 574 mbs on the nearby M1377 in SS-A2.
- Figure 33.** Time series of R from the ADCP for 3 bins (68, 148, 292m) on M1378 in SS-A2, and from the RCM8s on nearby M1377, from November 2000 to late May 2001.

**Figure 34.** Scatterplots and regression results of RCM Rate vs ADCP Rate for 149 and 148m, and 289 and 292m, from M1377 and M1378 in SS-A2.

**Figure 35.** PVDs for velocity from 5 different depth bins from the ADCP on M1388 in SS-A2, and from the RCM8 at a similar depth on nearby M1387 for 3 of the bins.

**Figure 36.** Time series of %GP in the bin at 80 mbs, and of R and D from the bins at 24, 32, 204 and 232 mbs, from the NB ADCP on M1387 in SS-A3.

**Figure 37.** Time series of %GP in the bin at 25 mbs, and of R and D from the bins at 17, 25, 89 and 177 mbs, from the NB ADCP on M1419 in SS-A4.

**Figure 38.** Time series of %GP in various bins from the LR ADCP on M1388 in SS-B1.

**Figure 39.** Time series of %GP in the 16m bins centered at 146, 194 and 242 mbs from the LR ADCP on M1412 in SS-B2, and of T from the ADCP at 395 mbs and the RCM8 at 545 mbs.

**Figure 40.** Time series of %GP and R for the 16m bin centered at 209mbs from the LR ADCP on M1429 in SS-B3, and of T from the ADCP at 409 mbs and the RCM8 at 565 mbs.

**Figure 41.** Time series of %GP at 16, 36 and 56 mbs from the WH ADCP at 86 mbs on M1414 in SS-C1, and of T from the ADCP and the RCM8 at 131 mbs.

**Figure 42.** Time series of %GP at 5, 35 and 556 mbs from the WH ADCP at 85 mbs on M1431 in SS-C2, and of T from the ADCP and the RCM8 at 130 mbs.

**Figure 43.** Approximate periods and depths with good velocity time series returned from the 3 sites in the 2000-04 program, and the 2 sites in the 2004-08 program.

**Figure 44.** Time series of U, V, R and D from the three current meters on M1413 at SS-C1 during the first 29 days of the deployment: S4 at 4 mab, RCM8 at 3 mab, and S4 at 2 mab.

**Figure 45.** (a) Time series of the differences between the R values measured by the 3 current meters on M1413 at SS-C1 from October 2001 to November 2002. (b) Scatterplots for the R values from the 3 meters.

**Figure 46.** Time series of T and S from the 4 MCs on M1377 in SS-A2, and P from 2 of the MCs. An earlier version of S from the 274m MC is also shown.

**Figure 47.** Time series of T and S from the 4 MCs on M1412 in SS-B2.

**Figure 48.** Time series of T, S and P from the 2 MCs on M1414 in SS-C1.

**Figure 49.** Time series of T, S and P from (a) the MC at 2415 mbs on M1623 in SS-D3, and (b) the MC at 3385 mbs on M1624 in SS-E3, from October 2006 to October 2007.

**Figure 50.** Time series of T from (a) the 5 MLs at SS-A1 over the entire deployment, and (b) two of the MLs and 3 nearby RCM8s on the moorings for ~2 days in June 2000.

**Figure 51.** Time series of (a) T and (b) P from the WLR8 on M1413 in SS-C1 from October 2001 to May 2002.

**Figure 52.** Time series of U from 3 depths at SS-A and 2 depths at SS-B, T from one depth at each of SS-A and SS-B, and the estimated geostrophic surface flow normal to the satellite altimetry track to the west of the mooring line for the 2-month period of May-June 2001.

**Figure 53.** Time series of U from 2 depths at SS-A, 3 depths at SS-B, and 1 depth at SS-C, and of T from 1 depth at each of SS-A, SS-B and SS-C during the period January-July 2002.

**Figure 54.** Time series of subsurface T at 5 approximate depths in the SS-A1 to SS-A4 deployments between June 2000 and June 2002, and of SST from AVHRR.

**Figure 55.** Time series of (a) T at 5 approximate depths in the SS-A1 to SS-A6 deployments between June 2000 and April 2004, and (b) S and (c) density at 2 approximate depths.

**Figure 56.** Time series of R from 6 different approximate depths in the SS-A1 to SS-A6 deployments between June 2000 and April 2004.

**Figure 57.** PVDs for the velocity in 4 different vertical intervals during deployments SS-A1 to SS-A3, from June 2000 to September 2001.

**Figure 58.** Time series of (a) U and (b) V from 5 different approximate depths in the SS-A1 to SS-A6 deployments between June 2000 and April 2004.

**Figure 59.** Time series of (a) R, (b) D, (c) U and (d) V from the deepest RCM in the 5 deployments at SS-B.

**Figure 60.** Time series of R from 7 approximate depth levels during the 5 deployments at SS-B.

**Figure 61.** Time series of T from 5 approximate depth intervals during the 5 deployments at SS-B.

**Figure 62.** Time series of R from 6 approximate depth levels during the 4 deployments at SS-C.

**Figure 63.** Time series of T from 3 approximate depth intervals during the 3 deployments at SS-C.

**Figure 64.** Time series of the seasonal means of (a) the along-shelf component of velocity, (b) T and (c) S at representative approximate depths in the moored measurements during the 2000-04 Scotian Slope program.

**Figure 65.** Time series of estimates of along-slope transport for each mooring site assuming that its velocities are representative of specified vertical intervals and cross-slope distances consistent with the separation of the sites.

**Figure 66.** Time series of seasonal-mean along-slope transport from the moored measurements, for individual mooring “sections” and combinations thereof.

**Figure 67.** Concatenated time series of (a) R and (b) T from the RCM11 at 50 mab in deployments SS-D1, -D2 and -D3, extending from October 2004 to October 2007.

**Figure 68.** PVD for the hourly velocity data from the RCM11 at 50 mab on M1547, M1585 and M1623 at SS-D1, -D2 and -D3, covering the period October 2004 to October 2007.

## **Appendix – Example Mooring Diagrams**

SS-A1

SS-A2

SS-A3

SS-B1

SS-C1

SS-C4

## LIST OF TABLES

- Table 1.** DFO-PERD Scotian Slope mooring sites, sequential deployment numbers at each site, latitude and longitude ranges of the mooring positions at each site, ranges of the water depths for the different deployments, BIO Consecutive Numbers for each mooring, and comments.
- Table 2a.** Listing of moorings deployed at SS-A and SS-B during the 2000-04 Scotian Slope program with their BIO #, deployment and recovery dates, water depth, and instrument depths.
- Table 2b.** Listing of moorings deployed at SS-C during the 2000-04 program, and at SS-D and SS-E during the 2004-08 program with their BIO #, deployment and recovery dates, water depth, and instrument depths.
- Table 3.** List of DFO cruises which contributed to, or complemented, the 2000-04 moored measurement program on the Scotian Slope with the time period, cruise designation, chief scientists, mooring sites and BIO numbers for moorings recovered and deployed, and CTD stations occupied.
- Table 4.** Chronology of mooring deployments and recoveries on the RAPID WAVE B Line between October 2004 and October 2008 during DFO AZMP survey cruises, with dates, cruise numbers, chief scientists, mooring sites and BIO numbers, and the POL Line B sites where CTD profiles were taken.
- Table 5a.** SS-A. Listing of RCM8s during the 2000-04 Scotian Slope program, organized by site and deployment #. The other columns are the BIO mooring #, RCM8 serial number, record start & end dates, water & RCM depths, variables sampled, the sampling interval, and comments.
- Table 5b.** SS-B. Listing of RCMs during the 2000-04 program, organized by site and deployment #.
- Table 5c.** SS-C, SS-D, SS-E. Listing of RCMs during the 2000-04 and 2004-08 programs, organized by site and deployment #.
- Table 6.** Listing of ADCP deployments during the 2000-2004 program, organized by site and deployment #. Other columns indicate the BIO mooring #, ADCP type and serial #, record start and end dates, water and ADCP depths, bin size, and center depths and vertical intervals of bins with good data.
- Table 7.** Listing of InterOcean S4 electromagnetic current meters deployed at site SS-C during the 2000-04 Scotian Slope program, organized by sequential deployment #.
- Table 8a, b, c.** Listing of MicroCAT and MinLog deployments during the 2000-04 and 2004-08 Scotian Slope programs, organized by site (SS-A, -B, -C, -D, -E) and deployment #.
- Table 9.** Listing of Water Level Recorders (WLRs) deployed during the 2000-04 Scotian Slope program, organized by site and sequential deployment #.

## Abstract

Loder, J.W., and Geshelin, Y. 2025. Moored current and hydrographic measurements near the Halifax Line across the Scotian Slope, 2000 to 2008. Can. Tech. Rep. Hydrogr. Ocean Sci. 399: x + 87 p.

Moored measurements of currents, temperature and salinity at 3 sites on the Halifax Line (HL) across the Scotian Slope between June 2000 and April 2004, and at 2 sites on Line B of the Rapid Climate Change Program between October 2004 and October 2008, are described with respect to location, time, quality control, good data return and salient features. The 2000-04 program involved tall moorings near the 300-, 1100- and 2000-m isobaths, typically with an upward-looking Acoustic Doppler Current Profiler (ADCP) sampling the upper ocean, and Aanderaa current meters (RCMs), MicroCAT temperature-conductivity-pressure recorders (MCs) and/or Minilog (ML) temperature recorders distributed below. The program also had water level recorders (WLRs) and near-bottom current meters on some moorings. Mostly good data were returned from 13 ADCPs, 78 current meters, 40 MCs, 11 MLs and 5 WLRs. The 2004-08 program had 4 deployments of year-long short moorings on the 2400- and 3400-m isobaths, each with a near-bottom RCM and MC. Mostly good data were obtained from 6 of the RCMs and 7 of the MCs. Complementary hydrographic survey data and satellite-derived Sea Surface Temperature composites from the Atlantic Zone Monitoring Program, and time series from earlier moored measurements in the area are used to discuss the oceanographic complexity and variability of the shelf-water/slope-water frontal zone on the HL during the study period. An apparent seasonal variation in southwestward transport in the Labrador Current Extension arose from the incursions of remnant warm eddies in spring-summer 2002 and summer-fall 2003, rather than from surface buoyancy changes over the shelf. The observed complexity indicates that a combination of oceanographic surveys, remote sensing, moored measurements with high-frequency sampling, and interpretative models will be needed to understand the physical variability and its biological and chemical implications.

## Résumé

Loder, J.W., and Geshelin, Y. 2025. Moored current and hydrographic measurements near the Halifax Line across the Scotian Slope, 2000 to 2008. Can. Tech. Rep. Hydrogr. Ocean Sci. 399: x + 87 p.

Cette étude décrit le lieu, le moment, le contrôle de la qualité, le bon retour des données et les caractéristiques principales relatifs aux mesures du courant, de la température et de la salinité par dispositifs ancrés effectuées à trois sites du transect d'Halifax, qui traverse le talus du plateau néo-écossais, entre juin 2000 et avril 2004, ainsi qu'à deux sites du transect B du programme sur les changements climatiques RAPID entre octobre 2004 et octobre 2008. Le programme de 2000 à 2004 comprenait de grands dispositifs ancrés près des isobathes de 300, 1 100 et 2 000 m, généralement avec un profileur de courant à effet Doppler (ADCP) orienté vers le haut qui échantillonnait la couche supérieure de l'océan, et des courantomètres Aanderaa (CA), des enregistreurs de température-conductivité-pression MicroCAT (MC) ou des enregistreurs de température Minilog (ML) répartis en dessous. Le programme comptait également des enregistreurs de niveau d'eau (ENE) et des courantomètres proches du fond sur certains dispositifs d'ancrage. Des données généralement bonnes ont été obtenues à l'aide de 13 ADCP, de 78 courantomètres, de 40 MC, de 11 ML et de 5 ENE. Le programme de 2004 à 2008 comprenait quatre déploiements de petits dispositifs d'ancrage d'une durée d'un an sur les isobathes de 2 400 et 3 400 m, chaque dispositif étant équipé d'un CA et d'un MC proches du fond. Des données généralement bonnes ont été obtenues à l'aide de 6 CA et de 7 MC. Des données de levés hydrographiques complémentaires et des images composites de la température de surface de la mer dérivées de données satellitaires du Programme de monitoring de la zone atlantique, ainsi que des séries chronologiques de mesures antérieures par dispositifs ancrés dans la zone, sont utilisées pour discuter de la complexité et de la variabilité océanographiques de la zone frontale des eaux du plateau et des eaux du talus sur le transect d'Halifax au cours de la période d'étude. Une variation saisonnière apparente du transport vers le sud-ouest dans le prolongement du courant du Labrador est due aux incursions de tourbillons chauds résiduels au printemps-été 2002 et à l'été-automne 2003, plutôt qu'à des changements de flottabilité près de la surface sur le plateau. La complexité observée indique qu'une combinaison de levés océanographiques, de télédétection, de mesures par dispositifs ancrés avec échantillonnage à haute fréquence et de modèles d'interprétation sera nécessaire pour comprendre la variabilité physique et ses effets biologiques et chimiques.

# 1. Introduction

The Halifax Line (HL) across the Scotian Shelf and Slope off Halifax is one of the most heavily sampled (at least with hydrographic profiles) parts of that shelf-slope region (Fig. 1). Regular seasonal sampling of the upper 500-1000m was carried out by the Fisheries Research Board of Canada between 1950 and the mid 1970s (e.g., Mann and Needler 1967; de la Ronde 1972), as a contribution to a broader-scale monitoring program under the auspices of the International Commission for the Northwest Atlantic Fisheries (ICNAF). The HL's slope area was included in the 1960s Gulf Stream '60 hydrographic survey of the broader Slope Water region (Fuglister 1960), whose results were used in an iconic schematic of different water masses on the outer HL and further south (Gatien 1976; see later - Fig. 8). Other early descriptions of the oceanography of the Scotian Shelf and Slope were provided by McLellan (1957) and Smith et al. (1978), and then later for the broader Slope Water by Csanady and Hamilton (1988).

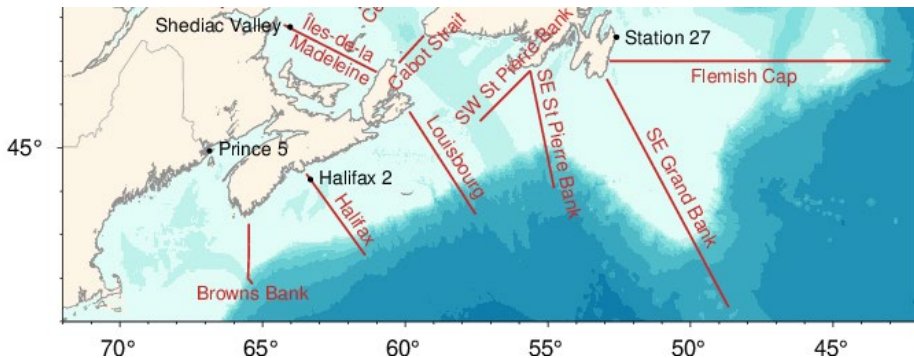
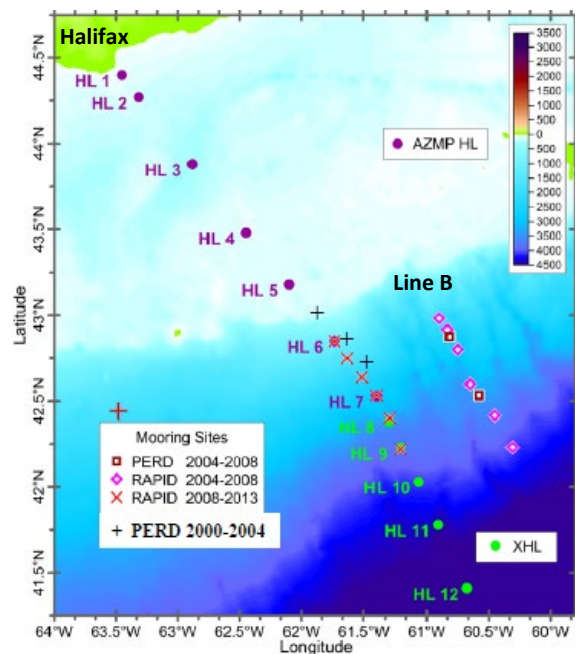


**Figure 1.** Lines of regular (typically tri-seasonal) oceanographic profile sampling in the Scotian Shelf and adjacent regions in DFO's Atlantic Zone Monitoring Program (AZMP; <https://www.dfo-mpo.gc.ca/science/data-donnees/azmp-pmza/index-eng.html> )

The ICNAF monitoring was followed by only limited measurements in the vicinity of the HL for over 2 decades. This changed with the initiation in 1998 of regular seasonal physical-biological-chemical profile sampling in Fisheries and Oceans Canada's (DFO's) Atlantic Zone Monitoring Program (AZMP 2002), at the same 7 HL sites of the earlier ICNAF program (Fig. 2). AZMP is now one of the few field physical oceanographic observational programs carried out by BIO, and hence a cornerstone of the DFO BIO

**Figure 2.** Locations of regular oceanographic profile sampling on the Halifax Line in DFO's AZMP (HL1-7; magenta closed circles ●) and on the eXtended Halifax Line (XHL) in DFO's AZOMP (HL8-12; green closed circles ●). Also shown are the sites of moored measurements of more than a year in duration. Those in the vicinity of the HL are the sites (SS-A, -B, -C) of the 2000-2004 DFO-PERD-industry moorings (blue plus signs +), and of the 2008-2014 RAPID WAVE moorings (red x signs). The red + sign near 43.5°N, 63.5°W is the site of the mooring on the 1000m isobath in the 1977-80 Shelf Break Experiment. To the east on RAPID WAVE's Line B, the pink open diamonds (◇) indicate the sites of the Proudman Oceanographic Laboratory's 2004-08 moorings, and the red open squares (◻) the sites (SS-D, -E) of the 2004-08 DFO PERD moorings.



Science program. However, its core sampling over the Scotian Slope where the primary larger-scale circulation arteries – the Labrador Current Extension (LCE), the Deep Western Boundary Current (DWBC) and the meandering Gulf Stream (GS) - are located remained sparse in its early years, with stations HL5, HL6 and HL7 having water depths of ~100, ~1000 and 2700 m, respectively.

Early multi-year moored oceanographic measurements over multiple years on the Scotian Slope were limited to those by Smith and Petrie (1982) in the late 1970s Shelf-Break Experiment which was sited about 150 km to the west of the HL. This contrasts the area of the ICNAF-AZMP Browns Bank Line off southwest Nova Scotia (Fig. 1) where long-term moored measurements were carried out at 4 sites during 1978-85 in the Cape Sable project (Smith 1983), then at 2 of these sites in the 1983-85 Fisheries Ecology Program (Smith 1989), and later at 2 of the sites during the 1990s in the US GLOBEC (Global Ocean Ecosystem Dynamics) program (Smith et al., 2001). At the time of the long-term hydrographic variability studies of Petrie and Drinkwater (1993) and Loder et al. (2003), and the pioneering numerical modelling studies of Han et al. (1997), Hannah et al. (2001) and Loder et al. (2001) in which observationally-based 3-d seasonal hydrographic and circulation fields were developed, no moored current and hydrographic measurements were available from the HL.

A unique opportunity for moored measurements over the Scotian Slope with multiple applications arose around 2000 associated with strong interest by the oil and gas industry in exploratory drilling. This is illustrated in Fig. 3 by the large number of lease blocks over the slope where a dozen or so companies had obtained exploration licences, following on from actual oil and gas production at multiple sites on Sable Island Bank (Cohasset-Panuke, Sable Offshore Energy Project). DFO had been collaborating since the 1980s with other Government of Canada departments and industry in oceanographic research relevant to operational and safety issues (e.g., currents, sea ice and waves), and environmental impacts (e.g., drilling discharges, oil spills) of oil and gas exploration, through the Federal Program on Energy Research and Development (PERD; e.g., Loder et al., 2005). More oceanographic information in deep-water frontier exploration areas was a particular priority of PERD’s Offshore Environmental Factors (OEF) program in 2000.

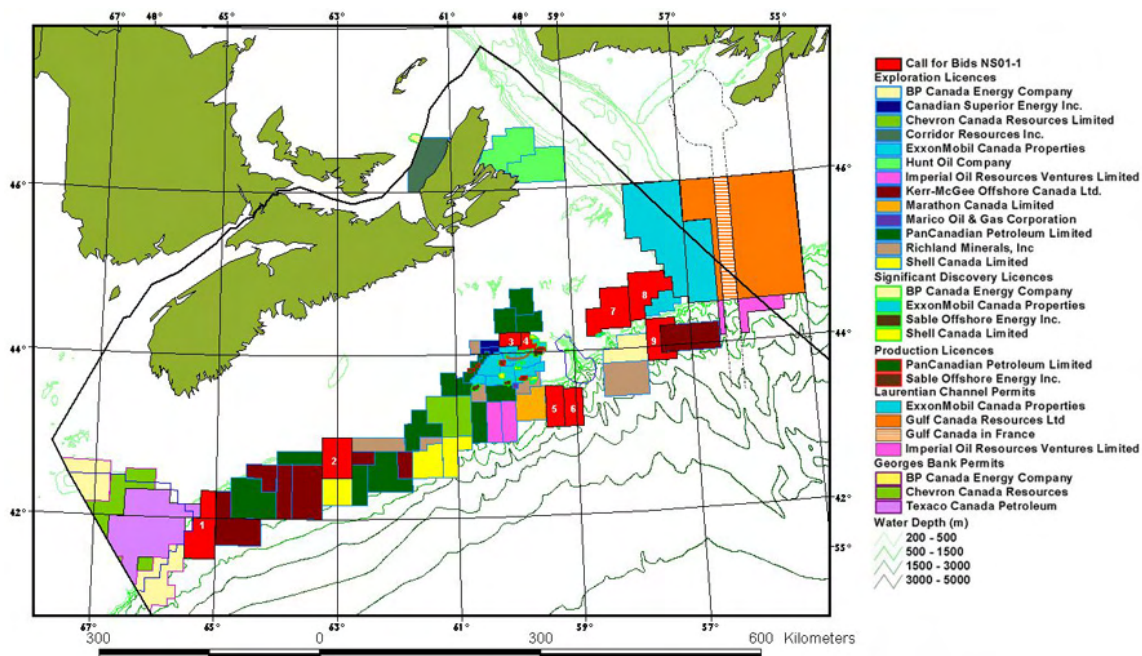


**Figure 3.** A map downloaded ca 2001 from the website of the then Canada Nova Scotia Offshore Petroleum Board (CNSOPB) showing blocks of “land” with Exploration and Production Licenses, and new blocks (in red) that were up for bids. The board is now known as the Canada Nova Scotia Offshore Energy Regulator (CNSOER) whose website is <https://cnsoer.ca/oil-gas-energy> .

With funding from the PERD OEF program and in-kind support from DFO BIO in the form of equipment, personnel, vessel time and other infrastructure, a multi-year moored current and hydrographic measurement program was initiated in spring 2000, with the deployment of a single tall mooring near AZMP hydrography station HL6. The site referred to as SS-A was near the 1100m isobath (Fig. 4), and the mooring included instrumentation distributed over the water column. With the HL crossing the central Scotian Slope and being at least somewhat representative of areas to the east and west, partnership agreements were developed with several oil and gas companies to provide increased instrumentation and further mooring deployments, complementing the initial SS-A deployments. This resulted in the DFO-PERD-industry program having tall moorings at a total of 3 sites between spring 2000 and spring 2004 – at SS-A for the entire period, at site SS-B on the 2000-m isobath starting in spring 2001, and at site SS-C on the 300-m isobath starting in fall 2001 (Fig. 2). Mooring deployments and recoveries were coordinated with AZMP surveys of the HL (e.g., AZMP 2002), and in later years with hydrographic surveys on an eXtended Halifax Line (XHL) as part of DFO BIO’s Atlantic Zone Off-shelf Monitoring Program (AZOMP) which was initiated to complement hydrographic monitoring on the AR7W Line across the Labrador Sea (e.g., Yashayaev 2007). A description of the moorings, instruments, and data return and quality from the 2000-04 moored measurement program, and mention of some complementary datasets, constitutes the bulk of this report.

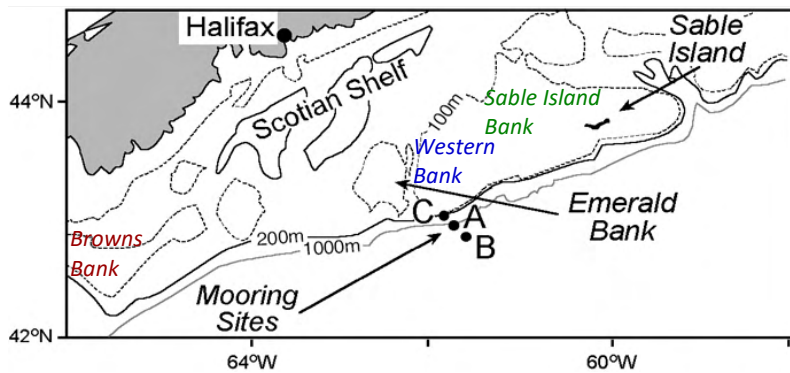


**Figure 4.** Location of mooring sites SS-A, SS-B and SS-C in relation to major topographic features on the outer Scotian Shelf and Slope.

Information on a second, much smaller DFO-PERD moored measurement program at 2 sites on the lower Scotian Slope/Rise about 50 km to the east of the HL/XHL, carried out from fall 2004 to fall 2008, is also provided in this report. Short moorings with near-bottom instrumentation only were deployed from fall 2004 to fall 2008 at sites SS-D on the (nominal) 2400m isobath and SS-E on the 3400m isobath, on a Line B corresponding to a satellite altimetry track (Fig. 2). This line had been chosen by the UK Rapid Climate Change (RAPID) Western Atlantic Variability Experiment (WAVE) for moorings at 6 sites (B0 to B5) across the Scotian Slope and Rise to obtain current, hydrographic and bottom pressure time series in order to estimate multi-year variability in the Atlantic Meridional Overturning Circulation (AMOC) (e.g., Elipot et al., 2013). The DFO-PERD moorings on Line B were part of a data exchange agreement between BIO and POL scientists, enhancing data availability for DFO and PERD issues.

As a result of technical mooring issues and for efficiency in RAPID WAVE operations, the latter’s mooring line on the Scotian Slope was switched in the fall of 2008 to the vicinity of the HL/XHL, in a partnership with DFO BIO. This has resulted in near-bottom moored measurements at 6 sites on the RAPID Scotian (RS) Line (adjacent to the HL/XHL) from fall 2008 to spring 2014, and continuation at 4 of those sites until spring 2018 (Loder et al., 2025a). The RS sites included RS1 near HL6, RS2 and RS3 between HL6 and HL7, RS4 near HL7, RS5 near HL8, and RS6 near HL 9. Together with the 2000-2004 DFO-PERD moored measurements, there are now moored time series near HL6 available from 2000-

2004 and 2008-2018, and near HL7 from 2001-2004 and 2008-2014 (as well as for other durations at the other RS sites indicated in Fig. 2).

In Section 2, a brief description of the oceanographic setting for the outer HL will be provided, followed by overviews of the 2000-04 and 2004-08 PERD moored measurement programs, a chronology of the mooring deployment and recoveries, and brief discussions of the complex topography of the HL's slope and of other datasets that are complementary to the moored measurements. The moored instrumentation will be described in Section 3, together with the data return and quality, and processing issues. Example displays of the data collected including concatenated time series over the mooring periods will be presented in Section 4, followed by a brief summary in Section 5. Examples of the mooring designs will be provided in the Appendix.

## 2. Background and Program Summary

### 2.1 Oceanographic Setting

The outer HL lies in a major large-scale frontal zone between the equatorward-flowing cold and relatively-fresh subpolar water in the LCE along the Scotian Shelf edge, and the warm and relatively-saline subtropical water of the GS (Figs. 5 and 6). This zone is particularly complex because the GS separates from the shelf edge near Cape Hatteras, and flows east-northeastward as a meandering and somewhat unstable open-ocean jet, shedding rings, eddies and filaments of various scale into the “Slope Water” region to the north. Note the contrast between the relative smoothness of the zone’s spatial temperature variation averaged over all months and many years (Fig. 5a), and the structure in the snapshot of sea surface temperature (SST) from satellite infrared imagery for 1-3 April 2002 during the moored measurement program (Fig. 6; see later for more detailed discussion). Note also the similar contrast

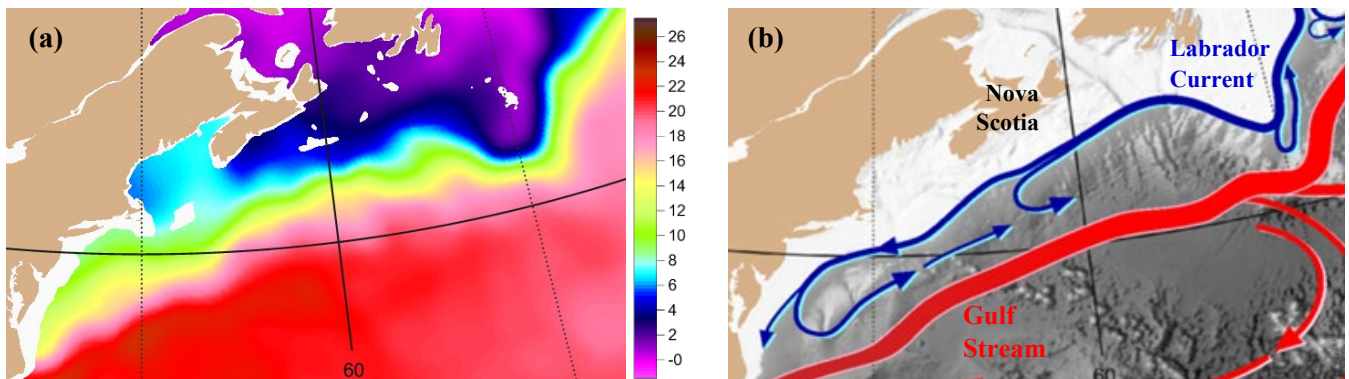
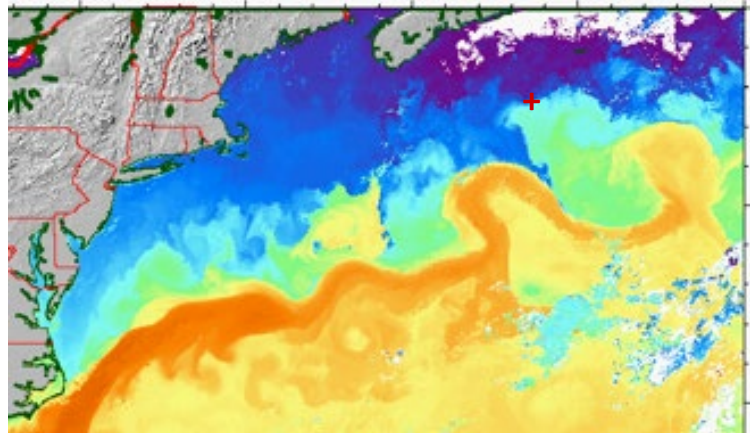
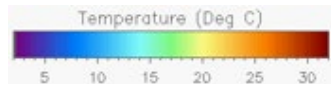


**Figure 5.** (a) Annual-mean ocean temperature (°C) at 100m, and (b) a schematic of the primary branches of the upper-ocean circulation in the Northwest Atlantic off Nova Scotia (blue denotes cold and red warm) (both courtesy of Dr. Igor Yashayaev of DFO BIO). The temperature distribution is interpolated objectively from historical observations, while the circulation pattern is based on a combination of current measurements and observed temperature and salinity distributions with some artistic licence; e.g., the cold offshore flow branch over the Scotian Slope represents episodic events over a broad area rather than a persistent local feature.

(c) Estimates of annual-mean transports (in units of Sverdrups, or 10<sup>6</sup> m<sup>3</sup>/s) in the major current branches (re-drawn from Loder et al., 1998). Those in solid blue are for subpolar waters with salinity below 34.8, based on moored measurements. The NADW/LSW arrow denotes the DWBC passing to the west of the Grand Bank.

**Figure 6.** Sea surface temperature (SST) in the Northwest Atlantic south of Nova Scotia from a composite of Advanced Very High Resolution Radiometer satellite images during 1-3 April 2002 (downloaded in 2003 from the website of the Johns Hopkins Applied Physics Laboratory). Note the temperature difference of  $\sim 25^{\circ}\text{C}$  between the Scotian Shelf and core of the Gulf Stream. The red + sign indicates the location of mooring site SS-A.

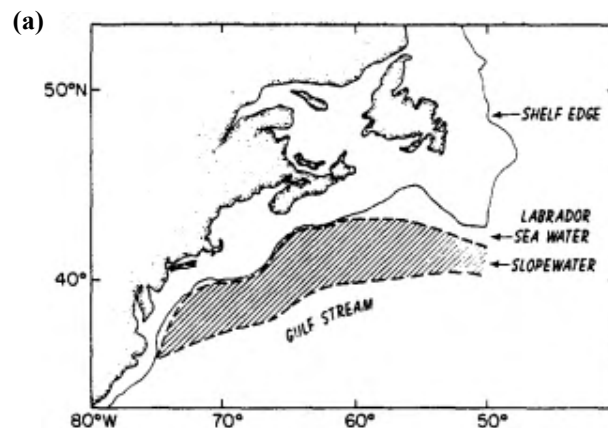


between the LCE and GS's structure in the mean-state schematic in Fig. 5c, and that apparent from the SST pattern in Fig. 6. An indication of the inadequacy of the moored measurements over the Scotian Slope prior to 2000 (Smith and Petrie 1982) is the computed eastward transport of 0.05 Sv along the Scotian Slope (Fig. 5c; Loder et al., 1998), in contrast to the collective evidence of water of subpolar origin reaching that location such as in the climatological temperature distribution (Fig. 5a).

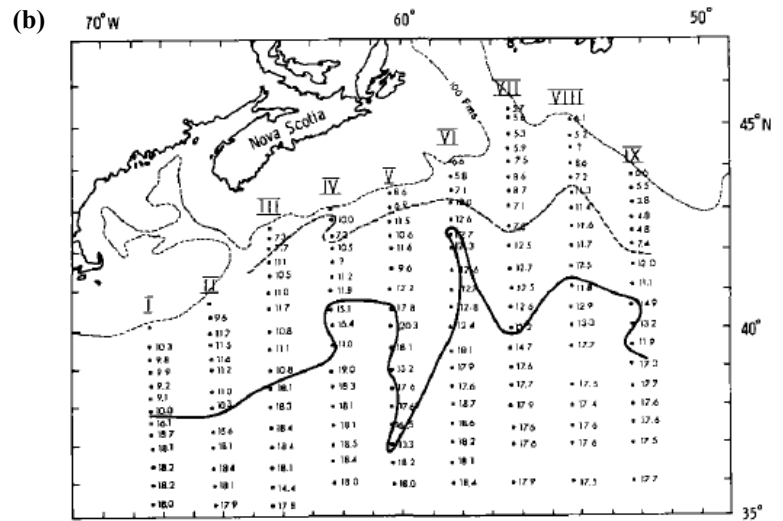
The name "Slope Water" was given (Lee 1970) to the admixture of remnant Labrador and GS waters that lies between the subpolar "coastal" water over the shelf and upper continental slope between the New England and Newfoundland Shelves, and the meandering GS. Different perspectives on its horizontal extent are shown in Fig. 7, and a schematic of its cross-slope vertical distribution in Fig. 8. The horizontal area that it typically occupies is shown schematically in Fig. 7a (from Csanady and Hamilton 1988), and a quasi-synoptic delineation of its southern extent in Fig. 7b (from Gatién 1976) based on the Gulf Stream '60 survey (Fuglister 1963). The spatial complexity of the currents in the Slope Water region is illustrated by the pattern (Fig. 7c) inferred by Gatién (1976) for the Gulf Stream survey, and the SST snapshot in Fig. 6 indicates that it can be much greater at particular times. The SST snapshot and the cross-slope schematic of water mass distributions (Fig. 8) show multiple weaker fronts within the larger-scale subpolar-subtropical (LCE-GS) frontal zone. In particular, the commonly discussed shelf-water / slope-water (or shelf-slope) front in the region (e.g., Herman and Denman 1979; Loder et al., 1998) usually refers to that between the Coastal and/or Labrador Slope Water, and the Warm Slope Water in Fig. 8, with the details varying with time.

Of relevance to the moored current measurements, the best picture of the seasonal variation of the shelf-edge Labrador Current Extension across the HL is probably provided by the circulation model (diagnostic

**Figure 7. (a)** Schematic of the typical extent of Slope Water (from Csanady and Hamilton 1988).



(b) Location of the boundary (solid curve) between the GS and Slope Water at 200m below the surface based on the Gulf Stream '60 temperature-salinity survey (Fuglister 1963), as interpreted by Gatién (1976). The dashed line indicates the boundary within the Slope Water of the two distinct types identified by Gatién (1976): Warm Slope Water adjoining the GS, and Labrador Slope Water to the north. (from Gatién 1976)



(c) Schematic of the circulation and water mass boundaries in the Slope Water region and over the Atlantic Canadian Shelf to its north, based on the Gulf Stream '60 survey (Fuglister (1963) and Gatién's (1976) analysis. Note the complexity including the recognition of eddies to the north and south of the GS (from Gatién 1976).

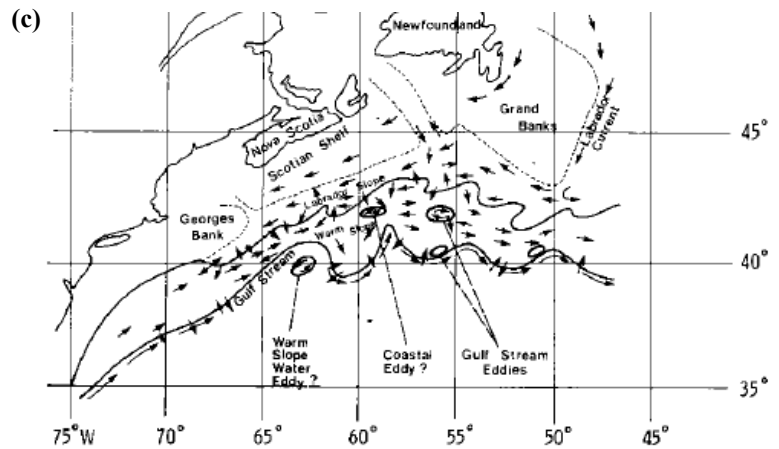
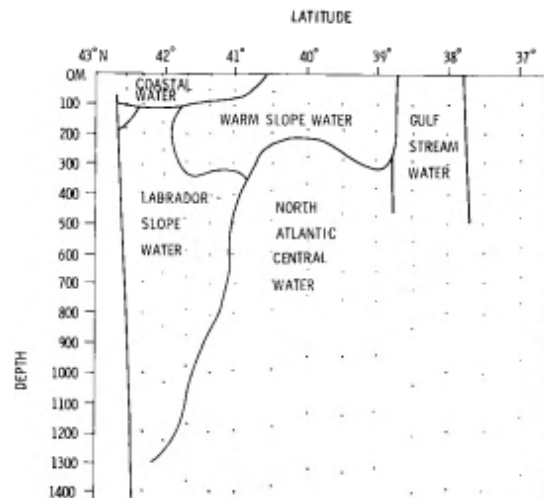
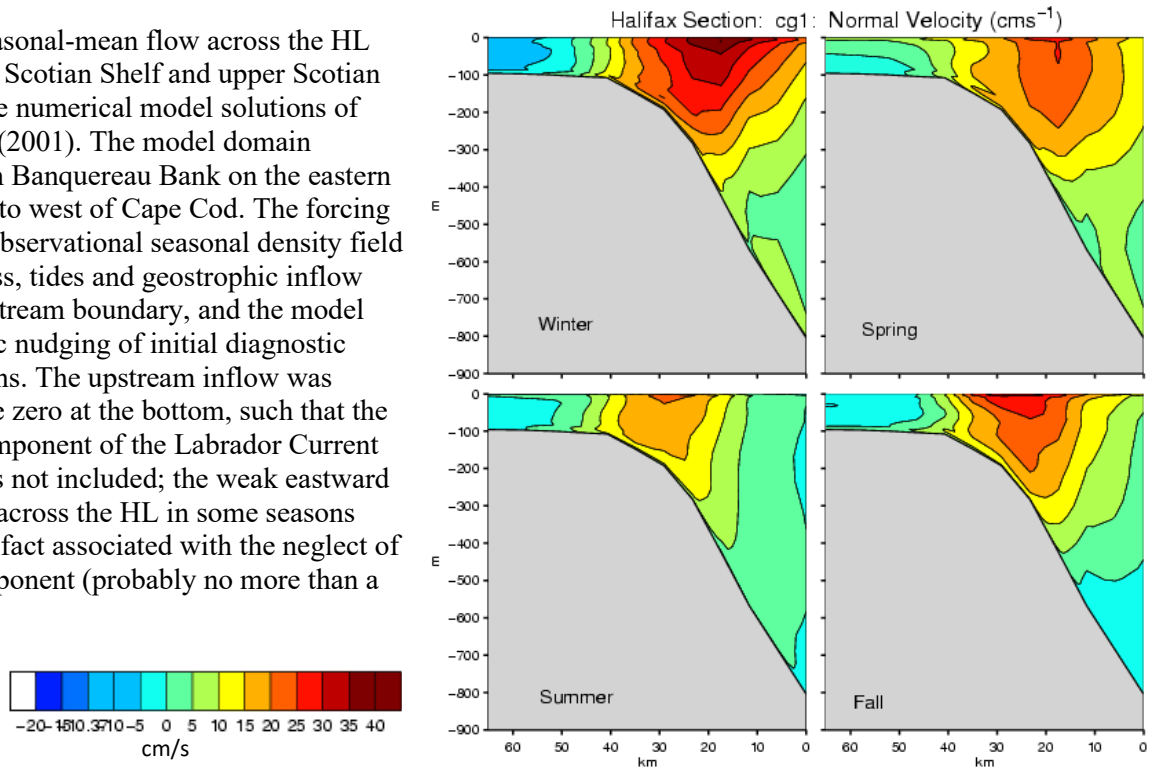


**Figure 8.** Schematic of the cross-slope vertical distribution of water masses over the Scotian Slope and Rise south of Nova Scotia (from Gatién 1976), based on the Gulf Stream '60 survey, and in particular on its Section III which extends south from the western Scotian Shelf (Fig. 7b). Note the indication of two types of Slope Water in the upper ~1000m between the upper slope and GS. The actual water mass distributions at a particular time and longitude in this frontal zone are usually somewhat different from this simplification, and generally much more complicated.



with prognostic nudging) results (Fig. 9) of Hannah et al. (2001) which shows a westward jet-like flow which is strongest in winter (2.5 Sv) and weakest in summer (1 Sv). However, the depth extent of westward flow in that model is not well represented since a barotropic inflow was not included in the upstream (Banquereau Bank) boundary condition.

**Figure 9.** Seasonal-mean flow across the HL over the outer Scotian Shelf and upper Scotian Slope from the numerical model solutions of Hannah et al. (2001). The model domain extended from Banquereau Bank on the eastern Scotian Shelf to west of Cape Cod. The forcing included the observational seasonal density field and wind stress, tides and geostrophic inflow across the upstream boundary, and the model had prognostic nudging of initial diagnostic model solutions. The upstream inflow was specified to be zero at the bottom, such that the barotropic component of the Labrador Current Extension was not included; the weak eastward flow at depth across the HL in some seasons may be an artifact associated with the neglect of this flow component (probably no more than a few cm/s).



## 2.2 Overview of the 2000-04 and 2004-08 Moored Measurement Programs

The objectives of the 2000-04 and 2004-08 PERD programs were to:

- describe and understand variability in currents and hydrography on the Scotian Slope, and
- obtain quantitative information on currents variability in potential deep-water oil and gas exploration areas in the region.

The broader approach, including for the Newfoundland Slope where the geographic focus was on Flemish Pass and Orphan Basin (Loder et al., 2025b,c), was to:

- make moored measurements over multiple years on representative cross-slope lines,
- obtain complementary surface current anomaly estimates from altimetry, and
- obtain complementary subsurface current estimates from vessel-mounted Acoustic Doppler Current Profiler (ADCP) measurements in conjunction with AZMP and AZOMP hydrographic surveys.

The HL/XHL and Line B were chosen as the focal areas for the Scotian Slope moored measurements, in view of the earlier (1950s-1970s) and ongoing AZMP/AZOMP hydrographic surveys on the HL/XHL (Figs. 1 and 2), supplementary financial support for the 2000-2004 moorings from multiple oil and gas companies with exploratory lease blocks on the Scotian Slope (Fig. 3; see Section 8), and the RAPID WAVE choice of the area for its 2004-2014 moorings (Elipot et al., 2013; Hughes et al., 2013; Loder et al., 2025a).

There were instrumented moorings deployed at 3 sites during the 2000-04 program and at 2 sites during the 2004-08 follow-up. The sequential deployment numbers for each site, and the overall periods, position and water depth ranges (among different deployments at the same approximate site), and BIO Consecutive Mooring Numbers (historical sequence) are summarized in Table 1. The specifics on each mooring are listed in Table 2, including the deployment and recovery dates, the actual positions and water depths, and the depths of the various instruments. The successive deployments at each site are indicated by a number after the site letter; e.g., SS-A1 in June 2000 and SS-A2 in November 2000.

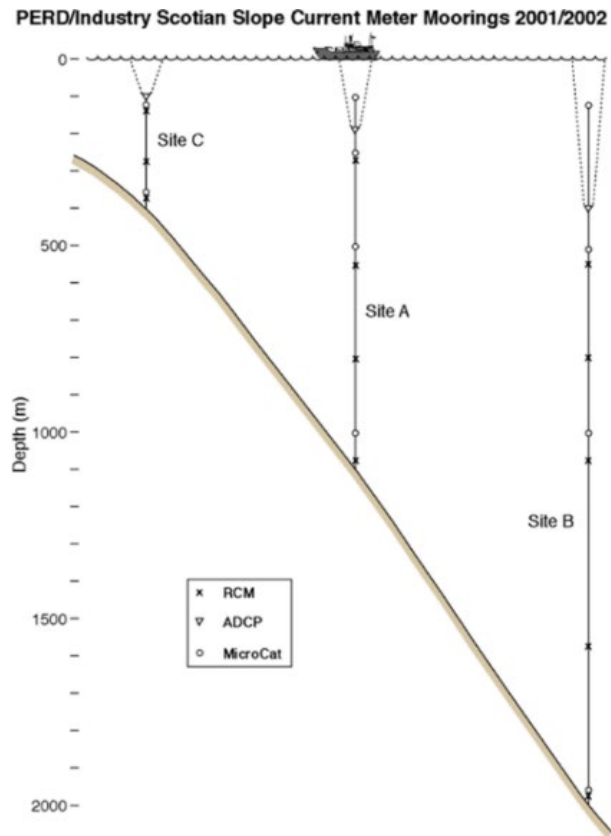
**Table 1.** DFO-PERD Scotian Slope mooring sites (SS-A, -B, -C, -D, -E), sequential deployment numbers (e.g., SS-A #) at each site, latitude and longitude ranges of the mooring positions at each site, ranges of the water depths for the different deployments, BIO Consecutive Mooring Numbers (BIO #'s, or M#'s) for each site, and comments. The range of positions at SS-A, SS-B and SS-E was related to at-sea positioning difficulties in the presence of winds, waves and currents. The CTD stations near SS-A and SS-B were sometimes denoted HL5.3 and HL6.5, respectively.

Site	D #'s	Period	Position Range		Water Depth Range (m)	BIO #s (or M#s)	Comments
			Lat. (N)	Long. (W)			
SS-A	1-6	Jun 2000 – Apr 2004	42° 49.90' – 42° 51.38'	61° 35.08' – 61° 39.10'	1115-1195	1352, 1377, 1378, 1379, 1387, 1395, 1419, 1432, 1433, 1478	East of HL6
SS-B	1-5	Jun 2001 – Apr 2004	42° 41.30' – 42° 41.59'	61° 30.48' – 61° 33.06'	1991–2101	1388, 1412, 1429, 1454, 1479	Between HL6 & HL7 (HL6.5)
SS-C	1-4	Oct 2001 – Apr 2004	42° 58.61' – 42° 59.15'	61° 44.87' – 61° 45.01'	295-317	1413, 144, 1430, 1431, 1455, 1480, 1491	Between HL5 & HL6 (HL5.3)
SS-D	1-4	Oct 2004 – Oct 2008	42° 52.46' – 42° 52.88'	60° 49.07' – 60° 49.39'	2383-2400	1547, 1585, 1623, 1666	On Line B
SS-E	1-4	Oct 2004 – Oct 2008	42° 31.53' – 42° 32.10'	60° 34.53' – 60° 35.64'	3298-3399	1548, 1586, 1624, 1667	On Line B

### 2.2.1 2000-04 Program

In the 2000-04 program, tall moorings were deployed at 3 sites near the HL (Fig. 10), with nominal water depths of 300m (SS-C), 1100m (SS-A) and 2000m (SS-B). The letter sequence in the site names reflects the order of the first deployments at each site, with the number of sites increasing with increased industry

**Figure 10.** Schematic of the nominal design of the primary mooring array in the 2000-04 program, with an upward-looking Acoustic Doppler Current Profiler (ADCP) for the near-surface region and Aanderaa current meters (RCMs) and MicroCATs (MCs) below. The instruments and their vertical positions on the actual moorings varied somewhat (Table 2). Site SS-C was chosen to be in the core of the shelf-edge current “jet” of the LCE based on the Hannah et al. (2001) model solutions (Fig. 9), site SS-A to be near AZMP station HL6, and site SS-B in the deeper water of primary industry interest. (Drawing courtesy of Bob Lively of BIO).



support. Because of fishing activity in the vicinity of the shelf edge, it was clear that surface guard buoys with lights and radar reflectors would need to be maintained around the mooring(s) at SS-C, in addition to active notifications to marine vessels via the Canadian Coast Guard's Notices to Mariners (NotShips) and communications to fishing companies and vessels about all the moorings. This turned out to be only partly successful since a mooring at SS-A was damaged by towed fishing gear, and a mooring at SS-C also damaged (in spite of the presence of the guard buoys). On the other hand, the guard buoys very likely contributed to the overall successful mooring and data return at SS-C.

The nominal mooring design included an upward-looking Acoustic Doppler Current Profiler (ADCP) near the top of each tall mooring, and Aanderaa current meters (RCMs) and MicroCAT (MC) temperature, conductivity and pressure recorders distributed over the water column below the ADCPs (Fig. 9). However, an ADCP and MCs were not available for some moorings, e.g., there was no ADCP in SS-A1 and SS-A5 (Table 2). When no ADCP was available, additional RCMs were included in the upper ocean. When no MCs were available, Minilog (ML) temperature recorders were sometimes added at selected depths; e.g., in SS-A1 and SS-C2. An ML was also attached to a surface guard buoy in deployments SS-C2 and SS-C4, providing a continuous record of near-surface temperature (at ~2m below the surface).

Two other types of recording instruments were included in some deployments, for potential use in data interpretation or collaborative studies (Table 2). Aanderaa bottom pressure recorders (BPSs), sometimes referred to as water level recorders (WLRs) or tide gauges, were included on a separate mooring in deployments SS-A2, SS-A3 and SS-A5, for potential use in numerical model studies. Electromagnetic S4 current meters with high-frequency sampling were deployed in the near-bottom region (2-4 mab), in addition to a WLR on separate short moorings, in SS-C1 and SS-C2, for potential collaboration with concurrent sediment transport studies being carried out by the Geological Survey of Canada Atlantic (GSCA) at BIO and Dalhousie University (Hill et al., 2004). Mobile bedforms on the upper Scotian Slope were also of concern to oil and gas drilling (and to PERD).

All but 2 of the 22 moorings deployed in the 2000-04 program were fully returned, with the other 2 only partly returned. Mooring #1387 deployed in May 2001 at SS-A3 was struck by towed fishing gear on 25 September 2001, and mooring #1455 deployed in October 2002 at SS-C3 was struck by towed gear on 24 December 2002. The returned instruments and the lengths of good record from all of the moorings will be discussed in Section 3.

### **2.2.2 2004-08 Program**

The more limited 2004-08 moored program, supported by only DFO and PERD, had short moorings at sites SS-D (water depth ~2400m) and SS-E (water depth ~3400m) on Line B (Fig. 11), with an RCM at 50 mab and an MC at 10 mab on each mooring (Table 1 and 2b). There were 4 successive year-long deployments at each site, referred to as deployments SS-D1 to SS-D4 and SS-E1 to SS-E4. All of the moorings were successfully recovered. The data return will be discussed in Section 3.

The DFO-PERD Line B moorings were designed to complement the 2004-08 RAPID WAVE (RW) moored measurements of the UK POL and NOC (Elipot et al., 2013), by adding an RCM and an MC at two sites among the six RAPID RW Line B sites (Fig. 11). The RW Line B moorings only had a combination of MCs and Bottom Pressure Recorders (BPRs), and no current meters. The RW program had also initiated a similar moored measurement program on a Line A across the Newfoundland Slope off the southwest Grand Bank, with the Line A and B programs complementing US moored measurement programs on Line W south of Cape Cod (Toole et al., 2017) and the long-term cross-basin AMOC monitoring line at 26.5°N (e.g., Smeed et al., 2014) (Fig. 11a). Unfortunately there were substantial mooring losses on Line A such that the program was not continued after the initial 2004 deployment.

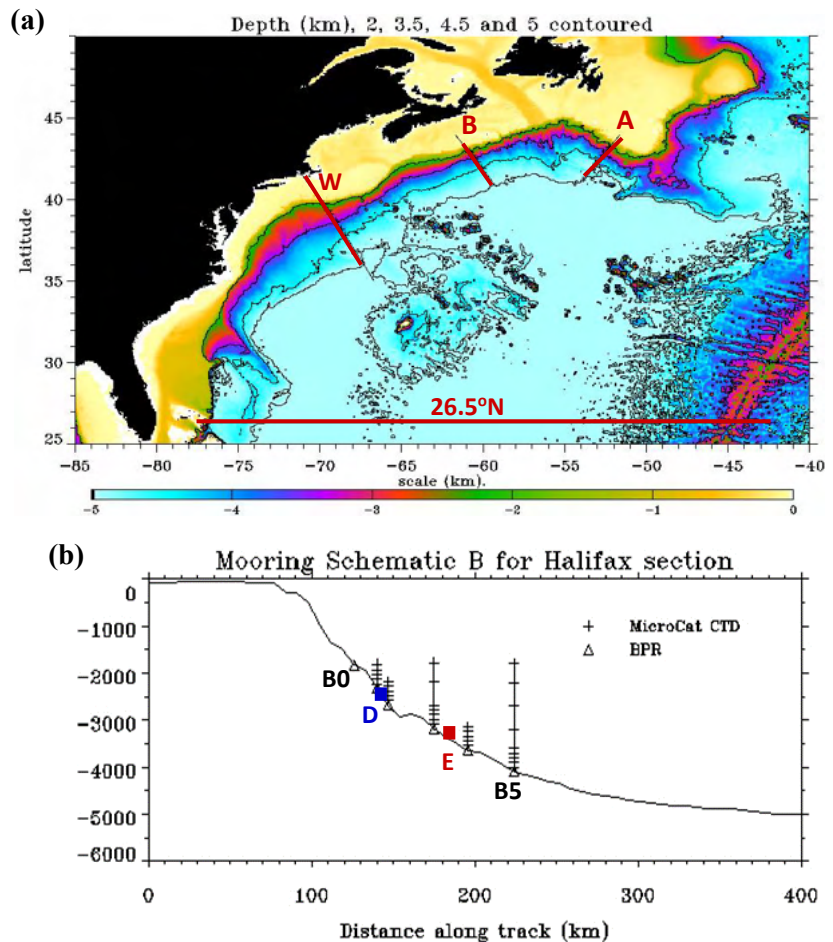
**Table 2a.** Listing of moorings deployed at **SS-A** and **SS-B** during the 2000-04 Scotian Slope program with their BIO #, deployment and recovery dates, water depth, and depths of various instruments (ADCP: Acoustic Doppler Current Profiler; RCM: Aanderaa RCM current meter (RCM8s except \*RCM11s and \*\*SeaGuard); MC: MicroCAT temperature (T) – conductivity (C) – pressure (P) recorder; ML: Minilog T recorder; WLR: Water Level Recorder). The listing is organized by site (SS-A to SS-E) and sequential deployment number (D #: e.g., 1 to 6 for SS-A). *Red italics* indicate that no good data were returned from the instrument. (continued on next page)

Site	D #	BIO #	Dates (dd/mo/yr-2000)		Position (N, W)		Depths (m)					
			Deployment	Recovery	Lat	Long	Water	AD-CP	RCMs	MCs	MLs	WLR
SS-A	1	1352	13/06/00	21/11/00	42° 50.98'	61° 37.81'	1119	-	74, 89, 144, 199, 294, 569, 819, 1096	-	68, 79, 99, 189, 225	
	2	1377	21/11/00	31/05/01	42° 50.99'	61° 36.89'	1124	-	149, 299, 574, 824, 1100	148, 274, 524, 1024	-	
		1378	21/11/00	31/05/01	42° 51.38'	61° 35.08'	1129	430		-	-	
		1379	21/11/00	31/05/01	42° 50.6'	61° 38.6'	1115	-	-	-	-	1115
	3	1387	31/05/01	25/09/01	42° 49.90'	61° 39.10'	1195	260	360, 635, 885, 1170	210, 335, 585, 1085	-	
		1395	31/05/01	24/05/02	42° 50.54'	61° 38.53'	1123	-	-	-	-	1123
	4	1419	21/10/01	24/06/02	42° 50.87'	61° 37.67'	1140	205	305, 580, 830, 1115	280, 530, 1030	-	-
	5	1432	25/06/02	22/05/03	42° 50.66'	61° 37.41'	1144	-	159, 309, 584, 834, 1119	284, 534, 1034	152	-
		1433	25/06/02	22/05/03	42° 50.8'	61° 37.58'	1114	-	-	-	-	1114
	6	1478	22/05/03	07/04/04	42° 50.88'	61° 37.67'	1125	153	268, 565, 815, 1100	74, 515, 1015	-	-
SS-B	1	1388	01/06/01	20/10/01	42° 41.31'	61° 33.04'	1991	391	541, 791, 1076, 1591, 1967	392, 991, 1592, 1966	-	-
	2	1412	21/10/01	24/06/02	42° 41.31'	61° 33.06'	1995	386	545, 795, 1080, 1595, 1971	396, 995, 1595, 1970	-	-
	3	1429	25/06/02	20/10/02	42° 41.41'	61° 31.21'	2015	409	565, 815, 1100, 2616, 1990	416, 1015, 1989	-	-
	4	1454	20/10/02	14/04/03	42° 41.59'	61° 30.48'	2101	495	651, 901, 1186, 1702, 2077	502, 1101, 2076		
	5	1479	23/05/03	09/04/04	42° 41.30'	61° 33.00'	1991	241	248, 541, 791, *792, 1076, 1592, 1967	92, 392, 991, 1966		
	6	1647	29/04/07	9/12/07	42° 41.27'	61° 31.45'	1979	-	<i>1874, *1877, **1880</i>	-	-	-

**Table 2b.** (continued from previous page) Listing of moorings deployed at **SS-C** during the 2000-04, and at **SS-D** and **SS-E** during the 2004-08, Scotian Slope programs with their BIO #, deployment and recovery dates, water depth, and depths of various instruments (ADCP: Acoustic Doppler Current Profiler; RCM: Aanderaa RCM current meter (RCM8s, except RCM11s indicated by an asterisk\*); **S4: InterOcean S4** electromagnetic current meter; MC: MicroCAT temperature-conductivity-pressure (T-C-P) recorder; ML: Minilog T recorder; WLR: Water Level Recorder). The listing is organized by site (SS-C to SS-E) and sequential deployment number (D #: 1 to 4 for SS-C).

Site	D #	BIO #	Dates (dd/mo/yr-2000)		Position (N, W)		Depths (m)					
			Deployment	Recovery	Lat	Long	Water	AD-CP	RCMs & S4s	MCs	MLs	WLR
SS-C	1	1413	19/10/01	22/05/02	42° 58.93'	61° 44.99'	317	-	314 313, 315	-		317
		1414	19/10/01	22/05/02	42° 59.09'	61° 44.88'	302	86	127, 202, 277, 292	84, 291	-	-
	2	1430	22/05/02	22/05/03	42° 58.96'	61° 44.93'	314	-	312, 311	-		314
		1431	22/05/02	19/10/02	42° 59.09'	61° 44.87'	305	85	130, 205, 280, 295	-	2, 85, 205, 280	-
	3	1455	19/10/02	24/12/02	42° 59.09'	61° 44.88'	302	85	130, 205, 280, 295	87, 294	-	-
	4	1480	22/05/03	07/04/04	42° 58.61'	61° 45.01'	340	-	330, 337	-	-	-
		1491	14/07/03	07/04/04	42° 59.15'	61° 44.92'	295	58	65, 120, 270	31	2	-
	SS-D	1	1547	22/10/04	01/11/05	42° 52.46'	60° 49.07'	2452	-	*2402	2442	-
2		1585	23/10/05	10/10/06	42° 52.88'	60° 49.39'	2419	-	*2369	2409	-	-
3		1623	10/10/06	07/10/07	42° 52.57'	60° 49.23'	2425	-	*2375	2415	-	-
4		1666	07/10/07	01/10/08	42° 52.58'	60° 49.20'	2438	-	*2388	2428	-	-
SS-E	1	1548	22/11/04	23/10/05	42° 31.96'	60° 34.63'	3418	-	3368	?	-	-
	2	1586	23/10/05	20/10/06	42° 32.10'	60° 34.53'	3414	-	3364	3404	-	-
	3	1624	11/10/06	07/10/07	42° 31.55'	60° 35.64'	3395	-	3345	3385	-	-
	4	1667	07/10/07	01/10/08	42° 31.53'	60° 35.59'	3414	-	*3364	3404	-	-

**Figure 11. (a)** Bathymetric map of the Western North Atlantic with the lines (red) with moored measurements during 2000-2004 for investigating multi-year variability in the Atlantic Meridional Overturning Circulation (AMOC). Lines A and B, on the Newfoundland and Scotian Slopes respectively, were part of the UK RAPID WAVE program, Line W was part of an ongoing US program carried out by the Woods Hole Oceanographic Institution, and the cross-basin line at 26.5°N was part of the ongoing UK/US RAPID/MOCHA program. (modified from Hughes et al., 2007)



**(b)** Schematic of moorings planned by POL/NOC (black) at six sites on Line B involving BPRs and MCs, with the two DFO PERD moorings at sites SS-D and SS-E included. The POL/NOC sites were named B0, B1, B2, B3, B4 and B5 proceeding offshore. The DFO PERD moorings comprised an RCM at 50 mab and MC at 10 mab. (modified from Hughes et al., 2007)

The 2004-08 POL/NOC measurements on Line B were used together with those from Line W and the 26.5°N line in the AMOC variability analysis of Elipot et al. (2013).

The RAPID WAVE Scotian Slope moored measurement sites were changed to be near the DFO AZMP/AZOMP HL/XHL in fall 2008, on a line referred to as RAPID Scotian (RS). See Hughes et al. (2013) and Loder et al. (2025a) for more information.

## 2.3 Program Chronologies

### 2.3.1 2000-04 DFO-PERD-Industry Program

In this subsection, we provide a chronology of the mooring work in the 2000-04 program, with indication of the moorings deployed and/or recovered on particular cruises, and of CTD stations between HL3 and HL7 that were occupied on those cruises (Table 3). Other AZMP surveys of the HL/XHL during the mooring period are included.

The 2000-04 program was initiated with the deployment of a single tall mooring (M1352) at SS-A1, about 2 km to the east of HL6 in slightly deeper water (~1100m), on cruise Parizeau 2000-075 in mid June 2000 (Table 2a and 3). No ADCP or MCs were available, but the mooring had 8 RCMs and 5 MLs including ones at ~70 mbs (or just “m”). CTD profiles were taken at HL3-HL6, and at 2 sites between HL5 and HL6 (HL5.2 and HL5.3 on the 200- and 300-m isobaths, respectively). While this mooring was in place, an AZMP survey which included HL3-HL7 was carried out in October 2000 on Hudson 2000-050.

Mooring M1352 was successfully recovered on Hudson 2000-066 in November 2000, and replaced by 3 moorings in SS-A2: a tall one (M1377) with RCMs and MCs distributed below ~150m, an intermediate-

**Table 3.** List of DFO cruises which contributed to, or complement, the 2000-04 moored measurement program on the Scotian Slope with the time period, cruise designation, chief scientists, mooring sites (SS-L# where L=A, B or C) and BIO consecutive numbers (#####'s) for moorings recovered and deployed, and CTD stations occupied. CTD stations 5.3 and 6.5 were near mooring sites SS-C and SS-B, respectively. Station HL5.2 was on the 200m isobath.

Dates	Cruise	Chief Scientist	Mooring Work		CTD Stations	Notes
			Recoveries	Deployments		
11-14 Jun 2000	Par 2000-075	G Bugden		A1:1352	HL 6, 5.5, 5.2, 5, 4, 3	
7-8 Oct 2000	Hud2000-050	E Horne			HL3-7	AZMP
20-22 Nov 2000	Hud 2000-066	G Bugden	A1:1352	A2:1377, 1378, 1379	HL 7, 6, 5.2, 5, 4, 3	
1 May	Hud2001-009	E Head			HL 6	AZMP
31May – 1Jun 2001	Hud 2001-022	A Clarke	A2:1377,1378, 1379	A3:1387, 1395 B1:1388	HL 7, 6, 5, 4, 3	AZMP
28 Sept 2001	Hud 2001-055	D Gordon	A3: 1387 (drifting portion)			
18-21 Oct 2001	Hud 2001-061: Leg1	M Mitchell	A3:1387 (remainder) B1:1388	A4:1419; B2: 1412 C1: 1413, 1414, 3gb	HL 7	
29-30 Oct 2001	Hud 2001-061: Leg2	E Horne			HL 3-7	AZMP
4-6 May 2002	SWA 2002-916	G Harrison			HL 3-7 (shallow only)	AZMP
22 May 2002	SWA 2002-912	M Scotney	C1: 1413, 1414	C2: 1430, 1431		RALPH deployed
24-26 Jun 2002	Hud 2002-032	A Clarke	A3: 1395; A4:1419 B2: 1412	A5:1432, 1433; B3: 1429	HL 3-7, 5.3, 6.5	
19-22 Oct 2002	Hud 2002-064	M Mitchell E Horne	B3: 1429 C2: 1431	B4: 1454 C3: 1455	HL 3-6, 5.3, 6.5	
9-12 Jan 2003	SV Bonavista		C3: 1455 (drifting portion)			
11 Apr 2003	Hud 2003-005	E Head	B4: 1454		HL 3-7, HL 6.5	AZMP
22-23 May 2003	Hud 2003-021	M Mitchell	A5:1432, 1433; C2: 1430; C3: 1455 (remainder)	A6: 1478; B5: 1479 C4: 1480	HL 5.3, 6, 6.5 Near 750 & 1500m isobaths	
14-15 Jul 2003	Hud 2003-038	A Clarke		C4: 1491	HL 3-7, HL5.3	RALPH deployed
1-13 Nov 2003	Hud 2003-072	M Mitchell	2 gb (S,T)	1 gb (H)	HL 5.3, 6, 6.5	RALPH recovered
18-21 Dec 2003	Hud 2003-078	E Head			HL 3-7	AZMP
6-9 Apr 2004	Hud 2004-005	M Scotney	A6: 1478; B5: 1479 C4: 1480, 1491		HL 5.3, 6, 6.5, 7; Near 750&1500m isobaths	

height mooring (M1378) with an upward-looking Long Ranger ADCP at ~400m, and a short mooring (M1379) with a WLR mounted in the train-wheel anchor (Table 2a and 3). CTD profiles were taken at HL3-HL7 and HL5.2.

The three SS-A2 moorings were successfully recovered on 31 May 2001 on Hudson 2001-002, and replaced by two moorings on the same day in SS-A3: a tall mooring (M1387) with an ADCP, 5 RCMs and 4 MCs, and a short mooring (M1395) with a WLR (Table 2a and 3). Also, the first mooring (M1388) at site SS-B(1) with water depth (~2000m) was deployed the next day. An AZMP survey including HL3-HL7 was carried out during this cruise.

Mooring M1387 was struck and severed at about 287 mbs on 25 September 2001, probably by fishing dragging gear. The upper portion with the main buoyancy float and ADCP (260 mbs), and a secondary buoyancy package and MC (~210 mbs), drifted away and was recovered on the Scotian Slope by Hudson 2001-055 on 29 September, aided by satellite tracking via an Argos transmitter on the main float.

On Leg 1 of Hudson 2001-061 during 18-21 October 2001, the remainder of M1387 from SS-A3, and M1388 from SS-B1, were successfully recovered, while M1395 was left in place (Table 2a and 3). Replacement tall moorings M1419 (SS-A4) and M1412 (SS-B2) were deployed at these respective sites, with instrumentation similar to that on the recovered moorings. In addition, the first moorings were deployed at site SS-C(1): a tall mooring (M1414) with an ADCP, 4 RCMs and 2 MCs; a short mooring (M1413) with 2 InterOcean S4 electromagnetic current meters and an RCM (all in the bottom 4m), and a WLR in the anchor; and 3 surface guard buoys (marked Q, AA and X) (Table 2b). An AZMP survey including HL3-HL7 was carried out during 29-30 October on Leg 2 of this cruise (but without profiles near SS-B2 or SS-C1). Also, an AZMP CTD survey which included profiles at HL3-HL7 (but only to a depth of ~300m) was carried out on 3-5 May 2002 on a special cruise by CCGS Sir William Alexander (SWA 2002-916) due to the unavailability of the CCGS Hudson.

Moorings M1413 and M1414 at SS-C1 were recovered on another special cruise - SWA 2002-912 - and replacement moorings M1430 and M1431 were deployed (SS-C2), all on 22 May 2002. The replacement moorings had similar instrumentation to the recovered ones, except that MLs were used instead of MCs on the tall mooring and there was one (instead of two) S4(s) on the short mooring. Two of the guard buoys (Q and AA deployed in Oct 2021) were no longer in place, and the other (X) was recovered. Since swordfishing line was tangled with the recovered tall mooring (but apparently did not affect instrument performance), the disappearance of the two guard buoys may have been related to fishing activity. Four replacement guard buoys (R, S, T and A) were deployed around the two replacement PERD moorings and the bottom quadrupod “Ralph” (Heffler et al., 1984) deployed by Dalhousie and GSCA collaborators (Hill et al. 2004). No CTD profiles were taken at the mooring sites.

Moorings M1395 (SS-A3), M1419 (SS-A4) and M1412 (SS-B2) were successfully recovered on 24 June 2002, and replacement moorings M1432 and M1433 (SS-A5) and M1429 (SS-B3) were deployed the next day, all on Hudson 2002-032. CTD profiles were taken at HL3-HL7 as part of AZMP, and also at HL5.3 (near SSC) and HL6.5 (near SSB), during 24-26 June.

On Hudson 2002-064 during 19-22 October 2002, M1431 (SS-C2) and M1429 (SS-B3) were successfully recovered, and replacement moorings M1455 (SS-C3) and M1454 (SS-B4) were deployed. All four of the guard buoys deployed in the preceding May were still in place; three were recovered and one (S) was left in place as a longevity test. Two new guard buoys were deployed, leaving three in place for the fall-winter period. CTD profiles were again taken at HL3-HL7 for AZMP, and near SSC (HL5.3) and SSB (HL6.5).

On 24 December 2002, the Argos beacon attached to M1431’s main float started transponding, indicating the float on this SS-C3 mooring had come to the surface and was drifting. The drifting portion of the

mooring, above roughly 250 mbs where the wire had been severed, was recovered on 9 January 2003 by the industry supply vessel (SV) Bonavista. All of the instruments on this portion were recovered in working order, as later (see below) were the instruments on the mooring's lower portion which did not break loose; however, none of the records after the day the mooring was struck were of use. It seems likely that this mooring was also struck by towed fishing gear (in spite of having guard buoys around it).

Mooring M1454 (SS-B4) was successfully recovered on 14 April 2003 on Hudson 2003-005, but not replaced until later. The acoustic release on the damaged mooring M1431 (SS-C3) also successfully transponded on that cruise. CTD profiles were taken at HL3-HL7 for AZMP, and near SSB (HL6.5).

Moorings M1432 and M1433 (SS-A5) were successfully recovered, and M1478 (SS-A6) successfully deployed, on 22 May 2003 on Hudson 2003-021. M1430 (SS-C2) and the remainder of M1455 (SS-C3) were also recovered, and a replacement short mooring M1480 (SS-C4) with two near-bottom RCMs was deployed, on that same day. A replacement guard buoy (T) was also deployed at site SSC. Replacement mooring M1479 (SS-B5) was deployed on 23 May, resulting in a gap of over 5 weeks in the moored measurements at site SSB. CTD profiles were taken near the three mooring sites, as well as on the 750- and 1500-m isobaths on the HL.

On Hudson 2003-038, two guard buoys (O, Q) were recovered at SS-C4, and a tall replacement mooring M1491, the GSCA quadrupod Ralph and three replacement guard buoys (L, P, S) were deployed there, all on 14 July 2003. CTD profiles were taken at HL3-HL7 for AZMP, and at HL5.3 (SSC).

On Hud 2003-072 in early November, two guard buoys (S, T) and the GSCA tripod RALPH were recovered at SS-C4, and a replacement guard buoy (H) was deployed there. CTD profiles were taken at the 3 mooring sites. Later on Hud 2003-078, CTD profiles were taken at HL3-HL7 as part of AZMP.

The 2000-04 moored measurement concluded with the successful recovery of M1480, M1491 and the remaining guard buoys at SS-C4, and M1478 at SS-A7, all on 7 April 2004 on Hudson 2004-005. M1479 at SS-B5 was recovered the next day. CTD profiles were taken at HL 5.3, 6, 6.5 and 7, and near the 750- and 1500-m isobaths.

### **2.3.2 2004-08 DFO-PERD-RAPID Program**

The short moorings at sites SS-D and SS-E on the RAPID B Line were deployed and recovered on the annual Fall AZMP survey cruise of the Scotian Shelf and Slope region. Dates, cruise numbers and BIO mooring numbers are provided in Table 4 (see Table 2 for more detail on the positions and depths). All of the instruments from the four year-long deployments were successfully recovered.

The PERD SS-D and SS-E moorings complemented the near-bottom RAPID WAVE moorings on Line B which had 2-year deployments starting in each of 2004 and 2006 (Elipot et al., 2013). These sites are denoted R-B# in Table 4 where R refers to RAPID, B to the B Line, and # to the site name: the sites B0 to B6 were positioned in water depths ranging from ~1800m to ~4100m. Each of those moorings had a SeaBird SBE53 Bottom Pressure Recorder (BPR) and most had at least one MC.

Five of the six POL moorings from the second (2006-08) B Line deployment were recovered on Hud 2008-037 in September-October 2008 (Table 4). Multiple dragging attempts for the R-B1 mooring were not successful.

CTD profiles near most of the POL Line B moorings were taken on each of the five deployment and/or recovery cruises for the SS-D and SS-E moorings (Table 4).

**Table 4.** Chronology of mooring deployments and recoveries on the RAPID WAVE Line B between October 2004 and October 2008 during DFO AZMP survey cruises, with dates, cruise numbers, chief scientists, mooring sites and BIO mooring numbers, and the POL Line B sites where CTD profiles were taken. The DFO PERD moorings were at sites SS-D and SS-E (Table 2), denoted below by the letters **D** and **E**. The number (1 to 4) after each letter denotes the sequential deployment at each site (e.g., **D1** to **D4** at SS-D). The POL mooring sites where the CTD profiles were taken are denoted R-B# where R refers to RAPID, B to the B line, and # to the different sites (B0 to B5 proceeding offshore).

Dates	Cruise	Chief Scientist	Mooring Work		CTD Stations	Other
			Recoveries	Deployments		
21-23 Oct <b>2004</b>	Hud 2004-055	E Head		<b>D1:</b> <i>M1548</i> <b>E1:</b> <i>M1547</i>	R-B0, -B2, -B4	
23-25 Oct, 1 Nov <b>2005</b>	Hud 2005-055	E Head	<b>D1:</b> <i>M1548</i> <b>E1:</b> <i>M1547</i>	<b>D2:</b> <i>M1585</i> <b>E2:</b> <i>M1586</i>	R-B0, -B1, -B2, -B3, -B4	
10-11 Oct <b>2006</b>	Hud 2006-052	E Head	<b>D2:</b> <i>M1585</i> <b>E2:</b> <i>M1586</i>	<b>D3:</b> <i>M1623</i> <b>E3:</b> <i>M1624</i>	R-B0, -B1, -B2, -B3, -B4; SS-D	
29 Sep – 7 Oct <b>2007</b>	Hud 2007-045	E Head	<b>D3:</b> <i>M1623</i> <b>E3:</b> <i>M1624</i>	<b>D4:</b> <i>M1666</i> <b>E4:</b> <i>M1667</i>	R-B0, -B1, -B2, -B3, -B4, -B5	
29 Sep- 6 Oct <b>2008</b>	Hud 2008-037	E Horne	<b>D4:</b> <i>M1666</i> ; <b>E4:</b> <i>M1667</i> R-B0, -B2, -B3, -B4, -B5	<b>RS1-RS6</b>	R-B0, -B1, -B2, -B3, -B4, -B5	R-B1 not recovered

## 2.4 Complementary Datasets

This section will provide examples of three types of physical oceanographic data which should be valuable in describing and interpreting the ocean variability apparent in the moored measurements.

### 2.4.1 CTD Sections from AZMP, AZOMP and Other

As discussed in the previous sections and indicated in Table 3, CTD profiles were taken along the HL on most of the cruises when the mooring deployments and recoveries were done, as part of AZMP. CTD/bottle surveys were done in spring and fall of each year, and also in late spring or summer of each year on the AZOMP cruise to the Labrador Sea. The latter surveys usually included profiles at the 2000-04 PERD mooring sites, providing improved spatial resolution of properties over the upper slope. Chemical variables such as Dissolved Oxygen (DO) and nutrients were measured on all of the surveys, as well as some biological variables related to phytoplankton and zooplankton (AZMP 2002, 2010).

Section displays of Potential Temperature ( $\theta$ ), Salinity (S) and Potential Density ( $\sigma_\theta$ ) over the shelf edge and upper slope from the AZOMP survey on Hud2002-032 on 24-25 June 2002 are shown in Figs. 12 and 13, for the upper 1000m and full depth, respectively. Water masses identified in the Gatién (1976) schematic (Fig. 8) are apparent in the upper ocean, such as the Warm Slope Water (WSW), in this case reaching the shelf edge.

Also apparent in Fig. 13 are the subpolar waters are the relatively-low salinity and relatively-high DO waters at depth over the middle slope, such as the Labrador Slope Water (LSW, Fig. 8) in the ~300-1200m depth range and the Labrador Sea Water (LSeaW) below associated with the DWBC.

Section displays of  $\theta$  and  $\sigma_\theta$  along Line B over the middle and lower Scotian Slope survey from the Hud2005-055 survey in October-November 2005 are shown in Fig. 14. The relatively-fresh subpolar waters at depth are again apparent, as well as the sloping isopycnals associated with the DWBC.

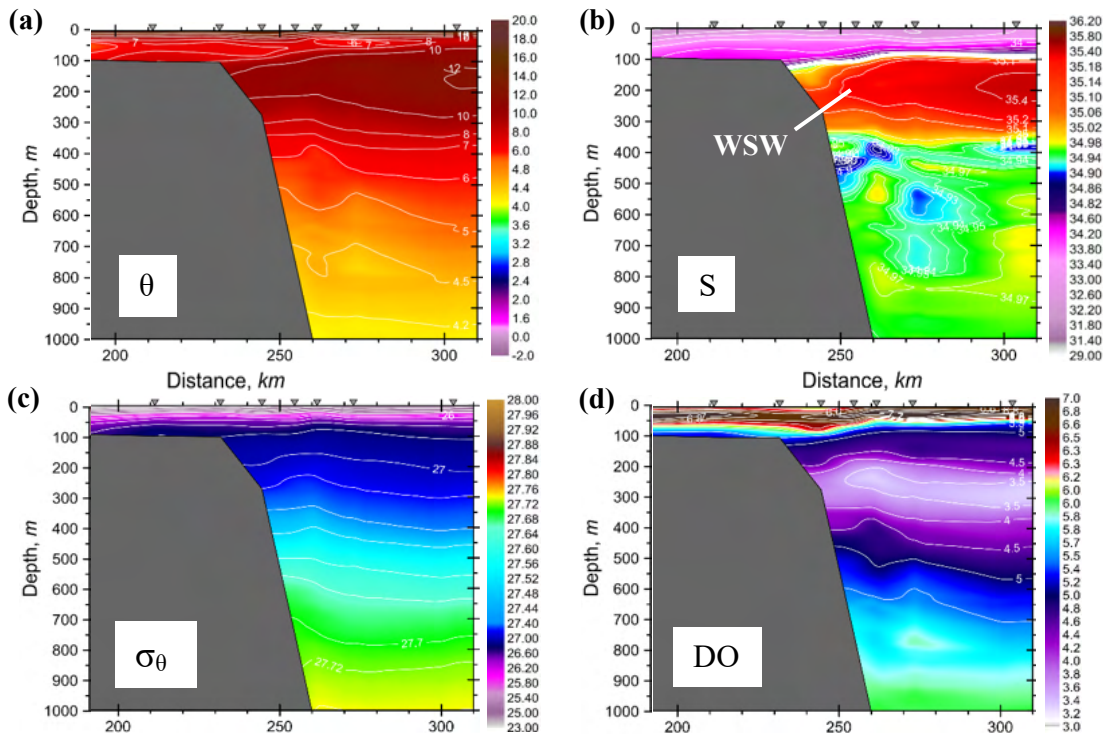


**Figure 12.** (a) Potential Temperature ( $\theta$ , °C), (b) Salinity (S), (c) Potential Density ( $\sigma_\theta$ ) and (d) Dissolved Oxygen (DO, mL/L) in the upper 1000m over the Scotian Shelf edge and Slope, from the Hud02-032 survey in June 2002.

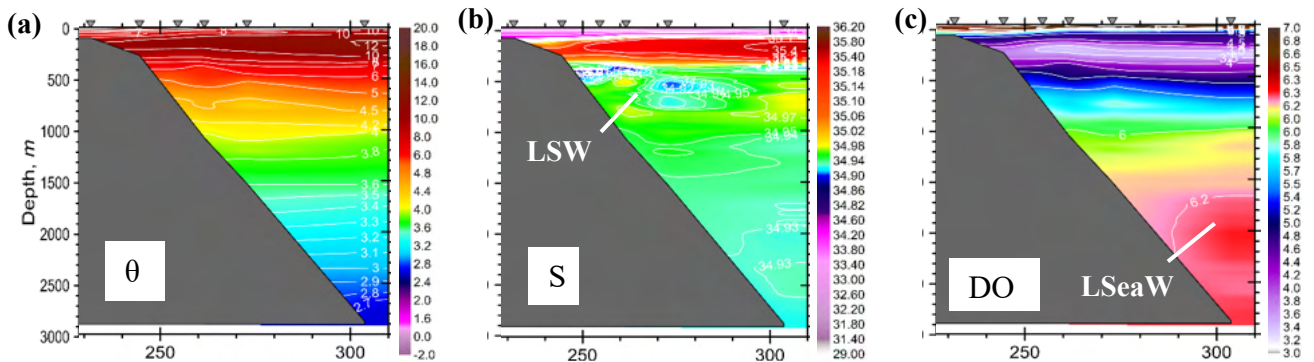


**Figure 13.** (a)  $\theta$  (°C), (b) S and (c) DO (mL/L) over the full water depth from the Hud02-032 survey in June 2002.

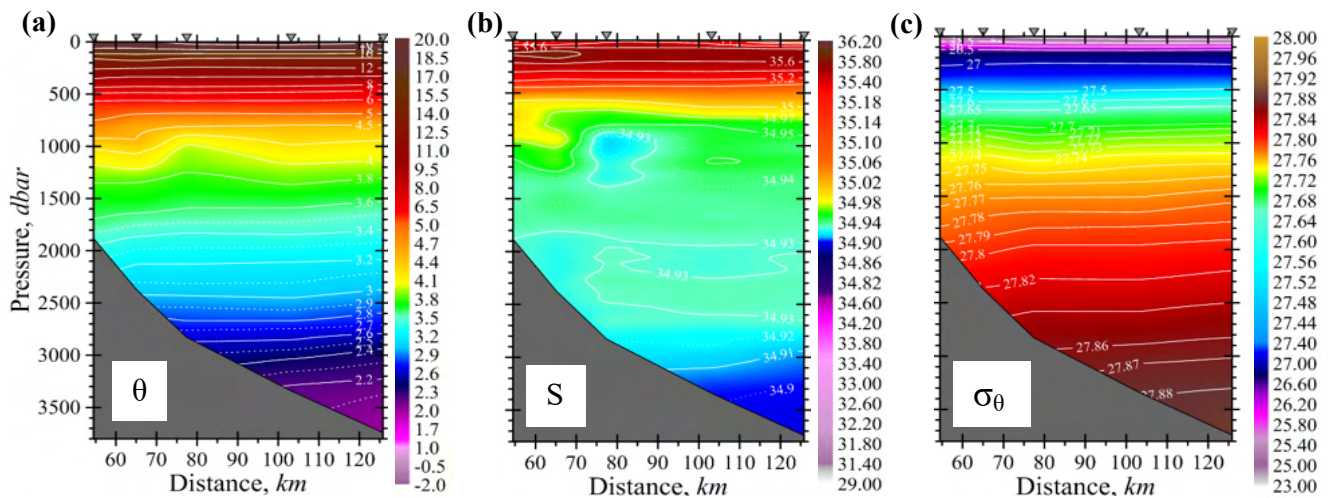


**Figure 14.** (a)  $\theta$  (°C), (b) S and (c)  $\sigma_\theta$  over the full water depth along Line B from the Hud05-055 survey in October-November 2005. The inverted triangles along the top of the section plots (here and in Figs. 12 and 13 indicate the locations of the CTD stations. (Plots in Figs. 12-14 courtesy of Inna Yashayaeva of BIO).

## 2.4.2 Sea Surface Temperature (SST) from Satellite Imagery

The value of satellite remote sensing in synoptic-scale sampling of the ocean is widely appreciated. Infrared imagery of SST is especially valuable for a complex frontal zone like the Slope Water region which has a large surface temperature contrast during most of the year. The monthly and semi-monthly SST composites from the BIO Remote Sensing Group available through AZMP, like those in Fig. 15, should be highly complementary to the moored and survey datasets in providing invaluable information on the location and structure of the GS and related frontal features. This was demonstrated by Loder

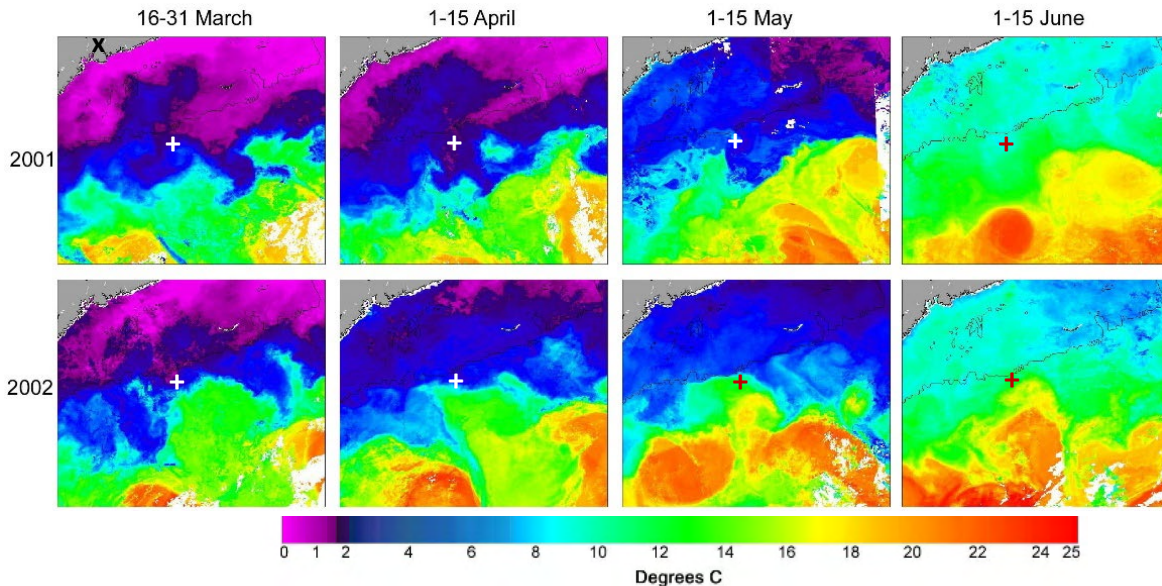


**Figure 15.** Composites of SST for four semi-monthly periods in the springs of 2001 and 2002 showing the complex structure of Gulf Stream meanders, rings and related features in the Scotian Shelf and Slope Water region. The location of Halifax is marked (x) in the upper left panel and the SS-A mooring site (+) in all panels.

and Geshelin (2009) who showed how the disruption of mean southwestward flow in the upper ~800m at the three PERD mooring sites in spring 2001 was associated with the incursion of the warm eddy feature apparent in Fig. 15 (note that it was not present in spring 2000). They also used the AZMP semi-monthly SST composites to show how a similar disruption in summer 2004 was related to another warm-eddy incursion (see their Fig. 9).

## 2.4.3 Sea Surface Elevation from Satellite Altimetry

In a series of papers and reports, Han (e.g., 2004, 2007) has computed estimates of the anomalies in sea surface elevation gradient across the Scotian Slope and then of the along-Slope (normal) component of surface velocity, from a combination of altimetry measurements from the TOPEX/Poseidon satellite at 10-day intervals, and the climatological seasonal-mean surface circulation from a diagnostic numerical model (Han et al., 1997). (The marine geoid and the mean oceanic topography were removed in the computation procedure.) The estimates were computed for four cross-Slope altimetry tracks on the central and western Scotian Slope, including a track (#050) ~100 km to the west of the HL and another (#089) ~150 km to its east (where the RAPID Line B was established). The time series was started in 1992 and continued through the 2000-04 and 2004-08 moored measurement programs.

Examples of the time series of along-slope current for two portions of Track #050, specifically between the 200- and 1000-m isobaths and the 1000- and 2000-m isobaths are shown in Fig. 16. The flow is generally westward across the 200-1000m portion but varies both seasonally and at higher-frequencies across both portions, as well as interannually (Han 2007). The high-frequency component indicates

complexity in the frontal zone, but its detailed variability and relation to the hierarchy of spatial structure apparent in SST (e.g., Figs. 6 and 15) need further examination (also in relation to the moored current and hydrographic measurements). Han (2004) has shown how the circulation in warm-core GS rings in earlier periods can be estimated from this altimetry data.

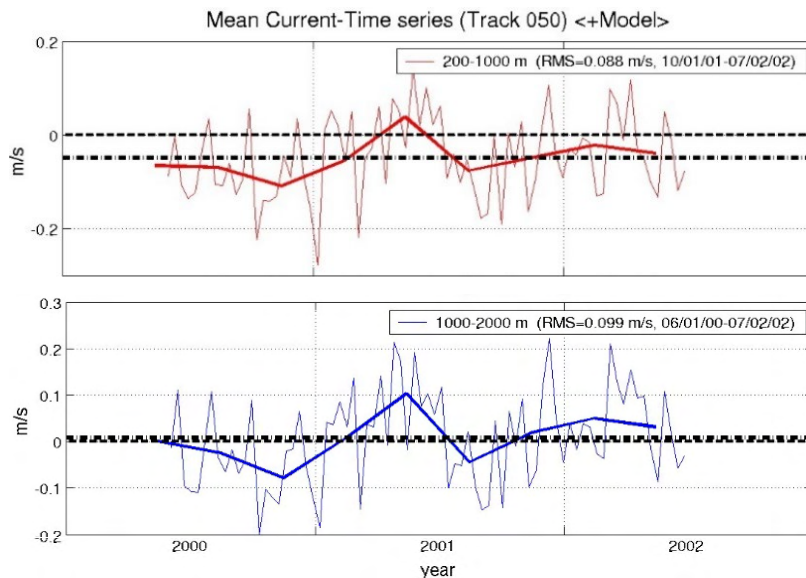


**Figure 16.** Time series of the along-slope surface current between (a) the **200- and 1000-m** isobaths, and (b) the **1000- and 2000-m isobaths** on Track 050 of the TOPEX/POSEIDON altimetry satellite to the west of the HL. Positive values indicate eastward flow. The faint lines are estimates from individual satellite passes at 10-day intervals, and the thick lines the seasonal means. Each individual-pass estimate comprises a high-frequency geostrophic variability component based on the surface elevation anomaly along the track, and a seasonal-mean component taken from circulation solutions of Han et al. (1997). The methodology and estimated current variability during 1992-2002 on four altimetry tracks across the Scotian Slope are described in Han (2007). (Courtesy of Dr. Guoqi Han, formerly of DFO Northwest Atlantic Fisheries Centre (NAFC))

### 3. Instrumentation, Data Return, Quality Control and Data Features

Before discussing individual instruments and records, we note that various sources of information on water and instrument depths were considered in developing best estimates for particular moorings and their instruments. These estimates are used in the final archived datafiles which also have notes on the quality issues discussed in this section.

#### 3.1 Aanderaa Current Meters

##### 3.1.1 Overall Summary

Following their traditional use at BIO, RCMs were the primary measurement device over the water column in the 2000-2004 program, positioned below upward-looking ADCPs (where available) for the near-surface zone. RCM8s with mechanical rotors were available from the BIO inventory at the time of this program, so were primarily used (Table 5). A total of 75 RCM8s were deployed at the 3 mooring sites during the 4-year program: 30 at site SS-A, 26 at SS-B and 19 at SS-C. One of the newer acoustic RCM11 meters (Drozdowski and Greenan 2013) was used at SS-B5 in an RCM8 vs RCM11 comparison experiment. The sampling interval was set at 60 minutes in all cases, except in SS-A1 and SS-A2 where it was 30 min in most cases, and 2 or 5 min in 3 cases at SS-A1 (for internal wave sampling).

All of the (76) RCMs were successfully recovered (Table 5), although one did not return any good currents data. Ten other RCMs had shortened good records because either their memory was full (3) because of the high-frequency sampling or they were no longer in their deployed position (7) after the two

moorings were struck (they were either adrift, or dangling near the seafloor). About a third of the RCMs had conductivity (C) sensors so that salinity (S) could be computed (most of these were at SS-A and SS-C), and about a fifth had pressure (P) sensors (although the reliability of the C and P measurements needed to be checked, which has been done).

Two particular data quality issues needed careful attention for the RCM8s, which slowed down the data processing. These issues will be summarized below and discussed in more detail in the next subsection in relation to data displays (Figs. 17-24) and the comments in Table 5.

The most significant data quality issue was the stalling of the RCM8's paddle-wheel rotors due to some combination of relatively-weak currents at times (especially at SS-A and SS-B), mechanical interference by organisms or objects, and possibly inadequately-mounted rotors. In most cases, the apparent or possible problems occurred during weak currents (as evidenced by other current meters on the mooring), such that it was not a significant issue from the perspective of the oil and gas industry's primary interest in the occurrence of strong current events (especially considering proximity to GS rings, but also in view of documented internal wave generation at the shelf edge; Sandstrom and Elliott 1984). The occurrences of rotor stalling can be grouped into two categories:

- i. Apparent mechanical interference for periods of hours or longer when currents were not weak (i.e., above 0.1 cm/s) in which case Rate (R) was set to a NoData value. In a few cases, there were no good R data after this occurred (e.g., Fig. 20a at 1595m); in others, it appeared that the interference disappeared, leaving good data (e.g., Fig. 18a at 791m); and
- ii. Much more commonly, especially at depth at SS-A and SS-B (e.g., Figs. 17a, 18a and 20a), there were successive cycles with zero rotor counts (during the 2-60 min sampling interval) when other instruments on the mooring indicated relatively weak (< 0.1 m/s) currents. In a few cases when the R value of 0.011 m/s (as per the rotor counts to R calibration relation) occurred for periods of a day or so, and there was an indication that currents may no longer have been very weak (<0.05 m/s), R was set to NoData (e.g., Fig. 20a at 795m and 1080m). In most cases, the R values of 0.011 m/s were not edited. This means that the measured Rates for some of these cycles may be low, resulting in underestimation of current magnitude in very weak currents. It had been previously recognized that RCM8 rotors often require a threshold speed of a few cm/s to start spinning, so this stalling during weak currents was not necessarily unusual; however, some mounting and alignment issues were identified in later RCM8 deployments in Flemish Pass and Orphan Basin (Loder et al., 2025b,c), so a contribution from the RCM8 preparation cannot be ruled out completely (but is considered unlikely).

As a result of the concerns about rotor stalling of the RCM8s and for input to decisions on new point-source current meters that were being acquired by BIO, several comparison experiments were carried out by BIO in the early 2000s with different current meters deployed in close proximity (e.g., Drozdowski et al., 2010; Drozdowski and Greenan 2012, 2013). One of these was on M1479 in SS-B5 which included an RCM8 at 791m and an RCM11 at 792m (Table 5b). It provided useful data confirming that RCM8 rotor stalling during very weak currents did not imply that the rotor spinning was being impeded at higher speeds (including weak currents of only 0.1 m/s or so), neither before nor after the stalling.

Another was the later deployment of a special mooring (M1647) at site SS-B during April to December 2007, referred to as SS-B6 in Tables 2a and 5b. In this case, an RCM8, an RCM11 and an Aanderaa SeaGuard were deployed at about 100 mab, at vertical intervals of 3m. Unfortunately, the main buoyancy on this mooring imploded during deployment, such that the 3 current meters lay on or near the seafloor and hence did not provide any good currents data upon recovery.

**Table 5a. SS-A.** Listing of RCM8s during the 2000-04 Scotian Slope program, organized by site and deployment # (D #). The other columns are the BIO mooring #, RCM8 serial number (Ser #), record start & end dates in the format Day/Month/(Year-2000), water & RCM depths, variables sampled, the sampling interval, and comments re-Salinity (S) reliability, rotor stalling and other issues. (continued on next page)

Ste	D #	BIO #	Ser #	Start Date	End Date	Depths (m)		Variables	Smpl-ing Intvl: min	Comments: $\Delta S$ =Salinity offset; hi="high by"; Ocs brf rtr still = occasional brief rotor stall duration; R NDt=R set to NoData; LnIntrp=LinearInterpolation
						Water	RCM			
SS-A	1	1352	4349	13/06/00	21/11/00	1119	74	RDTCP	30	$\Delta S < 0.1$
		1352	5578	13/06/00	10/08/00	1119	89	RDTC	2	$\Delta S < 0.1$ ; memory full by mid Aug
		1352	5567	13/06/00	21/11/00	1119	144	RDTCP	30	$\Delta S < 0.1$
		1352	5002	13/06/00	10/08/00	1119	219	RDTC	2	$\Delta S < 0.1$ ; memory full by mid Aug
		1352	7131	13/06/00	21/11/00	1119	294	RDTCP	30	S hi 0.2-0.3
		1352	1607	13/06/00	21/11/00	1119	569	RDTC	30	$\Delta S < 0.1$
		1352	4603	13/06/00	21/11/00	1119	819	RDT	30	
		1352	5574	13/06/00	08/11/00	1119	1096	RDT	5	Memory full by mid Nov
	2	1377	7013	21/11/00	31/05/01	1124	149	RDTCP	30	$\Delta S < 0.1$
		1377	4208	21/11/00	31/05/01	1124	299	RDTC	30	$\Delta S < 0.1$
		1377	7134	21/11/00	31/05/01	1124	574	RDT	30	R NDt 34dy rtr intfr
		1377	7127	21/11/00	31/05/01	1124	824	RDT	30	
		1377	6405	21/11/00	31/05/01	1124	1100	RDT	30	
	3	1387	2663	31/05/01	25/09/01	1195	360	RDT	60	Mooring struck
		1387	3299	31/05/01	25/09/01	1195	635	RDT	60	Ocs rtr stlls <7hr; Mrg struck
		1387	3306	31/05/01	25/09/01	1195	885	RDT	60	No good R,D; Setup issue
		1387	4406	31/05/01	25/09/01	1195	1170	RDT	60	Ocs rtr stlls <1dy; Mrg struck
	4	1419	8697	21/10/01	24/06/02	1140	305	RDTC	60	$\Delta S$ hi 0.2-0.3?
		1419	8695	21/10/01	24/06/02	1140	580	RDT	60	Ocs brf rtr stlls
		1419	7127	21/10/01	24/06/02	1140	830	RDT	60	Ocs brf rtr stlls; No R aft 13Nov
		1419	6405	21/10/01	24/06/02	1140	1115	RDT	60	Ocs brf rtr stlls; No R aft 27Nov
	5	1432	5359	25/06/02	22/05/03	1144	159	RDTP	60	Ocs rtr stlls <3hr
		1432	1607	25/06/02	22/05/03	1144	309	RDTC	60	Ocs rtr stlls <3hr; S hi 0.2
		1432	6410	25/06/02	22/05/03	1144	584	RDT	60	Ocs rtr stlls <8hr
		1432	7013	25/06/02	22/05/03	1144	834	RDT	60	R NDt 16dy rtr intfr; other ocs rtr stlls <10hr
		1432	9328	25/06/02	22/05/03	1144	1119	RDT	60	Ocs rtr stlls <16hr
	6	1478	9607	22/05/03	07/04/04	1125	268	RDTCP	60	LnIntrp R 31hr; S hi 0.06-0.16
		1478	4600	22/05/03	07/04/04	1125	565	RDT	60	Ocs rtr stlls <8hr
		1478	4602	22/05/03	07/04/04	1125	815	RDT	60	Ocs rtr stlls <9hr
		1478	4603	22/05/03	07/04/04	1125	1100	RDT	60	Ocs rtr stlls <32hr

**Table 5b. SS-B.** Listing of RCMs during the 2000-04 Scotian Slope program, organized by site and deployment # (D #). The other columns are the BIO mooring #, RCM serial number, record start and end dates in the format Day/Month/(Year-2000), water and RCM depths, variables sampled, the sampling interval, and comments. All RCMs are RCM8s except RCM11 #0225\* in D5. *(continued on next page)*

Ste	D #	BIO #	RCM Ser #	Start Date	End Date	Depths (m)		Variables	Smpl Intl: min	Comments: See Table 5a for explanation of abbreviations
						Water	RCM			
SS-B	1	1388	4600	01/06/01	20/10/01	1991	541	RDT	60	
		1388	4998	01/06/01	20/10/01	1991	791	RDT	60	R NDt 70dy rtr intfr; ocs other stlls <7hr
		1388	5002	01/06/01	20/10/01	1991	1076	RDT	60	Ocs rtr stlls <6hr
		1388	5575	01/06/01	20/10/01	1991	1591	RDT	60	Ocs rtr stlls <15hr
		1388	5578	01/06/01	20/10/01	1991	1967	RDT	60	Ocs rtr stlls <19hr
	2	1412	4600	21/10/01	24/06/02	1995	545	RDT	60	Ocs rtr stll <10hr
		1412	4998	21/10/01	24/06/02	1995	795	RDT	60	R NDt 49hr; Other ocs rtr stlls <19hr
		1412	5002	21/10/01	24/06/02	1995	1080	RDT	60	R NDt 90hr; Other ocs rtr stlls <19hr
		1412	5575	21/10/01	24/06/02	1995	1595	RDT	60	R NDt 11dy at end; Other ocs rtr stlls <14hr
		1412	5578	21/10/01	24/06/02	1995	1971	RDT	60	Ocs rtr stlls <22hr
	3	1429	2663	25/06/02	20/10/02	2015	565	RDT	60	
		1429	3306	25/06/02	20/10/02	2015	815	RDT	60	Ocs rtr stlls <19hr
		1429	3584	25/06/02	20/10/02	2015	1100	RDT	60	R NDt 40hr, 13dy, 59dy; Other ocs rtr stlls <14hr
		1429	4406	25/06/02	20/10/02	2015	1616	RDT	60	Ocs rtr stlls <14hr
		1429	4603	25/06/02	20/10/02	2015	1990	RDT	60	Ocs rtr stlls <26hr
	4	1454	2664	20/10/02	14/04/03	2101	651	RDTC	60	Ocs rtr stlls <14hr; S hi 0.1-0.25
		1454	4998	20/10/02	14/04/03	2101	901	RDT	60	R NDt 37dy; Other ocs rtr stlls <21hr
		1454	5574	20/10/02	14/04/03	2101	1186	RDT	60	Ocs rtr stlls <10hr
		1454	5575	20/10/02	14/04/03	2101	1702	RDT	60	Ocs rtr stlls <10hr
		1454	5578	20/10/02	14/04/03	2101	2077	RDT	60	Ocs rtr stlls <27hr
5	1479	7525	23/05/03	08/04/04	1991	248	RDTCP	60	Ocs rtr stlls <hr; S hi 0.07-0.19	
	1479	0217	23/05/03	08/04/04	1991	541	RDT	60	Ocs rtr stlls <8hr	
	1479	0225*	23/05/03	08/04/04	1991	791	RDTP	60		
	1479	1039	23/05/03	08/04/04	1991	792	RDT	60	Ocs rtr stlls <18hr	
	1479	1951	23/05/03	08/04/04	1991	1076	RDT	60		
	1479	3299	23/05/03	08/04/04	1991	1592	RDT	60	Ocs rtr stlls <10hr.	
	1479	4195	23/05/03	08/04/04	1991	1967	RDT	60	Ocs rtr stlls <19hr	
6	1647	4208	29/04/07	9/12/07	1979	1874	RDT	30	No good velocity data from RCMs which lay on/near seafloor after buoyancy float imploded upon deployment. Possibly good T data but not archived.	
	1647	0265*	29/04/07	9/12/07	1979	1877	RDT	30		
	1647	0019†	29/04/07	9/12/07	1979	1880	RDT	30		

**Table 5c. SS-C, SS-D, SS-E.** Listing of RCMs during the 2000-04 Scotian Slope and 2004-08 Scotian Rise programs, organized by site and deployment # (D #). The other columns are the BIO mooring #, RCM serial number, record start and end dates in the format Day/Month/(Year-2000), water and RCM depths, variables sampled, the sampling interval, and comments. All RCMs at SS-C are RCM8s. Some RCMs at SS-D and SS-E are RCM11s (indicated by \*).

Ste	D #	BIO #	RCM Ser #	Start Date	End Date	Depths (m)		Variables	Smpl Intl: (min)	Comments: See Table 5a for explanation of abbreviations
						Water	RCM			
SS-C	1	1414	7122	19/10/01	22/05/02	302	127	RDTCP	60	$\Delta S < 0.05$
		1414	5573	19/10/01	22/05/02	302	202	RDTCP	60	Ocs rtr stlls; $\Delta S < 0.1$
		1414	4208	19/10/01	22/05/02	302	277	RDTCP	60	Ocs rtr stlls; S hi 0.1
		1414	6409	19/10/01	22/05/02	302	292	RDT	60	Ocs rtr stlls
		1413	7134	19/10/01	22/05/02	317	314	RDT	60	Ocs rtr stlls
	2	1430	7131	22/05/02	22/05/03	314	312	RDTCP	60	Ocs rtr stlls; $\Delta S < 0.2$ to Jan'03; S NDt after
		1431	6403	22/05/02	19/10/02	305	130	RDTC	60	$\Delta S < 0.1$
		1431	2664	22/05/02	19/10/02	305	205	RDTC	60	R NDt 21 dy rtr stll; S hi 0.1-0.3
		1431	4195	22/05/02	19/10/02	305	280	RDTC	60	Ocs rtr stlls; S hi 0.1-0.3
		1431	6411	22/05/02	19/10/02	305	295	RDTC	60	Ocs rtr stlls; S hi 0.1
	3	1455	5032	19/10/02	24/12/02	305	130	RDTC	60	Mooring struck: S adjusted by -0.7; $\Delta S < 0.3$
		1455	4600	19/10/02	24/12/02	305	205	RDT	60	Mooring struck
		1455	5002	19/10/02	24/12/02	305	280	RDT	60	Mooring struck
		1455	5572	19/10/02	24/12/02	305	295	RDTC	60	Mooring struck; S hi 0.25
	4	1480	4342	22/05/03	07/04/04	340	330	RDTCP	60	P NDt; S drift to hi 0.3
		1480	4349	22/05/03	07/04/04	340	337	RDTCP	60	Ocs rtr stlls <9hr; $\Delta S < 0.05$ to Feb; drift to hi 0.3
		1491	5359	14/07/03	07/04/04	295	65	RDTCP	60	S hi 0.14-0.18
		1491	1607	14/07/03	07/04/04	295	120	RDTC	60	$\Delta S < 0.1$
		1491	2664	14/07/03	07/04/04	295	270	RDTC	60	Ocs rtr stlls; $\Delta S < 0.1$
	SS-D	1	1547	0397*	22/10/04	01/11/05	2452	2402	RDT	60
2		1585	0265*	23/10/05	10/10/06	2419	2369	RDT	60	
3		1623	0376*	10/10/06	07/10/07	2425	2375	RDT	60	
4		1666	0453*	07/10/07	01/10/08	2438	2388	RDTP	60	P unreliable
SS-E	1	1548	3300	22/10/04	23/10/05	3418	3368	RDT	60	R,D NDt 83hr Nov & after 6Dec; other occs rtr stlls
	2	1586	4208	23/10/05	20/10/06	3414	3364	RDT	60	R NDt 73&109hr Dec rtr stlls; other occs rtr stlls <19hr
	3	1624	6411	11/10/06	07/10/07	3395	3345	RDTC	60	R counter & C sensor failed
	4	1667	456*	07/10/07	01/10/08	3414	3364	RDTP	60	P unreliable

By the time of the 2004-08 PERD moored measurement program on Line B (Tables 4 and 5b), it was recognized that current meters other than RCM8s were desirable for moored measurements at depth over the middle and lower Scotian Slope. Consequently, acoustic RCM11s were used in the 4 year-long deployments at 50 mab at site SS-D, all returning good R, D and T datasets. However, RCM11s were still in limited supply at BIO, such that RCM8s were used in the first 3 deployments at the lower-priority site SS-E until an RCM11 was available for the 4<sup>th</sup> deployment. As a result there was a limited return of good R data from deployments SS-E1, -E2 and -E3.

In the 2000-04 program, Salinity (S) was computed from Conductivity, and measured (when apparently reliable) or specified Pressure (P), on a total of 26 RCM8s. In a few cases, there was an obvious problem with the computed S, such as a drift or temporary offset (e.g., due to a deposit or growth, or an object or organism in the C cell), in which case S was set to NoData (see Comments in Table 5).

Comparisons were made between the T and S values from the RCM8s, and those from the same depth in nearby CTD profiles (typically 1-4 km away). The T comparisons provided an indication of whether there were significant horizontal water mass property gradients in the area of each RCM8, and the S comparisons were used to indicate the approximate reliability of the S values from the RCM8s (**Table 5**). In most cases, S from the RCMs appears to have been reliable within 0.1. However, in a few cases, S appears to have been too high or low by 0.1-0.3; in one case (SS-C3), S appears to have been systematically high by 0.7 such that a negative offset was applied. Considering the locations of SS-A and SS-C in the shelf-slope frontal zone, the archived S data should be useful for describing and understanding oceanographic variability during the study period and more generally.

### 3.1.2 Example RCM Data Displays

Examples of the time series from the RCM8s at site SS-A are shown in Fig. 17 for deployment SS-A1. Considerable vertical coherence in the variability in R and Direction (D) at high- and mid- (periods of weeks) frequencies is apparent (Fig. 17a,b). Speeds were less than 0.2 m/s most of the time at 285m and deeper, and less than 0.3 m/s most of the time at the shallower depths, but periods with R less than 0.1 m/s and occasions of rotor stalls (probably speed < 0.05 m/s) occurred at all depths. There are also many similarities as well as some differences in the flow directions with depth. These qualitative features and also the primary quantitative current features should not be affected by the rotor issues discussed above.

Further features of the currents variability at SS-A1 can be seen in the eastward (U) and northward (V) flow components in Fig. 17c,d. The weak westward (-U) mean flow at all depths is barely apparent in the presence of the variability on various time scales. Of particular note, the two strongest flow events in the upper 300m, in early July and early November, are associated with persistent westward-to-northwestward flow over periods of a week or two.

The T and S time series from the RCMs at SS-A1 are shown in Figs. 17e and 17f, respectively. The range of T variability during the 5-month June-November period varied from about 6C° at 74-144 m RCMs, to 4C° at the 219-294 m RCMs, to less than 1C° at the 519-1096 m ones. The range of S variability varied from ~2 at 74m to ~1 at 144-219 m, to ~0.2 at 569m.

There were notable periods of warmer and saltier water, by >4C° and >1 (S unit) respectively, in the upper ~200m for about 6 weeks in July-August, possibly associated with northwestward flow. There were shorter periods (~1 week) of warmer and saltier water at 74 and 144m in late August and early October, again with unclear origin without further investigation. At greater depths (569-1096 m), there were some similarities in the mid-frequency T variability but also a lot of differences. There was an abrupt drop in both T and S for about a day around 19 July at depths between 74 and 194 m, but most pronounced at 144m, followed by an abrupt recovery, without an obvious strong velocity signal. There was enhanced high-frequency variability in both T and S at both 219 and 294 m, probably of tidal origin. However,

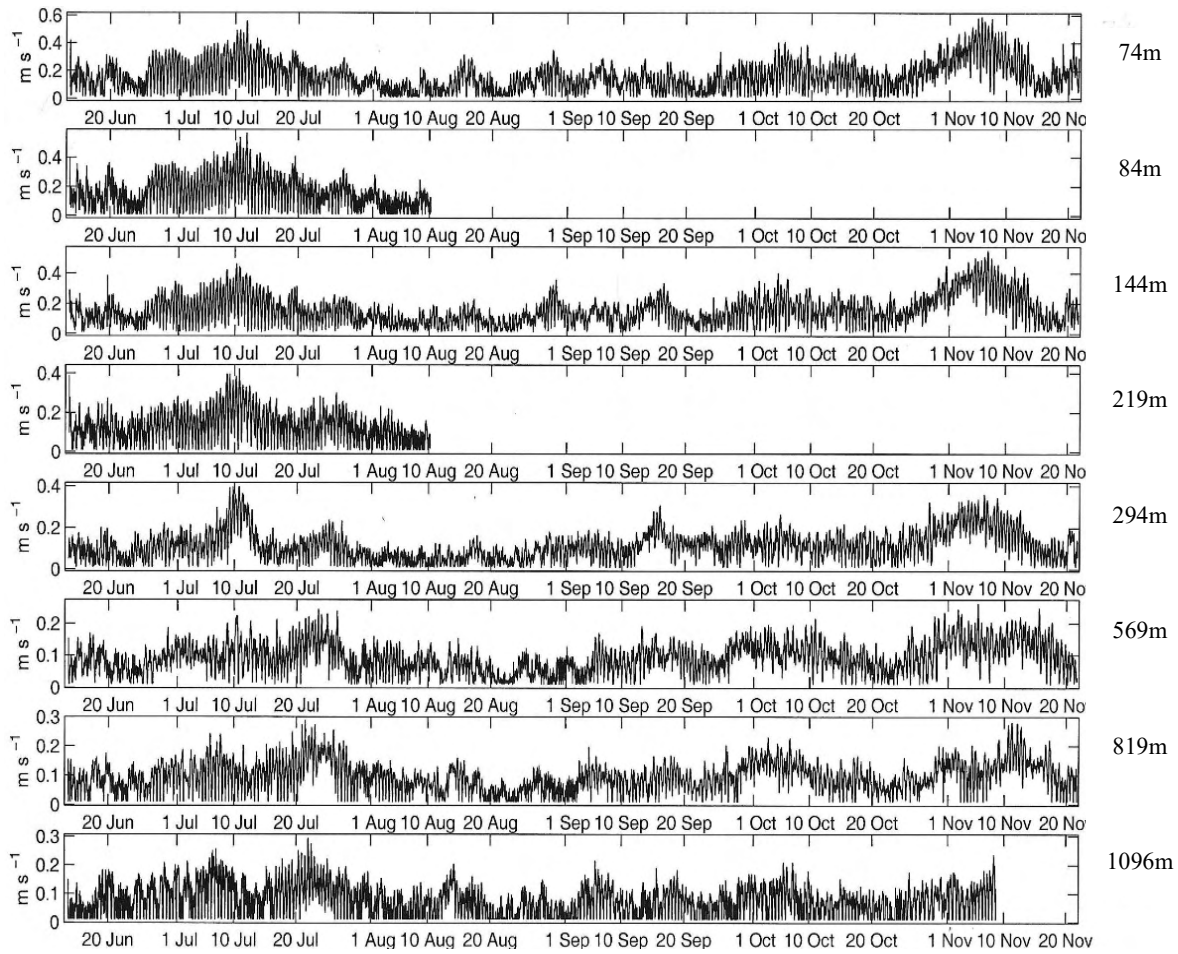


**Figure 17a.** Time series of Rate ( $R$ , m/s) from the 8 RCMs on M1352 at SS-A1 during Jun-November 2000. Note the occurrence of  $R=0.011$  m/s values, especially at the deeper levels during periods of weak currents at all depths. In the cases of the RCMs at 84, 219 and 1096 m, the memory was full before the mooring was recovered due to the specified high-frequency sampling. Note the different scales on the  $R$  axis and the nominal depths.

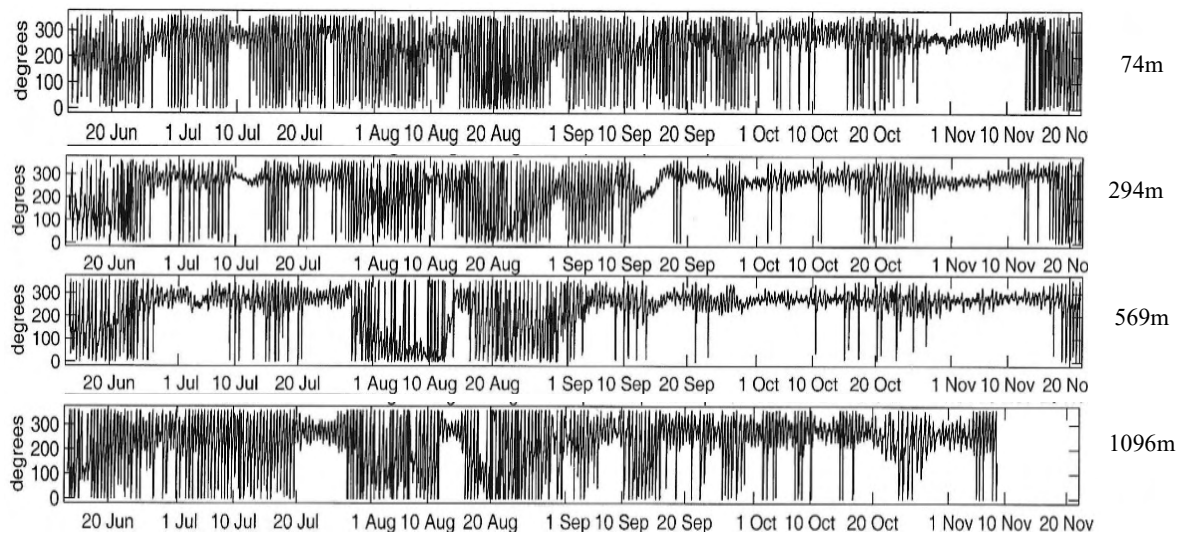


**Figure 17b.** Time series of velocity Direction ( $D$ , ° clockwise from True North) from 4 of the RCMs on M1352 at SS-A1 during June-November 2000 which reflect the differences with depth. Note that the most common flow direction at all depths is roughly westward (especially at 285m and deeper), but there are also periods of a week or longer at all depths when the flow direction fluctuates regularly.

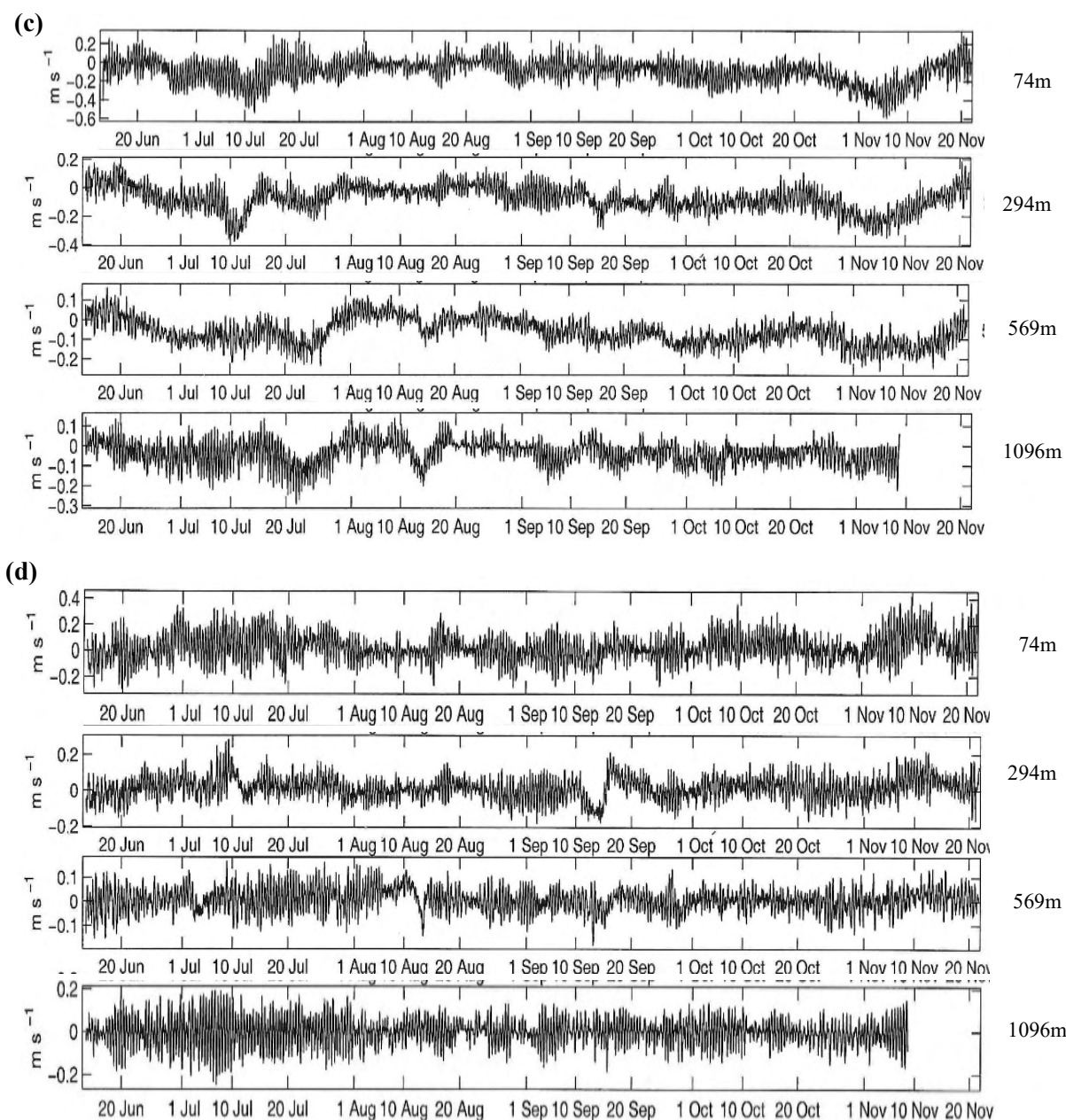


**Figure 17c,d.** Time series of the **(c)** eastward ( $U$ ) and **(d)** northward ( $V$ ) components of velocity from the same 4 of the RCMs on M1352 at SS-A1 as in Fig 17b. Note the different velocity scales in each panel.

more detailed investigation, especially considering the MC time series and AZMP datasets discussed earlier, is needed to interpret the variability on the multiple time scales apparent in this example from site SS-A.

A comparison of  $U$  and  $T$  from the upper 2 RCM8s (at 74 and 294 m) at SS-A1 in October-November 2000 when the westnorthwestward flow event discussed above (Fig. 17c,d) occurred, and the estimated geostrophic surface flow normal to the altimetry satellite tracks to the east and west of the mooring line (Han 2007) is shown in Fig. 18. There is a clear indication of a westward flow event on the same time scale in the RCM8 records, and of cooler water at the 274m RCM, but further investigation is needed.

The progressive vector diagrams for the 5 primary RCMs in SS-A1 are shown in Fig. 19, indicating primarily westward low-frequency flow during the deployment, with northwestward veering near the end.

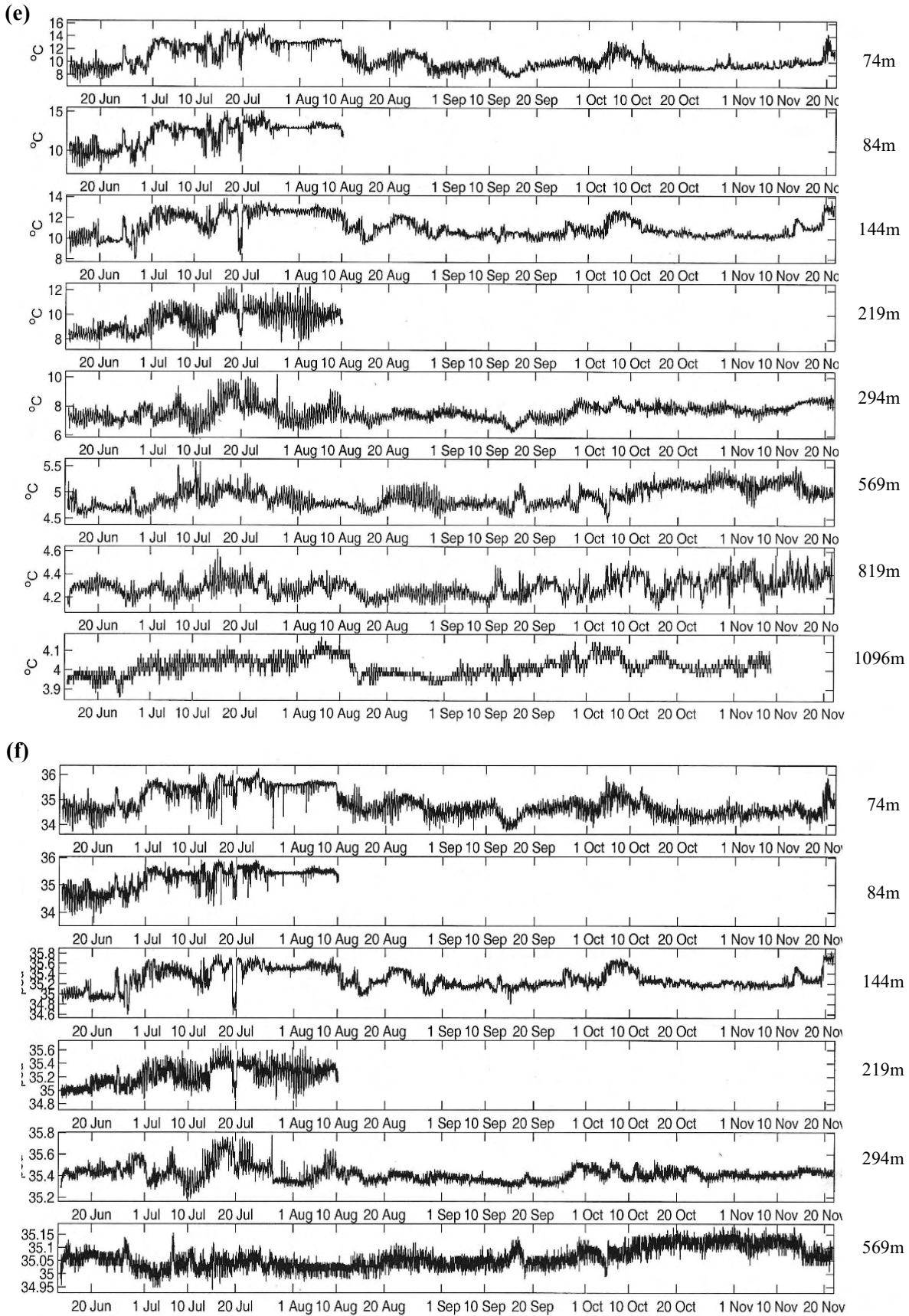


**Figure 17e,f.** Time series of (e) Temperature (T) from all 8 of the RCM8s at SS-A1, and (f) Salinity (S) from the upper 6 ones. Note the different T and S scales in each panel, the similarities in each of the T and S variabilities in the upper 4 RCMs, and the greater variability in the temporal structure among each at the deeper levels.

**Figure 18.** Time series of U and T from the upper two RCM8s (at 74 and 294 mbs, respectively) on M1352 at SS-A1 in October-November 2000 (upper 4 panels), and of the approximate eastward component of velocity (i.e., normal to the satellite track) on the nearest TOPEX/Poseidon altimetry tracks to the east and west of the mooring line (lower panels). (Courtesy of Dr. Guoqi Han of DFO NAFC).

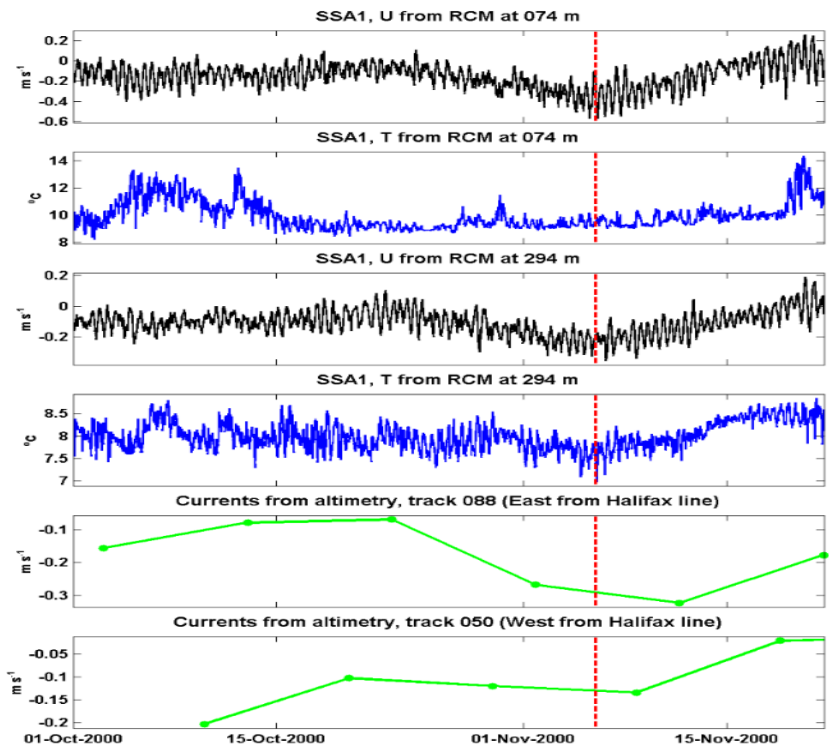
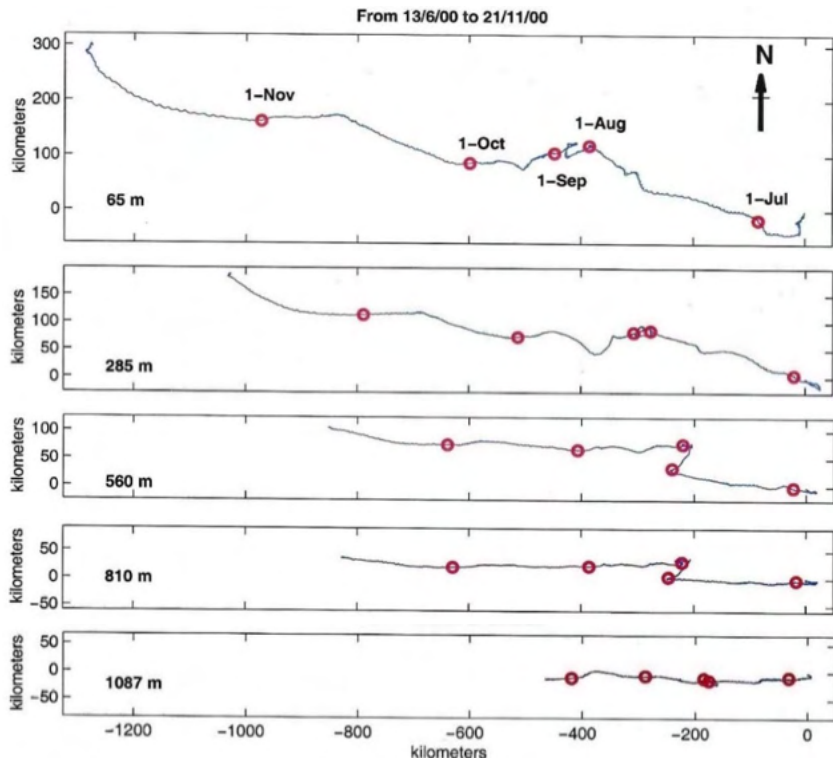


**Figure 19.** Progressive vector diagrams (PVDs) for velocity from the 5 RCM8s with full record lengths on M1352 at SS-A1 during June-November 2000. The circles are at 1-month intervals.



Moving to example displays of RCM8 data from site SS-B, time series of R and T from the 5 RCM8s at 541m and deeper during SS-B1 from early June to late October 2001 are shown in Fig. 20, and progressive vector diagrams (PVDs) for the velocity time series in Fig. 21. Note the occurrence of periods (Fig. 20a) with stronger currents of about a week duration at all depths in early June, early July, and early and mid September, and a period with stronger currents in mid October at 541-1076 m preceded by stronger currents at the two deeper levels starting about a week earlier. Also, the weak currents at all depths starting in mid-late June and early-mid August. The peak currents at all depths were  $\sim 0.25$  m/s.

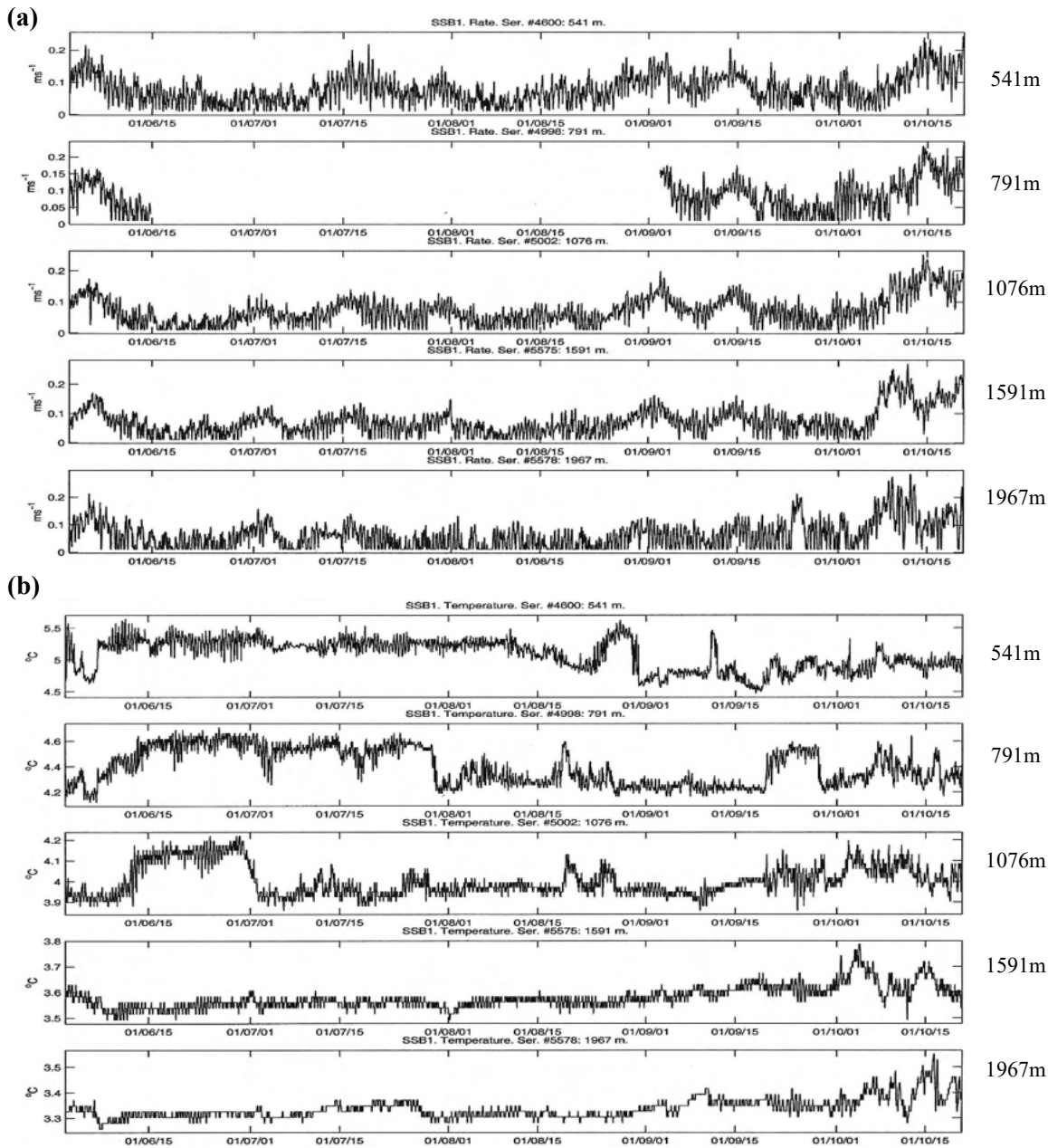
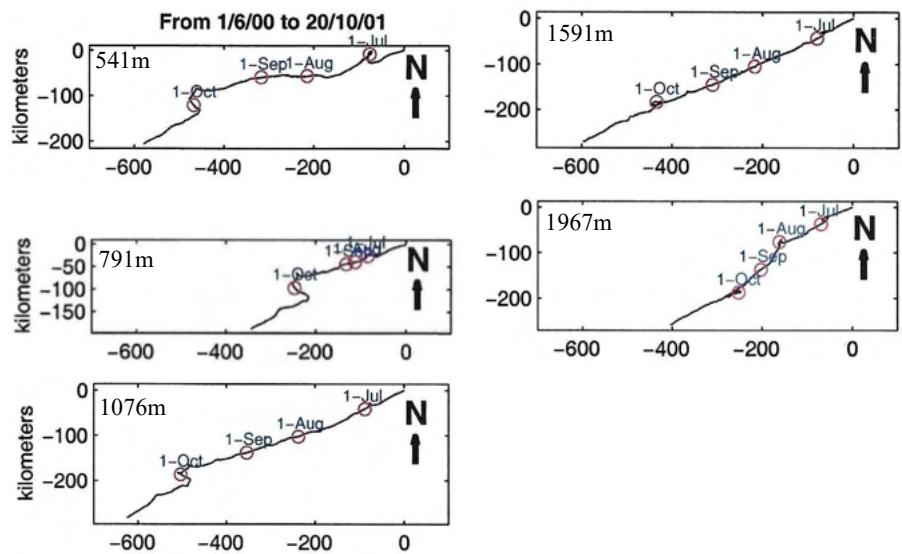


**Figure 20.** Time series of (a) R (m/s) and (b) T ( $^{\circ}$ C) from the 5 RCM8s on M1388 deployed at SS-B1 from May to October 2001. Note the different R and T scales in each panel. In (a), note the 2.5-month period when R at 791m was set to NoData (due to a prolonged rotor stall), starting at a time with weak currents at all the depths; persistent plausible R values were not recorded again by this RCM8 until the measured R at the adjacent RCM8s above and below were  $\sim 0.15$ m/s. Also, note the frequent occurrence of shorter stall periods at greater depths, with increasing frequency at the deepest instrument where the currents were weakest. In (b), note the decrease in the magnitude of the T variability with increased depth, and the different frequency structure of the variability at the different depths,  $\sim 250$ m and  $\sim 500$ m apart above and below 1076m.

There were major differences in the T variability at the different depths (Fig. 20b) except for 1591 and 1957 m, but also some similarities between other adjacent depths at times, e.g., between 541 and 791 m, and between 791 and 1076 m. The range of T variability was  $1^{\circ}$ C at 541m, and  $0.3$ - $0.5^{\circ}$ C at the deeper levels.

The SS-B1 PVDs (Fig. 21) indicate that this mooring period had relatively persistent west-southwestward low-frequency flow with variable magnitude, such as weakest overall at 791m and weaker at all depths in August-September, and a notable southeastward disruption in early October at 541, 991 and 1076m.

**Figure 21.** PVDs for hourly velocity from the 5 RCM8s on M1388 deployed at SS-B1 from May to October 2001. The positions, relative to the origin (0,0 km), at the start of each month are indicated.



Selected time series from the 5 RCM8s at 541 m and deeper at SS-B2 between October 2001 and June 2002 are shown in Fig. 22, and the PVDs for 3 of the RCMs in Fig. 23. Together with the examples from SS-B1 (Figs. 20 and 21), these datasets cover a full year. There were periods of persistent west-southwestward flow at all depths in late November (2 weeks) and February-March (6 weeks) involving the strongest currents (0.2-0.3 m/s) in the records at most depths. In contrast, there were also periods with relatively weak currents (speed <0.15 m/s) at all depths, e.g., for 2 weeks in December and for 2 months in April and May. On the other hand, there was a bottom-intensified flow reversal for ~2 weeks in March with peak speed near 0.15 m/s. There were also flow reversals, or periods with variable flow direction, for shorter durations, generally with weak currents.

Some rotor stalls (i.e.,  $R=0.11$  m/s) are apparent at all depths in the RCM8 Rate time series from SS-B1 (Fig. 20a) and SS-B2 (Fig. 22a), associated with the occurrence at times of weak currents in the sluggish areas of the Slope Water, especially at depth. At ~540m these were of limited duration (Table 5b), probably resulting in only very short-term (up to several hours) underestimation of current speed by a few cm/s which should have little impacts on overall record stats. At greater depths, they occurred more frequently. At ~790m, there was the multi-month period of rotor stall at SS-B1 discussed earlier, and also a period of ~2 days at SS-B2, in both cases where  $R$  was set to NoData.  $R$  was also set to NoData for a period of ~4 days at 1080m in SS-B2, and for ~11 days at the end of the record at 1595m at SS-B2 (Table 5b). Rotor stalls for periods of less than a day during weak currents occurred multiple times in all of the deeper RCM8 records from the 5 deployments at SS-B, such that the records during weak currents need to be used with caution. In the 2000-04 Scotian Slope study, a strategy was adopted to minimize the number of cycles in which  $R$  was set to NoData (e.g., for purposes needing continuous time series like PVDs), and many  $R$  values of 0.011 m/s were left in the time series when the actual speeds was a few cm/s higher. In later field studies in Orphan Basin where weak currents and RCM8 rotor stalling also occurred (Loder et al., 2025c),  $R$  was set to a default value of 0.03 or 0.05 m/s when there were more than some minimum number (e.g., 6 or 10) of consecutive cycles with stalls, in order to better represent the frequency of occurrence of speeds in the 0.02-0.06 m/s range, and have continuous time series.

There was greater similarity in the  $T$  variability at the different depths in SS-B2 (Fig. 20e) (than in SS-B1), especially among the 545, 795 and 1080 m RCMs, which showed slow warming during March-May (2002) after a warming and then cooling event in February, and then followed by slow cooling in June. The range of  $T$  variability was  $2C^\circ$  at 545m,  $1C^\circ$  at 795m, and  $0.3-0.5C^\circ$  at the deeper levels. The vertical variation was similar to that in SS-B1, except larger at 545m.

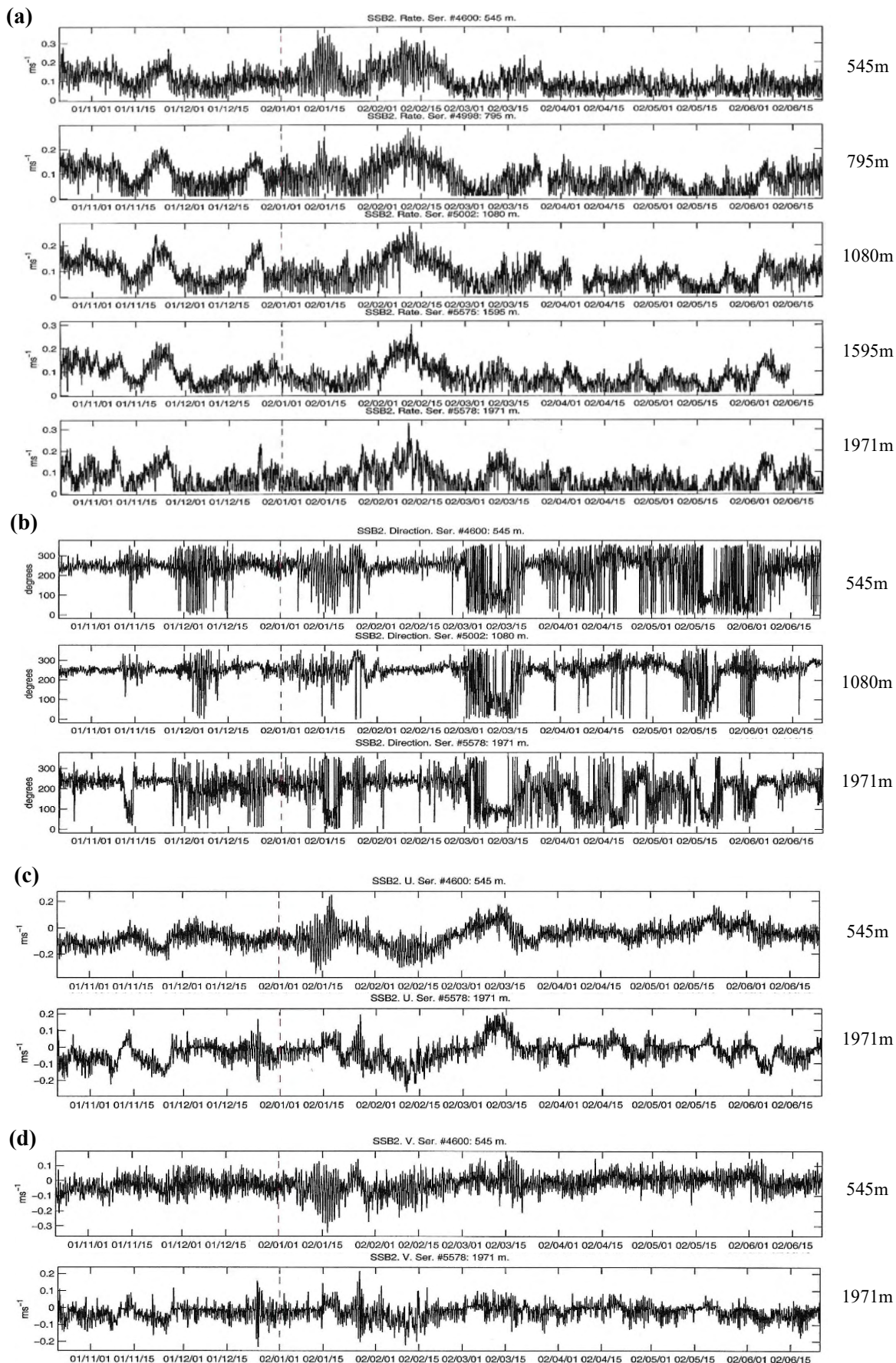


**Figure 22.** Time series of (a)  $R$  (m/s) from the 5 RCM8s on M1412 at SS-B2 from October 2001 to June 2002, (b)  $D$  ( $^{\circ}$ T) from 3 of the RCMs, and (c)  $U$  and (d)  $V$  from 2 of them. Note the different scales in some panels.

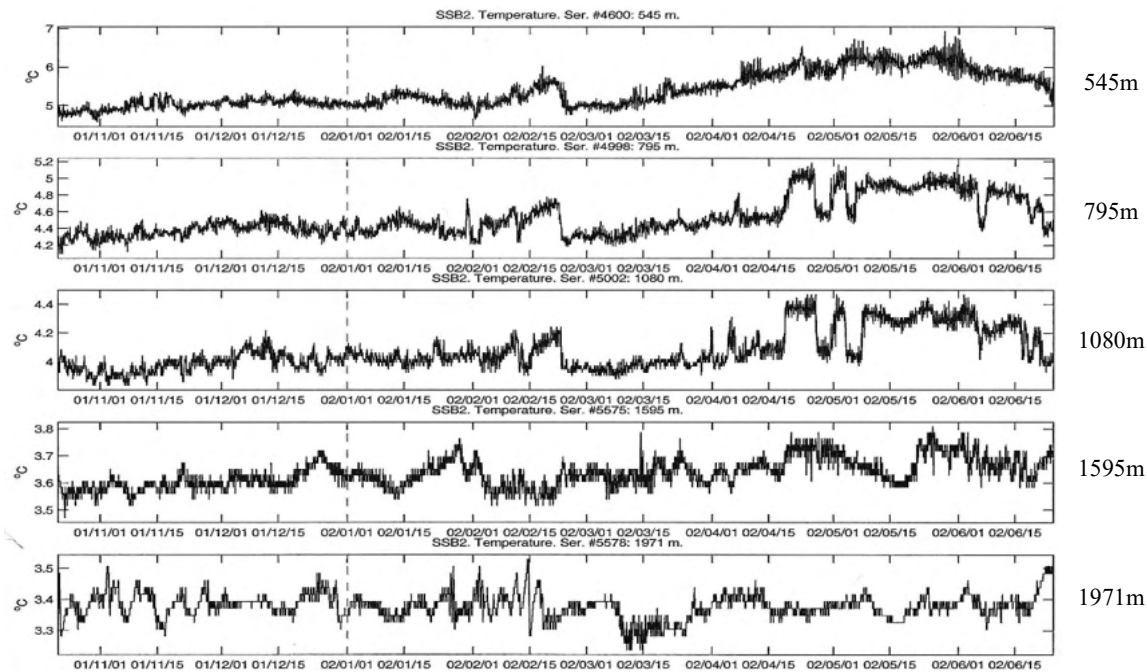
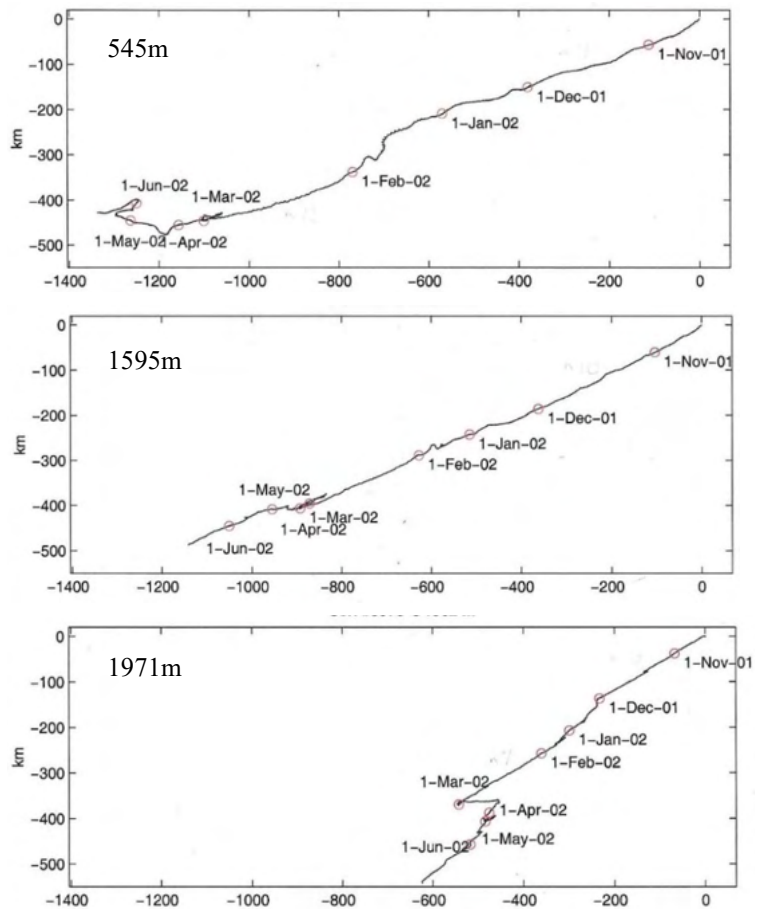


Figure 22e. Time series of T (°C) from the 5 RCM8s on M1412 at SS-B2 from October 2001 to June 2002.

Figure 23. PVDs for hourly velocity from 3 of the RCM8s on M1412 deployed at SS-B2 from October 2001 to June 2002. The positions at the start of each month are indicated.



As a final example of the RCM time series from SSB, Fig. 24 shows T, D and R from the RCM11 and RCM8 on M1479 during SS-B5. These instruments were positioned only 1m apart in an intercomparison experiment in a location with weak currents part of the time. The expected similarity in magnitudes and variability is apparent. Amongst the details, it appears that (i) D measured by the RCM11 varied more

than that measured by the RCM8 during very weak currents (perhaps due to a sluggish rotational response of the RCM8 with its vane assembly), (ii) the occurrences of very low R values ( $< 0.03$  m/s) was greater for the RCM8 (consistent with rotor stalling, and (iii) Rates measured by the RCM8s were higher during relatively strong currents (here  $< 0.25$  m/s).

Further info on these and other differences can be seen in the scatterplots (Fig. 25). Scatter about the 1:1 line is limited for T but larger for D, consistent with a mechanical instrument/mooring response by the RCM8. The origin of an apparent slight counterclockwise D bias from the RCM8 for D values other than the predominant 180-330° range is unclear. An RCM8 bias towards stronger R values, by 10% or so, for speeds above 0.1 m/s is clearly apparent. This is inconsistent with earlier findings (Loder et al., 1992) that the manufacturer’s R calibration relation may result in overestimation of current speeds for moderate current speeds. However, in the absence of a community consensus on this, considering the primary industry interest in the occurrence of strong currents on the Scotian Slope (also the tendency for R underestimation because of rotor stalling at low speeds) and following institutional protocol at BIO, the manufacturer’s relation was used in the study’s RCM8 data. (The possibility of R overestimation, as well as the occurrence of rotor stalling, are noted in the archived RCM8 files).

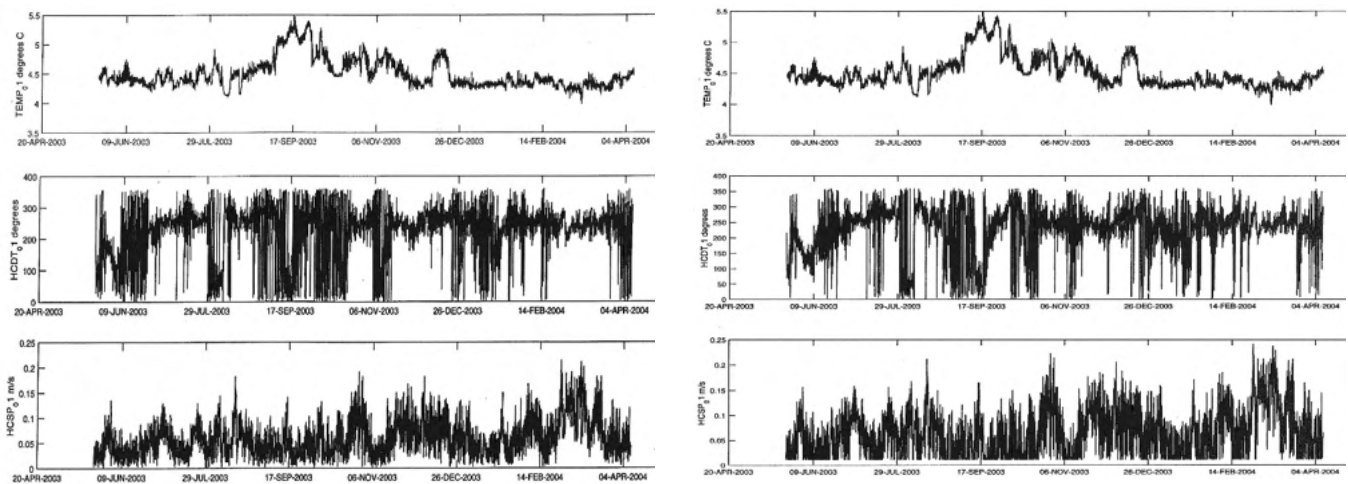


**Figure 24.** Time series of T (°C, upper panels), D (°T, middle) and R (m/s, lower) from the RCM11 at 791 mbs (left column) and the RCM8 at 792 mbs (right) on M1479 at SS-B5 from April 2023 to May 2024.

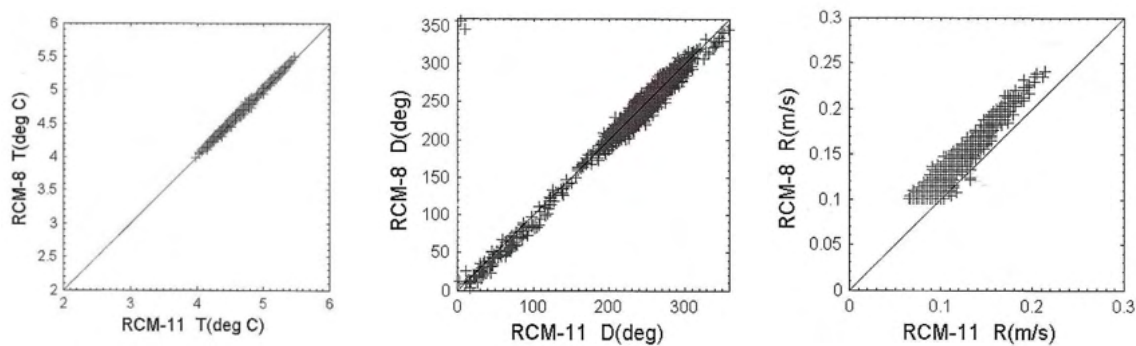


**Figure 25.** Scatterplots of T (left), D (middle) and R (right) from the RCM8 at 792m versus those from the RCM11 at 791m on M1479 at SS-B5 from April 2023 to May 2024. For R, only data for  $R > 0.1$  m/s are shown.

Moving to example RCM8 data displays from the shallowest site SS-C in the 2000-04 program, Fig. 26 shows time series of R, D, U and V from selected depths in SS-C1, and Fig. 27 shows the time series of T, S and P that were returned from the RCM8s. Current speeds were generally higher at this site and rotor stalling occurred less frequently, especially at 202m and above, partly but not entirely related to tidal currents. A 2-week period of relatively strong eastward currents occurred in May 2002 at all depths, with

peak speeds of  $\sim 0.8$  and  $\sim 0.5$  m/s at 127 and 277 m (25 mab), respectively, associated with the incursion of the remnant of a warm-core eddy (Fig. 15; Loder and Geshelin 2009). The top of M1414 was knocked

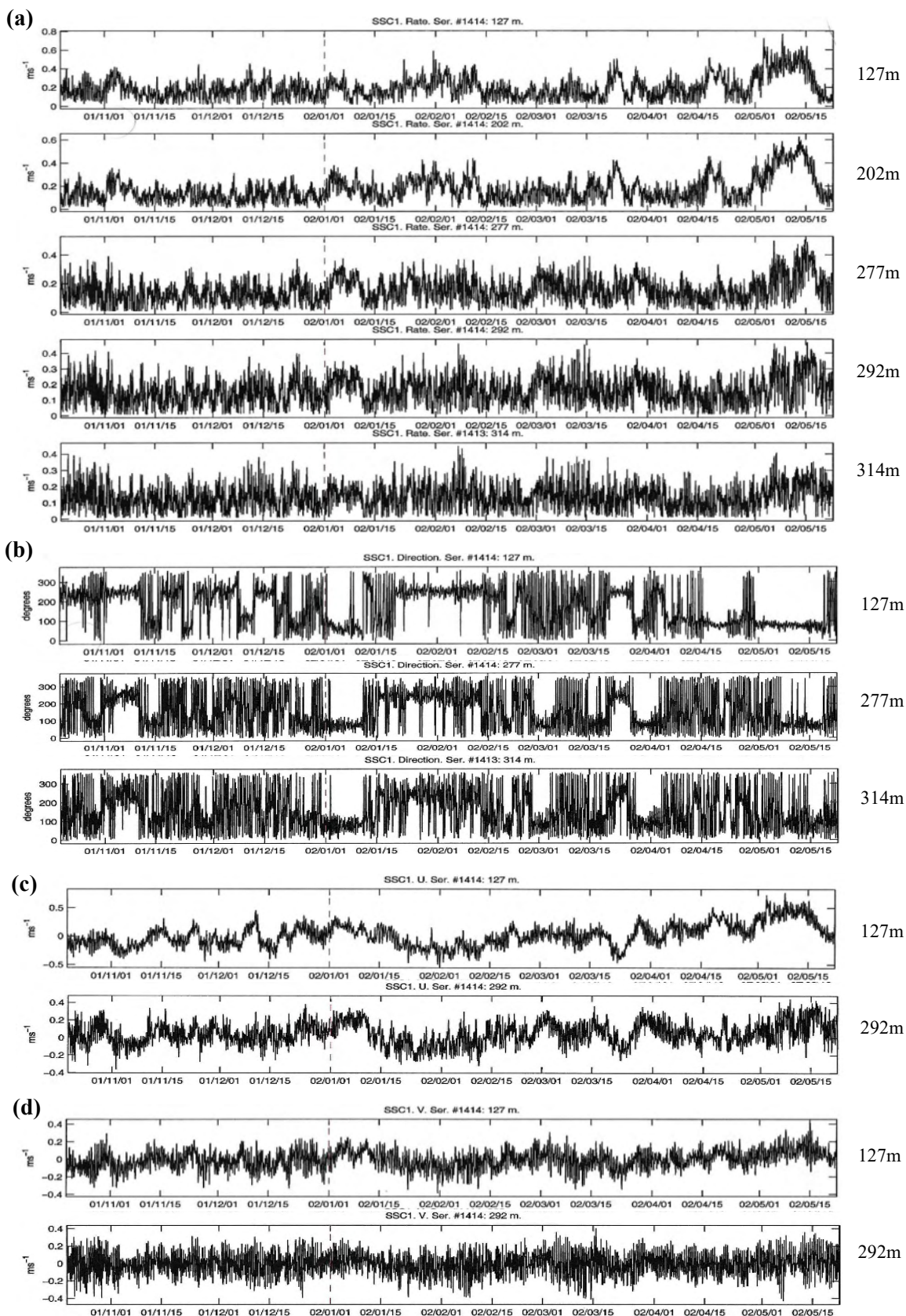
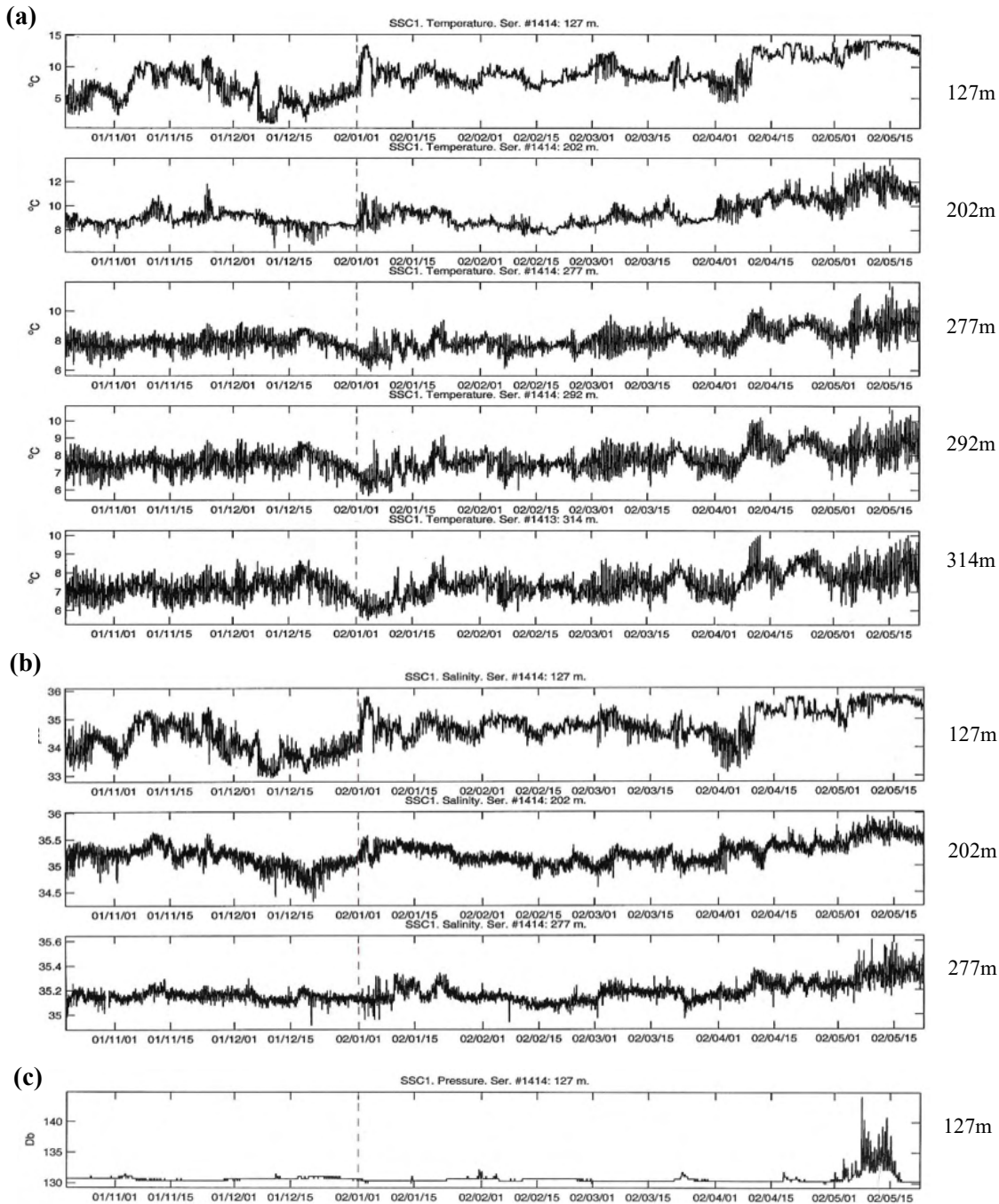


Figure 26. Time series of (a) R (m/s), (b) D, (c) U and (d) V from the RCM8s at different depths on M1414 and M1413 at SS-C1, from October 2001 to May 2002. Note the different ordinate scales, except in (b).

down by up to 10m during this event. Rotor stalling still occurred frequently at 277m and 292m (25 & 10 mab) on M1414, and 314m (2 mab) on M1413, but did not last for more than a few hours (Table 5) (in contrast to site SS-B where tidal currents were generally very weak). Only one period (~21 days) with a prolonged rotor stall occurred in the RCM8 data from SS-C (at 205m in SS-C2), with R set to NoData.

Other periods of 1-2 week duration with persistent eastward flow at all depths occurred in the SS-C1 RCM8 time series, as well as longer periods with persistent westward flow (Fig. 26b). These are apparent in the PVDs for various depths in Fig. 28.

The range of T variability varied from  $<10\text{C}^\circ$  at 127m to  $4\text{-}5\text{C}^\circ$  in the lower water column (below 200m; Fig. 27a). The range of S variability varied from 3 units at 127m to 0.6 units in the near-bottom region.



**Figure 27.** Time series of (a) T ( $^\circ\text{C}$ ), (b) S, and (c) P (db) from the RCM8s at different depths on M1414 and M1413 at SS-C1, from October 2001 to May 2002. Note the different ordinate scales in different panels.

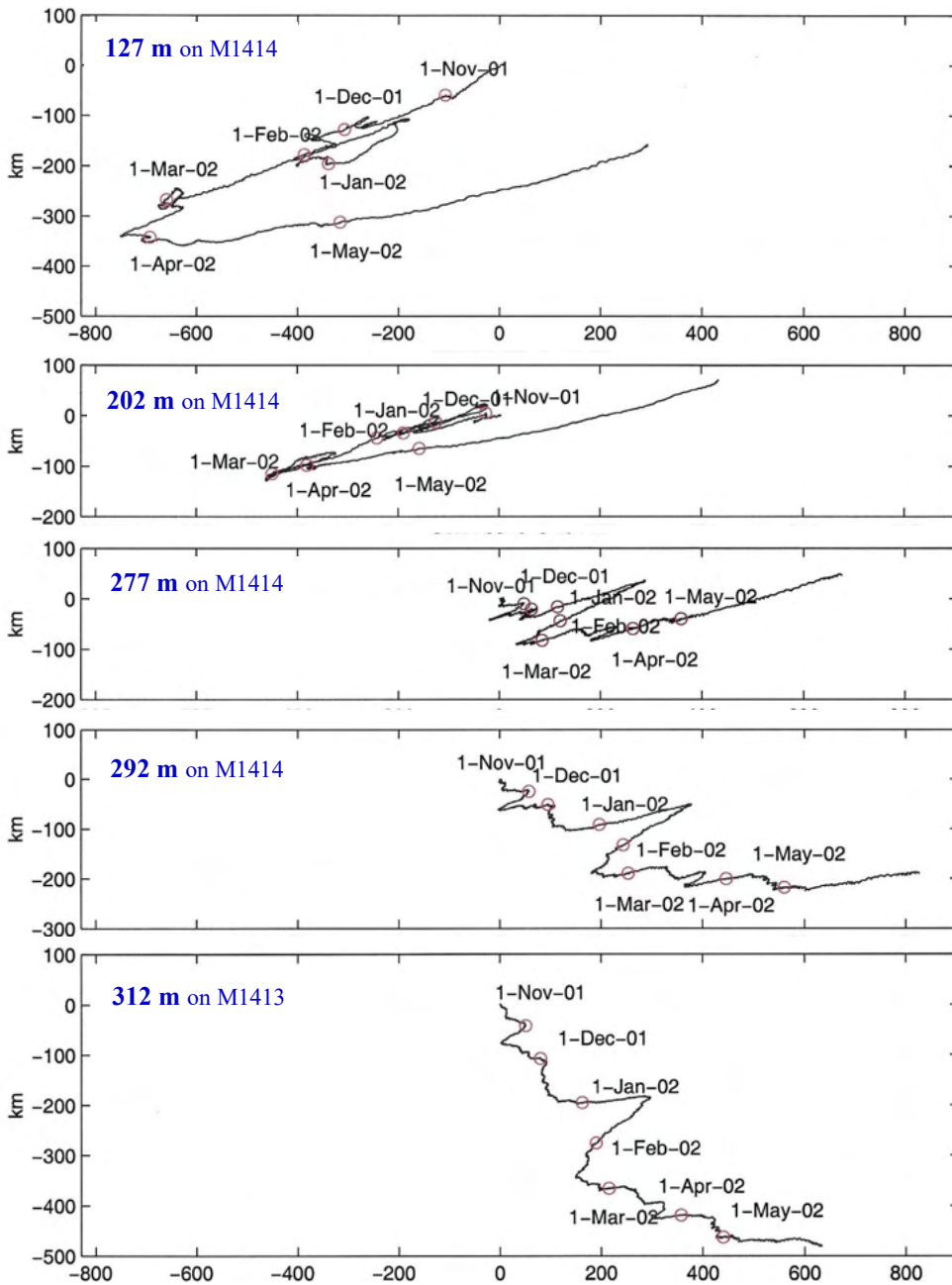


**Figure 28.** PVDs for hourly velocity from the 4 RCM8s on M1414 and the RCM8 on M1413 deployed at SS-C1 from October 2001 to June 2002. The positions at the start of each month are indicated.

Considering the rotor stalling at SS-A and SS-B in the 2000-04 measurement program, it was anticipated that stalling during weak currents would be a problem with the use of RCM8s at the 2400m and 3350m depth sites in the 2004-08 program, especially for currents at 50 mab (Table 2b). Consequently, RCM11s were used at the highest-priority site SS-D (Table 5). In view of industry interest in the occurrence of strong currents (and with additional RCM11s not available), RCM8s were still used in the first 3 of the year-long deployments at SS-E, with an RCM11 used in the final deployment (2007-08).

As examples, Fig. 29 shows the time series of T, R, D, U and V from the RCM11 in SS-D1 (2004-05), Fig. 30 those from the RCM8 in SS-E2 (2005-06), and Fig. 31 those from the RCM11 in SS-E4 (2007-08). Currents were typically  $\sim 0.05$  m/s towards the south-southwest in SS-D1 with occasional values over 0.1 m/s and peak values  $\sim 0.16$  m/s (Fig. 29). Good R, D and T time series were obtained from the 4 deployments at SS-D, and peak speeds were  $< 0.2$  m/s.

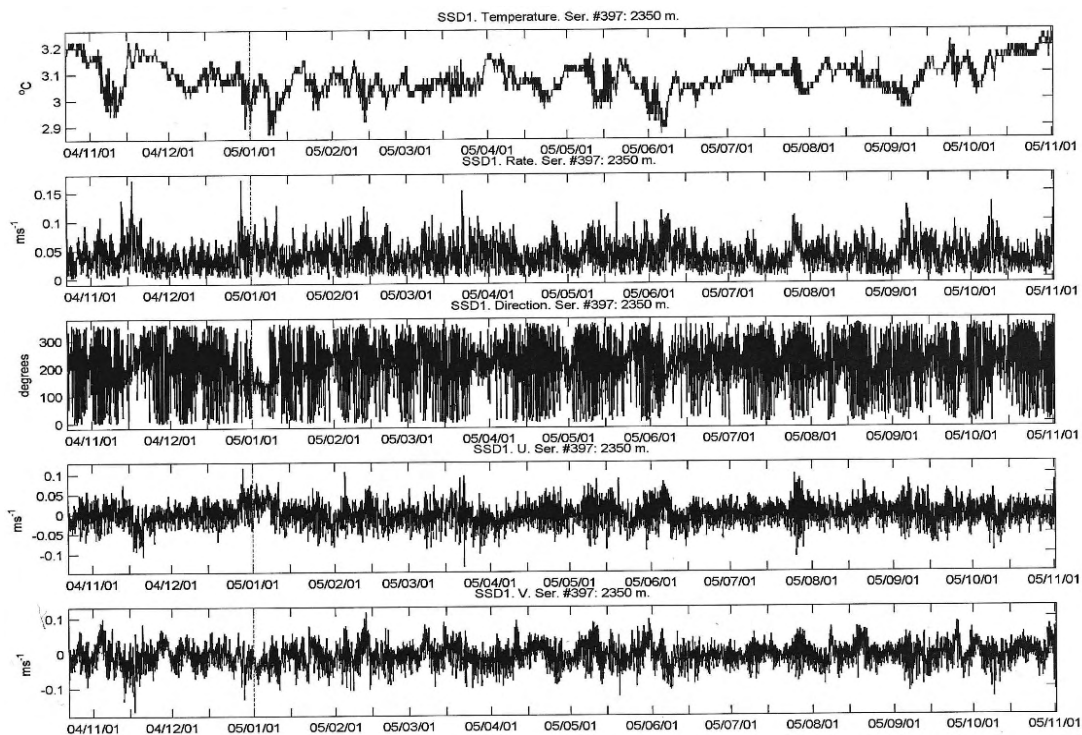


**Figure 29.** Time series of T (°C), R (m/s), D (°T), and U and V (m/s) from the RCM8 at 2402 mbs on M1547 at SS-D1, from October 2004 to November 2005. Note the different ordinate scales for U and V (and the incorrect depth in the subtitles above each panel).

The only good time series returned from all 4 deployments at SS-E were for T. At SS-E-1, prolonged rotor stalling started after ~2 weeks and then continued for the rest of the record after ~6 weeks. At SS-E3, the rotor counter failed for the entire deployment. Time series for the entire deployment were

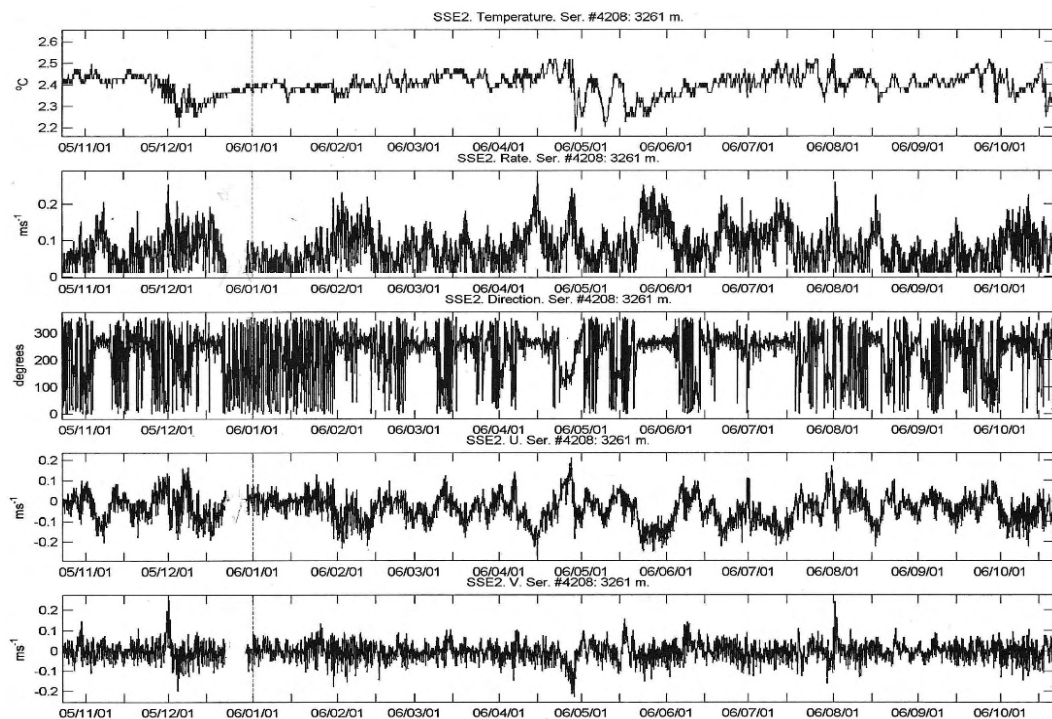


**Figure 30.** Time series of T (°C), R (m/s), D (°T), and U and V (m/s) from the RCM8 at 3345 mbs on M1624 at SS-E2, from October 2006 to October 2007. Note the different ordinate scales for U and V (and the incorrect depth in the subtitles above each panel).

obtained in SS-E2 (Fig. 30), but with a 10-day period of prolonged rotor stalling in December (2005) in which R was set to NoData, and with many other shorter periods with  $R=0.011$  m/s which were not edited (since they appeared to be during very weak currents).

A complete time series of good data for T, R and D was obtained from the RCM11 in SS-E4 (Fig. 31). Note that the current speeds at SS-E (Figs. 30 and 31) are generally larger than at SS-D (Fig. 29), and largest during periods with westward flow, implying either variable speed in the DWBC or a variable latitudinal position (e.g., cross-slope shift or meandering) of the DWBC. In SS-E4, there were many occurrence of  $R < 0.05$  m/s during which some rotor stalling of an RCM8 would have occurred.

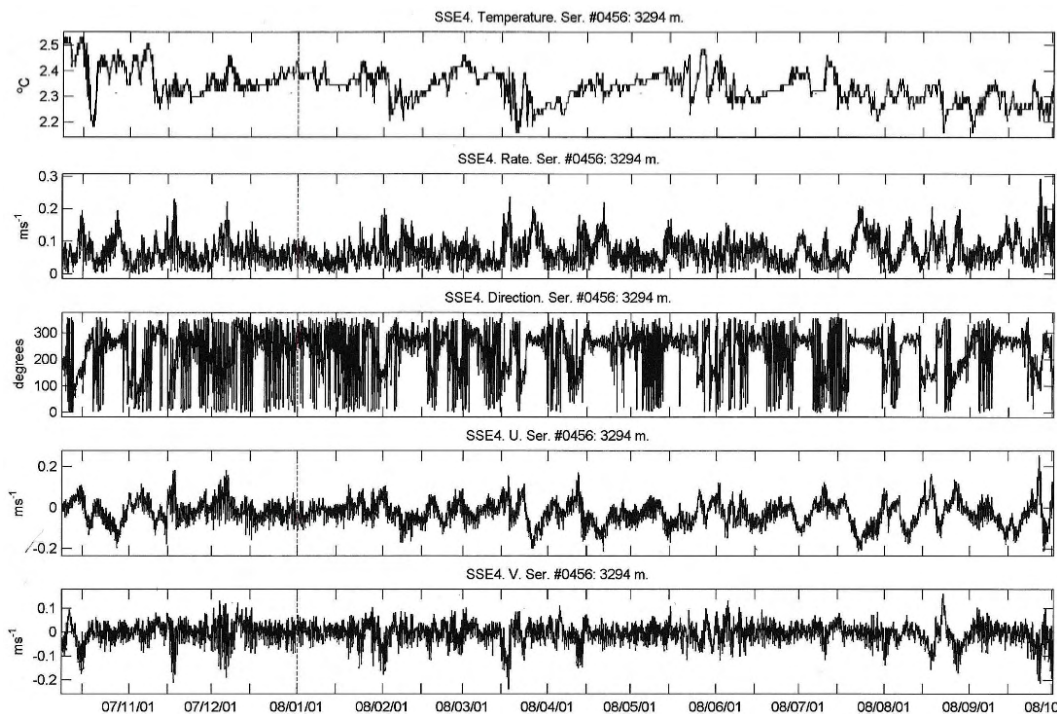


**Figure 31.** Time series of T ( $^{\circ}$ C), R (m/s), D ( $^{\circ}$ T), and U and V (m/s) from the RCM11 at 3414 mbs on M1667 at SS-E4, from October 2007 to October 2008. Note the different ordinate scales for U and V (and the incorrect depth in the subtitles above each panel).

The range of variability of T in each of SS-D1, SS-E2 and SS-E4 was  $\sim 0.3^{\circ}$ C which is comparable to that near the bottom at site SS-B (e.g., Figs. 20b and 22e). There is an indication of variability in T on the same time scale as some of the variability in R and D in the SS-D and SS-E records, but further analysis is required to determine the interrelation.

## 3.2 Acoustic Doppler Current Profilers

### 3.2.1 Overall Summary

A total of 13 Teledyne – RD Instruments ADCPs were deployed during the 2000-04 program, each in an upward-looking position at (or near) the top of a mooring. The deployment sites and numbers, start and end dates, depth information, comments, and other information are provided in Table 6. Four of the moorings at SS-A had an ADCP, all 5 of the moorings at SS-B had one, and all 4 of the deployments at SS-C had one. An ADCP was not available for the initial SS-A1 deployment, nor for SS-A5.

Long Ranger (LR) ADCPs were used in 2 of the SS-A deployments, and the same LR ADCP was used in all 5 SS-B deployments (with the data downloaded, and batteries replaced, at sea at SS-B). Averaging over 60-ping ensembles with pinging at 5-sec intervals was set for all the LR ADCPs, except for 40-ping ensembles at SS-B5. An older Narrow-Band (NB) ADCP was used in 2 of the SS-A deployments, with

averaging over 80-ping ensembles and pinging at 7-sec intervals (with data download and battery replacement done at sea). A WorkHorse (WH) ADCP was used in the SS-C deployments, with averaging over 80-ping ensembles and pinging at 4-sec intervals. The bin size was 4m for the WH ADCPs, 8m for NB ADCP, and 16m for the LR ADCPs, reflecting the different ranges of return data expected from the different ADCP models. The recording interval was 60 minutes in all cases, except 30 min in SS-A2.

**Table 6.** Listing of ADCP deployments during the 2000-04 Scotian Slope program, organized by site and sequential deployment #. Other columns have the BIO mooring #, ADCP type and serial #, record start and end dates in format day/month/(year-2000), water and ADCP depths, bin size, and center depths and vertical intervals of bins with good (QCed) data. NB refers to Narrow-Band , LR to Long Ranger and WH to Workhorse (ADCPs).

Site	D #	BIO #	ADCP & Ser #	Start Date	End Date	Depths (m)					Comments: Number of bins with some good data ( <i>bin #s for caution</i> )
						Water	AD-CP	Bin size	QCed Bins	Vrt Invl	
SS-A	2	1378	LR 1432	22/11/00	31/05/01	1129	430	16	36-404	384	24 bins (#24)
	3	1387	NB 0239	01/06/01	20/10/01	1195	260	8	24-232	216	27 bins ( <i>n/a</i> )
	4	1419	NB 0239	21/10/01	24/06/02	1140	205	8	17-177	168	21 bins ( <i>n/a</i> )
	6	1478	LR 3367	22/05/03	07/04/04	1125	153	16	18-130	128	8 bins (#8)
SS-B	1	1388	LR 1646	01/06/01	20/10/01	1991	391	16	46-366	336	21 bins (#s 13-21)
	2	1412	LR 1646	21/10/01	24/06/02	1995	395	16	50-370	336	21 bins (#s 16-21)
	3	1429	LR 1646	25/06/02	20/10/02	2015	409	16	49-385	352	22 bins (#s 15-22)
	4	1454	LR 1646	20/10/02	14/04/03	2101	495	16	51-467	432	27 bins (#s 19-27)
	5	1479	LR 1646	23/05/03	08/04/04	1991	241	16	24-216	208	13 bins (#13)
SS-C	1	1414	WH 0039	19/10/01	22/05/02	302	86	4	12-76	68	17 bins (#s 14-17)
	2	1431	WH 2456	22/05/02	19/10/02	305	85	4	10-78	72	18 bins (#s 17, 18)
	3	1455	WH 0104	19/10/02	24/12/02	305	85	4	22-78	60	15 bins (#s 10-15)
	4	1491	WH 0039	14/07/03	07/04/04	295	58	4	11-51	44	11 bins (#s 11, 12)

All of the ADCPs returned a large amount of good data over the entire deployment period (excepting of course the periods when the ADCPs at SS-A3 and SS-C3 were adrift). However, the distance (“range”) from the ADCP with good data return was less than expected (based on instrument specifications) in most cases, apparently related to a high density of zooplankton scatterers in the water column above the ADCP during substantial parts of the year (which attenuated the acoustic transmission). This was particularly the case at SS-B in summer and fall. Example displays of the time-varying acoustic return at the different sites will be included in the next subsection.

The time-varying range of the good data return posed difficulties in the data quality control, especially considering the interest in getting good velocity data as close to the sea surface as possible where speeds were expected to be highest. The standard BIO procedure of screening whether there were good ADCP velocity data from a particular bin based on the record-average value of the percentage of good pings (%GPs) in each ensemble would have left many flawed velocity estimates in the time series when the acoustic range was low (attenuation high due to dense scatters), and also excluded good velocity estimates for portions of the records when the range was high. Consequently, an ensemble-by-ensemble strategy was adopted in the quality control (QC) of the horizontal velocity data from the ADCPs, with the primary criterion being whether at least 25% of the return pings within each ensemble (in a particular bin) were good, supplemented by consideration of spikes in the vertical (average of estimates from the 2 orthogonal

beam planes) and error (difference in the 2 vertical velocity estimates) velocities. In ensembles in which the above screening criteria were not met, the horizontal velocity components were replaced with linearly interpolated (in time) values. Histograms of the occurrence of consecutive ensembles requiring linear interpolation were computed, and the total number of ensembles with interpolation and the largest number of consecutive ensembles with interpolation were recorded in the comments in the archived datasets. The record averages of the %GPs in each bin were also computed and considered. Based on the above diagnostics, a further comment was added in each archived file indicating the bins for which velocities should be used with caution considering the interpolations and reduced acoustic return. These comments are cursorily summarized in Table 6, where the bin #'s from which data are to be used with caution are indicated in parentheses (the bin closest to the ADCP with good data is #1, and then the bin # increases proceeding away from the ADCP).

Summarizing in relation to Table 6, it was initially expected that the LR ADCPs would provide good velocity data up to the near-surface sidelobe reflection zone (~8% of depth below the surface) if deployed at ~400 mbs, as was done in SS-A2 and SS-B1, -B2, -B3 and -B4. Good data were routinely returned over this range during portions of the deployments, but there was substantial intermittency (possibly related to vertical migration of the scatterers) during other portions. The first LR ADCP deployment (SS-A2) provided optimism with substantial good data returned from the 16m bin centered at 36 mbs (thus covering the vertical interval between 28 and 44mbs), and limited interpolation required in the deeper bins. However, the shallowest bin with a substantial amount of good (non-interpolated) data from the subsequent LR ADCP deployments at ~400 mbs at SS-B (B1-B4) was centered around 50 mbs (so a vertical interval of 42-58 mbs), and at least several of the bins immediately below it required a substantial amount of interpolation (at depths of 110 to 160 mbs, or deeper in the case of SS-B4 where the ADCP was deployed deeper than planned) (Table 6). In the last LR ADCP deployments at SS-A6 and SS-B5, the ADCP was positioned closer to the surface and a substantial amount of good data was obtained from the 16-m bins centered at 18 mbs and 24 mbs, respectively; also, none of the other bins in these cases were flagged as needing particular caution with respect to data quality.

In the 2 NB ADCP deployments at SS-A where the ADCP was positioned at 260 mbs (SS-A2) and 205 mbs (SS-A4), a substantial amount of good data was obtained from the 8m bins centered near 20 mbs. In the 4 WH ADCP deployments at SS-C where the ADCP was positioned at ~85 mbs (C1-C3) or 58 mbs (C4), a substantial amount of good data was obtained from the 4m bins centered as shallow as 10 mbs.

In spite of all the caveats above, the moored ADCP data from the 2000-04 program should be viewed as a large and unique dataset from the primary Maritimes AZMP sampling line, of high potential value to describing and understanding both currents and zooplankton variability. Counting all the bins with some good data, there are 245 time series of hourly velocity and echo intensity observations, in most cases over durations of 5-12 months. However, it should also be recognized that there is inherent averaging across adjacent bins (1:2:1 weighting) in the internal ADCP data processing, and the specified bin size provided some additional oversampling in the vertical, such that the number of different "representative" time series is only a fraction of the total (perhaps only 50-60, assuming 4-5 representative bins per ADCP).

### **3.2.2 Example ADCP Data Displays**

The example displays here are chosen based on a combination of representativeness and ready availability in order to provide useful information.

We start with the ADCP positioned at 430 mbs in SS-A2 which at times provided good data over a 384-m vertical interval up to within 28m of the surface. However, the range was more limited during the first month of the deployment, as indicated by some reduction in the %GP at a distance of only 250m from the ADCP (bin at 188 mbs) (Fig. 32a). Since %GP is generally considered to be an adequate indicator of good velocity estimates, especially when the number of pings per ensemble is in the 60-80 m range as was the case in the present program, good velocity time series were obtained for depths much shallower than

this: the record-average %GP was 81 for the bin centered at 36 mbs and >90 for all the other bins, such that only the 36 mbs bin would have been rejected in standard BIO processing. With the ensemble-by-ensemble screening used here (see above), a potentially-good time series was obtained for the 36 mbs bin, assuming that it is used carefully. Examination of the velocity time series in this and other cases with reduced acoustic backscatter in the 2000-04 program has indicated that this was indeed the case.

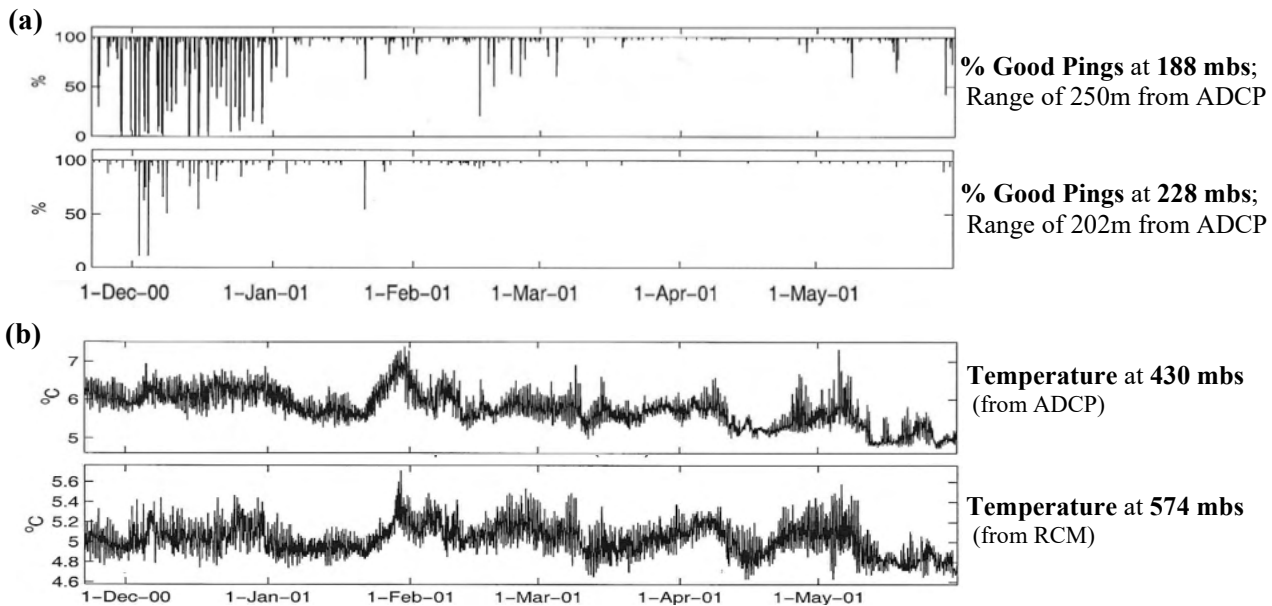


**Figure 32.** Time series of (a) %GP in the bins at 188 and 228 mbs from the ADCP on M1378 at SS-A2, and (b) T from that same ADCP and from the RCM8 at 574mbs on the nearby M1377 in SS-A2. Note the different ordinate scales in (b).

As an aside, time series of T are also available from each ADCP, as illustrated in Fig. 32b which shows the T series from the ADCP on M1378 and also that from the RCM8 on M1377 which was positioned about 3 km away. In SS-A2, the ADCP was the only measurement instrument on a separate mooring. It was deployed within a reasonable distance of the primary tall mooring which had instruments as shallow as 148 mbs (closer proximity would have been desirable but caution was used in consideration of variable at-sea weather conditions in order to avoid tangled moorings). In all of the other 12 ADCP deployments, the ADCP was included on the primary tall mooring.

As expected there are some similarities and some differences, including a higher mean value, between the T series from the ADCP and that from the RCM8 positioned 144m deeper and to the northeast. Since there was no instrument between 274 and 574 mbs on M1377, the T record from the ADCP may be of use. However, the T records from the ADCPs in the 2000-04 SS program were not added to the MTR (Moored Temperature Recorder) archive so they would need to be retrieved from the ADCP NetCDF files. In the later Flemish Pass and Orphan Basin moored measurement programs (Loder et al., 2025b,c), the T records from the ADCP were placed in the BIO MTR archive.

Time series of Rate from 3 depths (68, 148, 292m) from the ADCP on M1378 in SS-A2 are shown in Fig. 33, together with those from the 5 RCM8s on nearby M1377. The RCM8s at 149m and 289m were well within the ADCP range of good data, as illustrated by the ADCP R time series at 68m. An overall decrease with depth in the magnitude of the stronger currents is apparent.

The separate ADCP and RCM moorings in SS-A2 allow comparisons of the Rates from the different instruments for the same depth below surface (Fig. 34), although separated horizontally by ~3 km. The best-fit regression lines with (0,0) intercepts have  $R_{RCM} = 0.97 \times R_{ADCP}$  for both depths, although slightly better fits are obtained with non-zero intercepts. However, there is substantial scatter about the regression

lines, not completely unexpected considering the horizontal separation in a frontal zone with currents variability on a variety of time scales (including tides with horizontal phase structure), and considering the RCM8 rotor stalling during weak currents. Further analysis with phase lagging may be instructive.

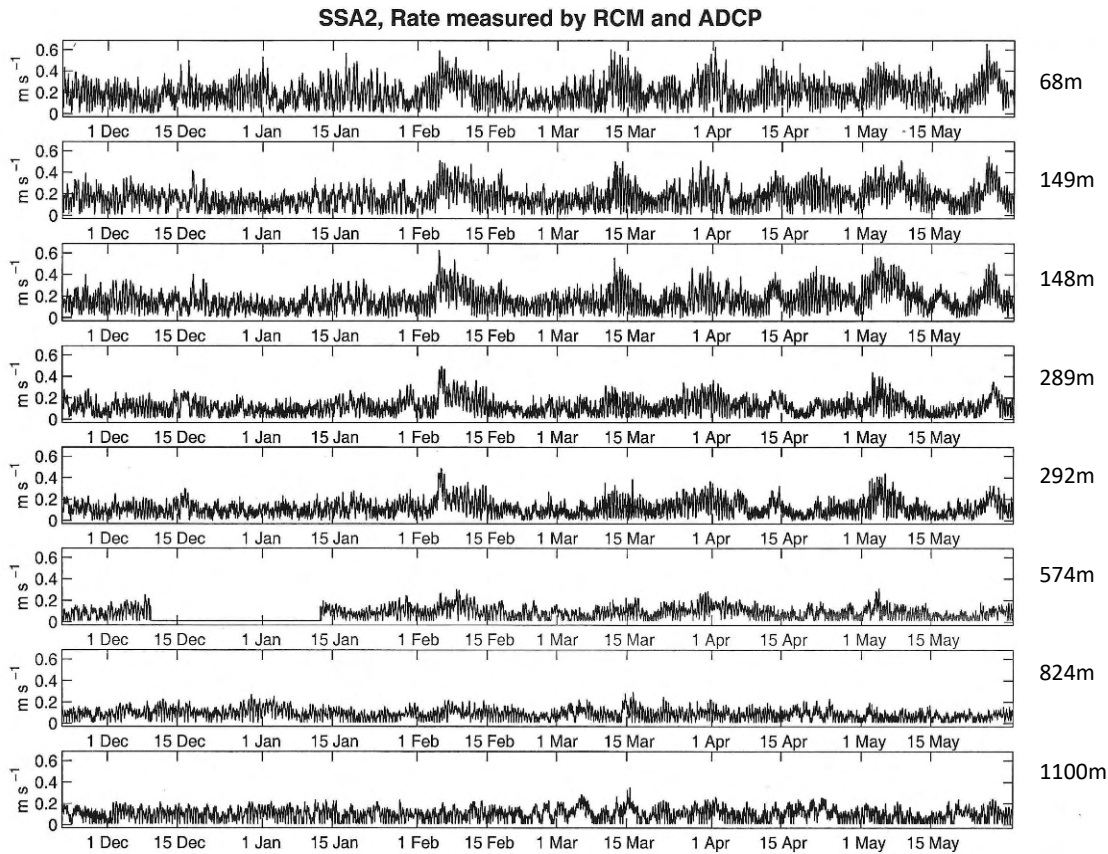


**Figure 33.** Time series of R from the ADCP for 3 bins (68, 148, 292m) on M1378 in SS-A2, and from the RCM8s on nearby M1377, from November 2000 to late May 2001. Note the period of rotor stalling at 574m.

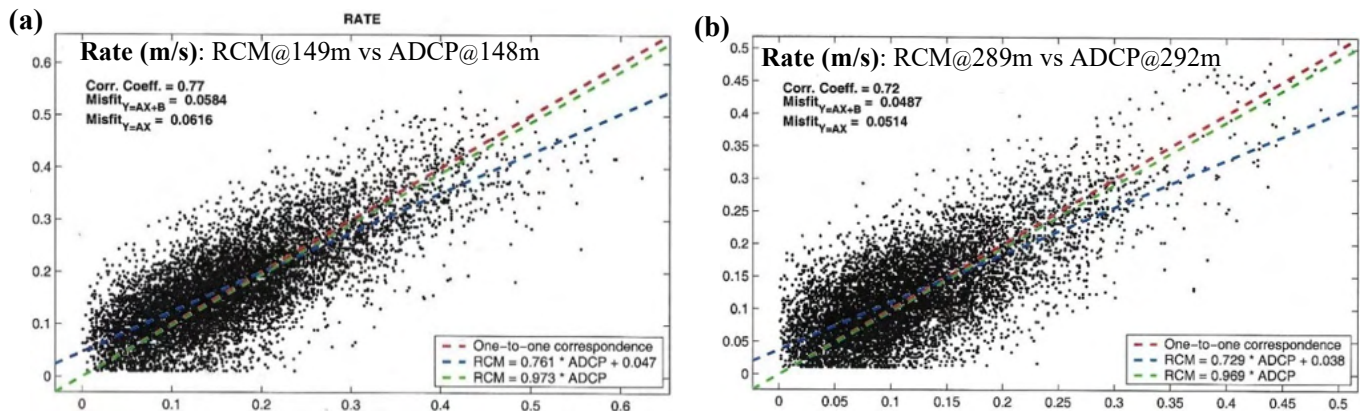


**Figure 34.** Scatterplots and regression results of RCM Rate (m/s) vs ADCP Rate (m/s) for (a) 149 and 148m, and (b) 289 and 292m, from M1377 (RCM8s) and M1378 (ADCP) in SS-A2. The dashed lines are the **1:1 line**, and the regression lines with a **(0,0) intercept** and a **best-fit intercept**. Regression results are included on the plots.

PVDs for velocity from 5 of the ADCP bins on M1378 (Fig. 35) show the vertical structure of the low-frequency drift implied by the data, and also confirm reasonable agreement between the ADCP and RCM8 measurements of low-frequency current variability at two of the levels. After a short initial period of generally northward flow, the flow was generally west-southwestward at all depths until mid April when it shifted to southeastward for about a month. However, at 84m and above, there was also another

short (couple of weeks) period of northward flow starting in late February. Thus, different disruptions of the primary south-southwestward flow occurred over different depths below the surface.

The close similarity of the implied drifts from the closest RCMs and ADCP bins provides support for the RCM8 rotors working reasonably well, other than in very weak currents. The noticeable difference in the drifts in the ADCP bins at 148m and 164m indicates a weak vertical shear in the low-frequency flow.

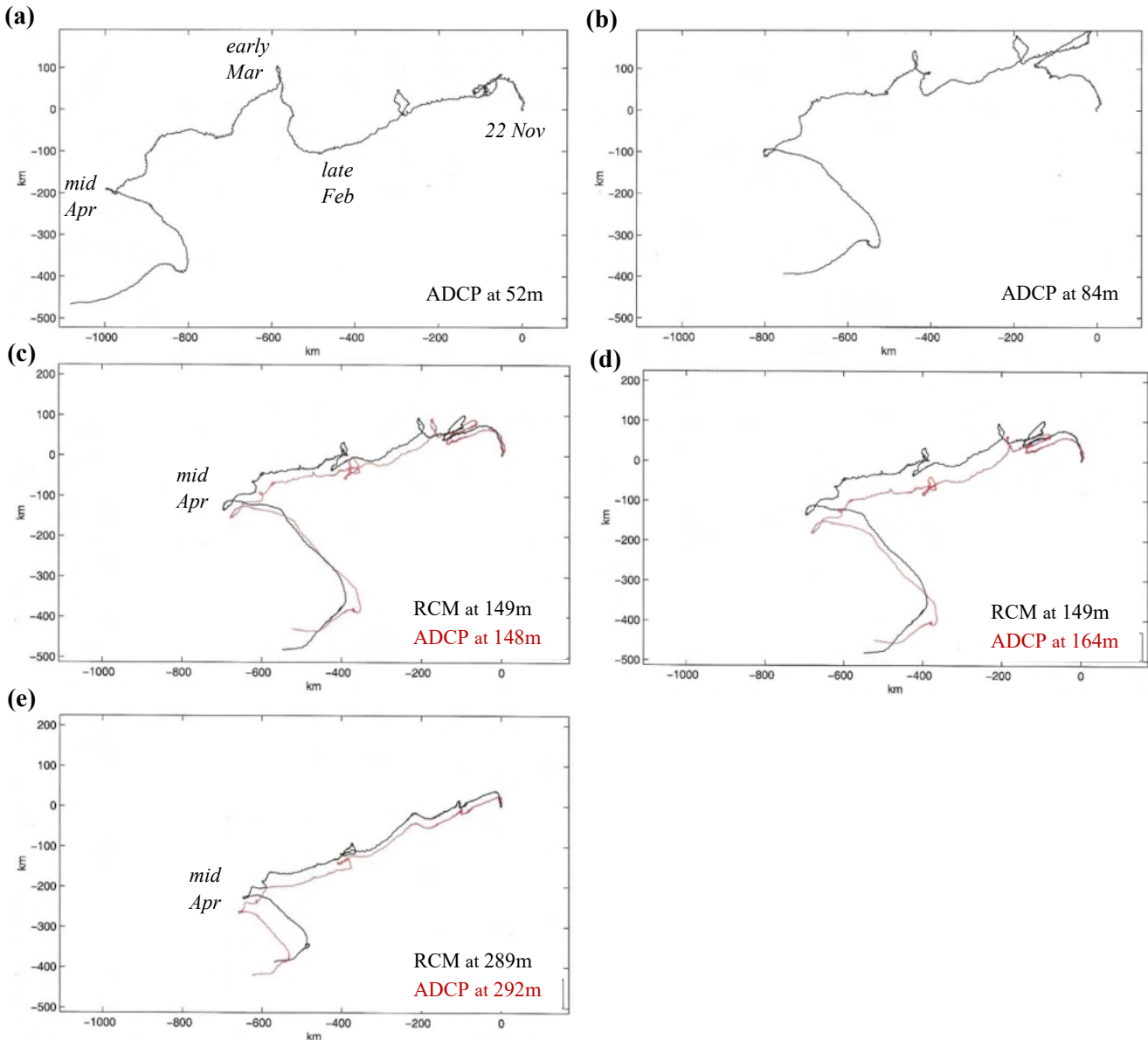


**Figure 35.** PVDs for velocity from 5 different depth bins from the ADCP on M1388 at SS-A2, from late November 2000 to late May 2001. The PVD from the RCM8 at a similar depth on nearby M1387 is included for 3 of the bins. In each case, the vector sequence starts at (0,0) km.

A glimpse at the data from the NB ADCP 260 mbs at SS-A3 is provided in Fig. 36. There was a similar range of good data return as at SS-A2 - compare the %GP at 180m away from the NB ADCP in Fig. 36a with that at 202m away from the LR ADCP in Fig. 32a. However, the shallower position of the ADCP in SS-A3 provided better velocity coverage close to the surface. This is illustrated by the time series of R and D from the bins at 24 and 32 mbs in Fig. 36b,c. It can be seen that the peak current magnitudes at these depths during the June-September (2001) summer period were not much larger than at 104 mbs, but those at 232 mbs were noticeably reduced.

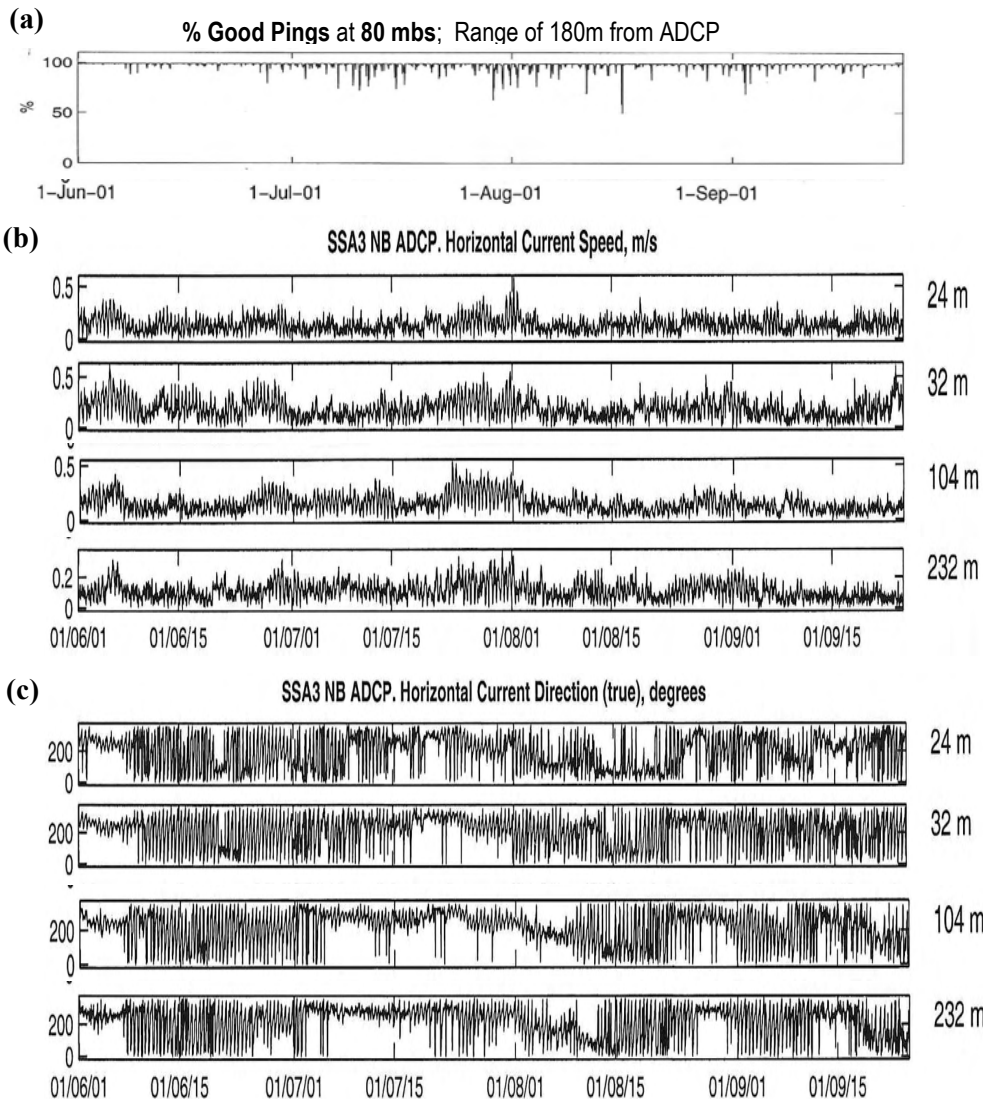


**Figure 36.** Time series of (a) %GP in the bin at 80 mbs, and of (b) R and (c) D from the bins at 24, 32, 204 and 232 mbs, from the NB ADCP on M1387 in SS-A3, from 31 May to 25 September 2001.

Substantial vertical coherence in the velocity variability between 16 and 240 mbs in SS-A3 is apparent from the R and D time series in Fig. 36b,c. Prolonged periods with persistent flow generally towards the southwest can be seen at all depths, as well as periods with an increased occurrence of flow reversals at all depths. However, it can also be seen that at times there is more coherence in the variability in the 104m and 232m depths, than with the variability at 24 and 32 mbs.

A similar glimpse at the NB ADCP data from the “fall-winter-spring” period in SS-A4 is provided in Fig. 37, where the ADCP was at 205m. The %GP in the bin at 180m from the ADCP (Fig. 37a) was slightly lower than in SS-A3 (Fig. 36a), perhaps related to surface sidelobe reflection since this bin was centered at 25 mbs in SS-A4, but still well above the 25% threshold at all times. The highest R values (Fig. 37b) were notably higher at all depths than those at comparable depths in SS-A3 (Fig. 36b), probably partly reflecting a seasonal change, but note also a contribution from the remnant GS eddy which encroached on the area in spring 2002 (Figs. 15, 26; Loder and Geshelin 2006, 2009). The latter is supported by the predominantly eastward flow at all depths (17-177 mbs) in April-June (Fig. 37c). Multi-week periods of predominantly westward flow also occurred at all depths, as well as multi-week periods with the flow at all depths veering gradually from northward (clockwise) to southward and then westward again (consistent with an anticyclonic eddy drifting westward). This again illustrates the potential value of the multiple types of moored measurements together with the evolving SST field from satellite imagery.

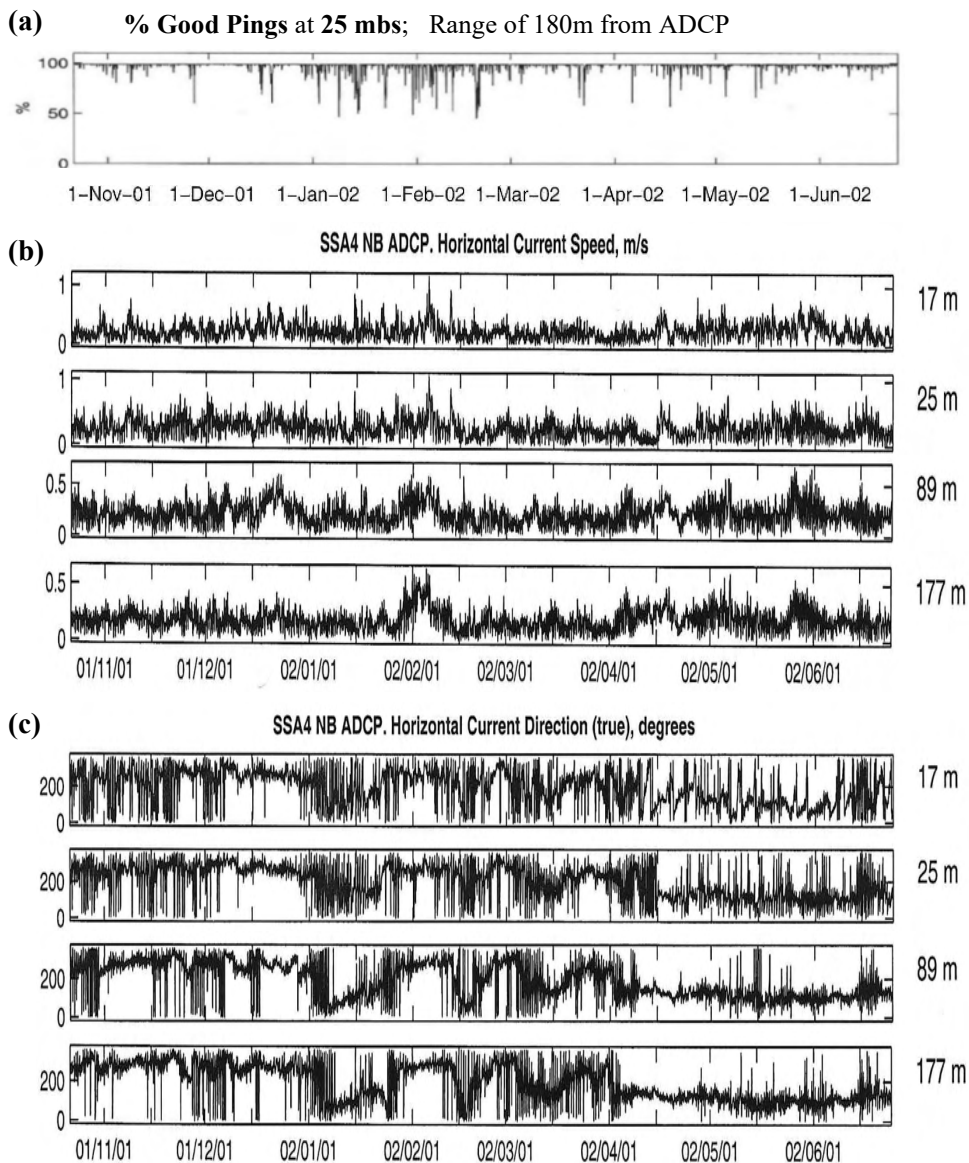


**Figure 37.** Time series of (a) %GP in the bin at 25 mbs, and of (b) R and (c) D from the bins at 17, 25, 89 and 177 mbs, from the NB ADCP on M1419 in SS-A4, from October 2001 to June 2002.

The time-varying vertical structure of the good data return from the LR ADCP deployed at 391m at SS-B1 is indicated with the time series of %GP for most of the vertical bins shown in Fig. 38. A full record with %GP > 25 was only obtained for the bins at 254 mbs (137m away from the ADCP) and below. However, the QC and linear interpolation provided reasonable time series of horizontal velocity for all the bins below 100 mbs and, for portions of the deployment period, for all of the bins centered at 46 mbs and lower. Note that there was the expected full range (up to surface sidelobe contamination zone which included the 30 mbs bin) for the first month or so (June) but that the range was intermittently reduced over the remainder (July-October) of the record. It seems most likely that this reduction was caused by attenuation of the acoustic transmission and return signals by the vertical migration of zooplankton, from their primary deeper water habitat, into the upper ocean for summer feeding, with an indication of a diel (daily) migration pattern apparent. This needs further investigation but points to the moored ADCP time series from the 2000-04 SS program being of potential value to the zooplankton monitoring and studies carried out by DFO AZMP colleagues for the program period.

Velocity time series from this deployment will be included in the later section of this report showing variability over the entire study period.

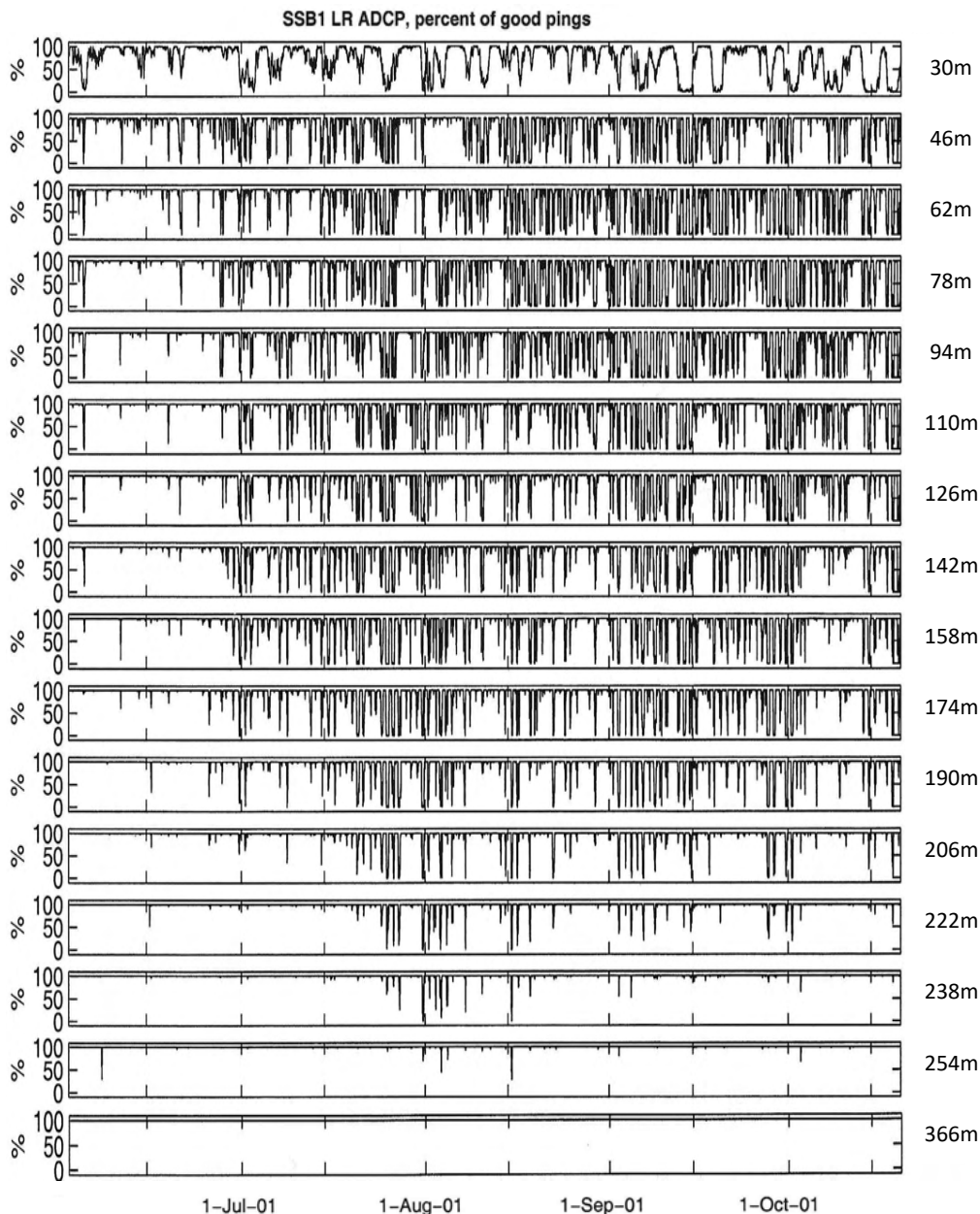


**Figure 38.** Time series of %GP in various bins from the LR ADCP at 391 mbs on M1388 in SS-B1, proceeding (top panel) from the bin centered at 30 mbs in which the velocity estimates were severely contaminated by surface reflection, down to the bin centered at 254 mbs in which the %GP was near 100 most of the time. The bin closest to the ADCP (at 366 mbs) in which the %GP was always 100 is also included.

Glimpses at the LR ADCP datasets from SS-B2 and SS-B3 are provided in Figs. 39 and 40, respectively. In both cases, the ADCP was positioned near 400 mbs, and the range of good data return was intermittently reduced, apparently by a high density of scatterers (zooplankton) in the water column above the ADCPs. However, after the QC and linear interpolation, good velocity time series for the entire deployment periods were obtained for the bins around 200 mbs and below, and for most of the time, for shallower bins up to the one at 50 mbs (Table 6).

The T time series from the ADCP and the closest RCM8 (below it) in SS-B2 and SS-B3 are included in Figs. 39 and 40, respectively, and also the R time series from the SS-B3 bin at 209 mbs in Fig. 40. The latter shows the occurrence of a period of stronger (but time-varying) currents in September 2002 associated with decreasing T during that period, just one example of many intriguing features in the moored datasets during that period.

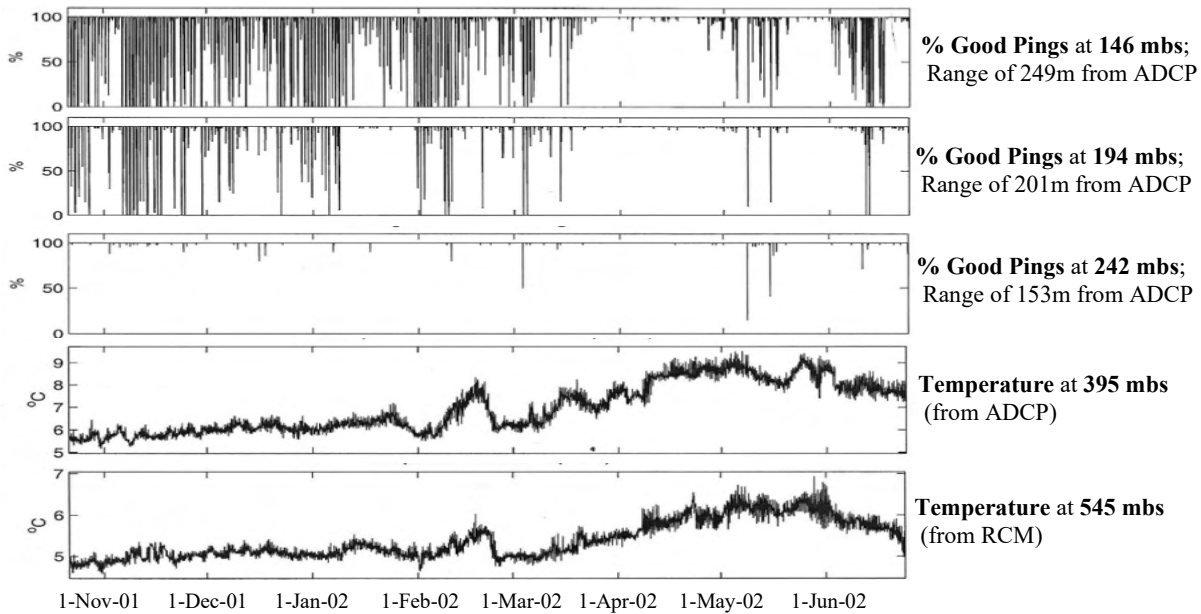


**Figure 39.** Time series of %GP in the 16m bins centered at 146, 194 and 242 mbs (upper 3 panels) from the LR ADCP on M1412 in SS-B2, from late October 2001 to late June 2002, and of T from the ADCP at 395 mbs and the RCM8 at 545 mbs (lower 2 panels).

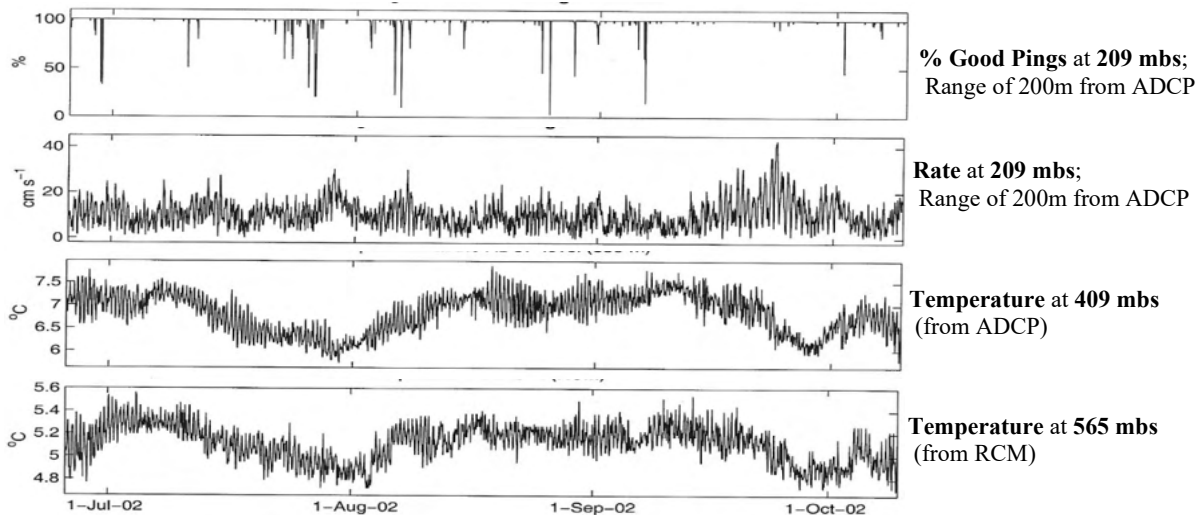


**Figure 40.** Time series of %GP (upper panel) and R (next panel) for the 16m bin centered at 209mbs from the LR ADCP on M1429 in SS-B3, and of T from the ADCP at 409 mbs and the RCM8 at 565 mbs (lower 2 panels).

Glimpses at the WH ADCP datasets from SS-C1 and SS-C2 are provided in Figs. 41 and 42, respectively. In both cases, the ADCP was positioned near 85 mbs, and the range of good data return was intermittently reduced, probably also by a high density of scatterers (zooplankton) in the water column above the ADCPs. However, after the QC and interpolation, good velocity series for almost the entire deployment periods were obtained for the bins at 35 mbs and below in both cases, and for most of the time, for shallower bins up to the one at 15 mbs in SS-C2 during the May-October “summer” period (also see Table 6). On the other hand, there were only limited good velocity data returned for the upper 2 bins (at 12 and 16 mbs) in SS-C-1 during parts of November -January; the record-mean values of %GP were only 77-78 for those bins. Nevertheless, there are good velocity series over a 50m interval for both deployments.

There are both similarities and differences in the T variability detected by the ADCP and the deeper (by ~50m) RCM in both SS-C1 and SS-C2 (Figs. 41 and 42), as expected and confirming the potential value

of the ADCP T records (although not archived as MTR files, as mentioned). The warming event in April-June 2002 associated with the remnant GS eddy is apparent.

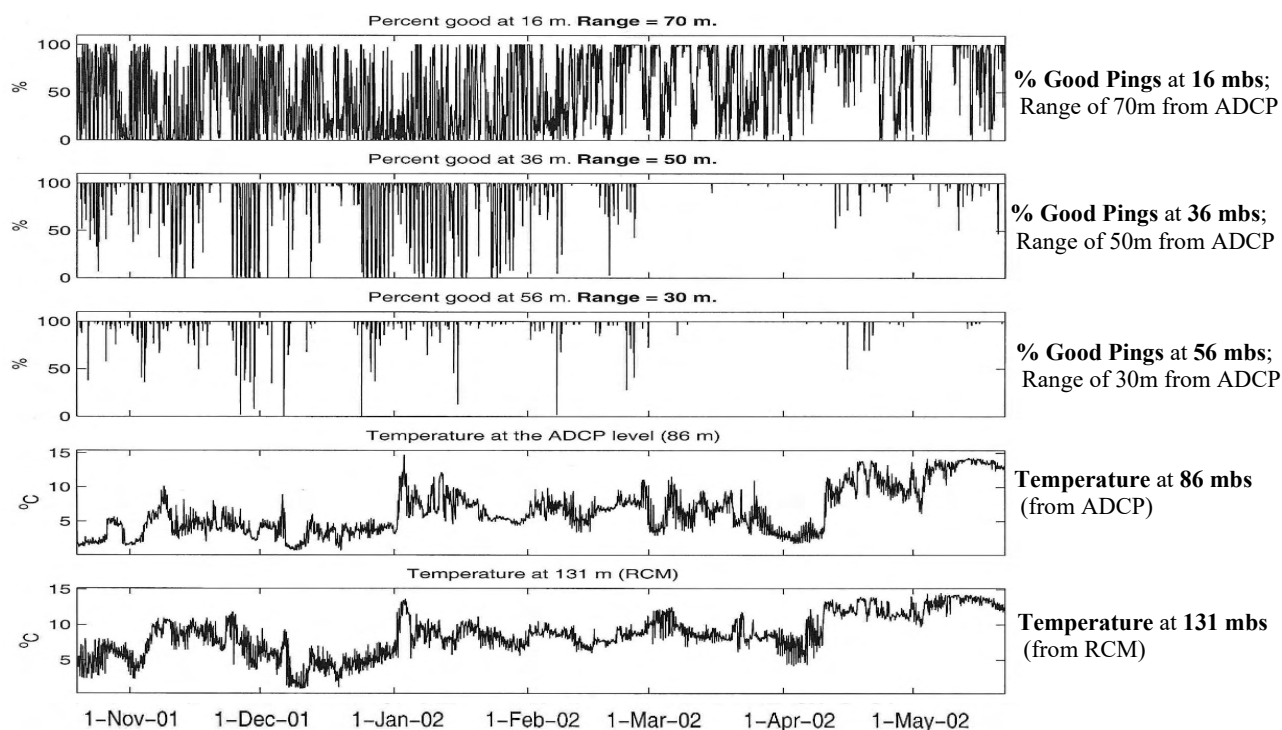


**Figure 41.** Time series of %GP (upper 3 panels) at 16, 36 and 56 mbs from the WH ADCP at 86 mbs on M1414 in SS-C1, and of T from the ADCP and the RCM8 at 131 mbs (lower 2 panels).

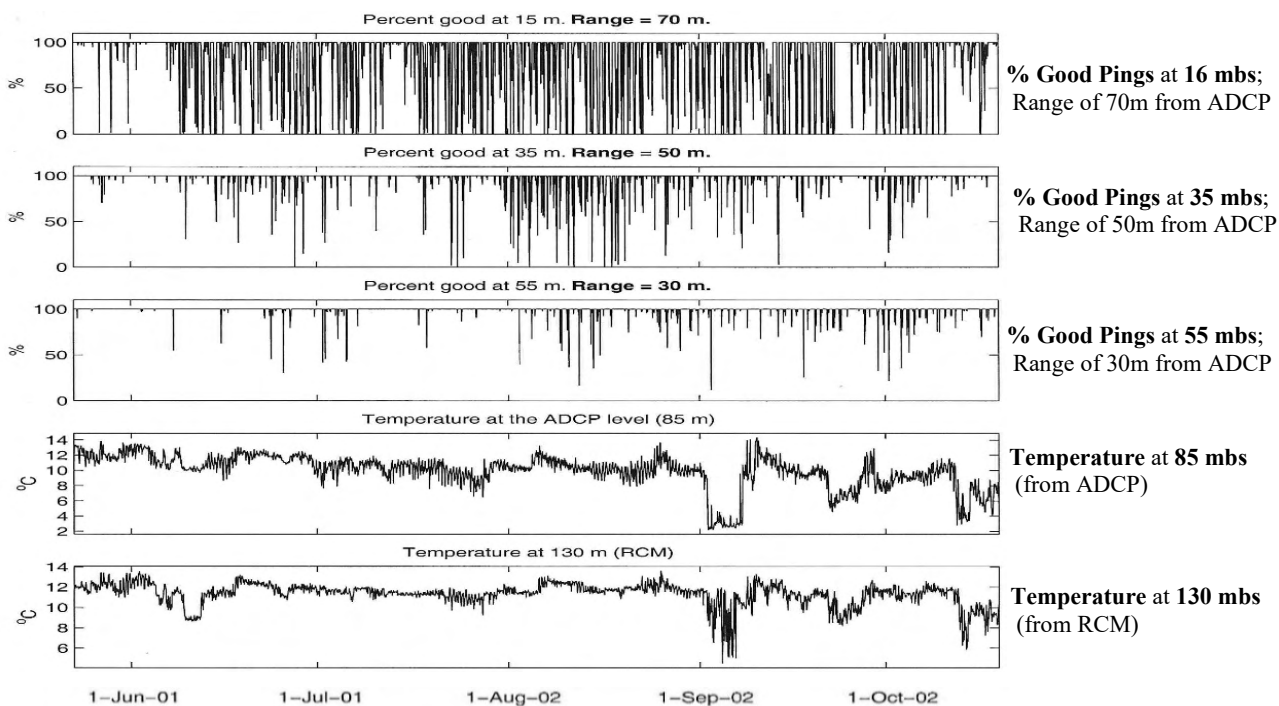


**Figure 42.** Time series of %GP (upper 3 panels) at 5, 35 and 55 mbs from the WH ADCP at 85 mbs on M1431 in SS-C2, and of T from the ADCP and the RCM8 at 130 mbs (lower 2 panels).

To conclude these two subsections on the primary currents time series from the 2000-04 and 2004-08 programs, we present a graphical depiction in Fig. 43 of the timeline of good Rate datasets from various

depths at the 5 mooring deployment sites. Good D data are also available for the periods and depths indicated by the coloured bars, as well as a few other periods when serious rotor stalling affected the R measurements. This display complements the more detailed information in Tables 5 and 6.

Site SS-A has the longest velocity time series, almost continuous over the 47-month of the 2000-04 program at the ~300 mbs and ~600 mbs levels there if the data from the deeper (by 70m) SS-A3 deployment are included. There are ~3.4 years of good velocity data from 25mab with those from SS-A3 included, and ~3 years of good data from the upper ocean at SS-A, if the RCM8 data at 74 mbs in SS-A1 are included, and also ~3 years at the ~800 mbs level.

There are good velocity time series of ~35 months duration at multiple depths at site SS-B, including the upper ocean at ~50 mbs. At SS-C, there are good velocity data from the near-surface (20-70 mbs) and near-bottom (25 mab) regions over the entire 31-month deployment period, and about 24 months of data at ~100 mbs and ~200 mbs. Additional time series from the electromagnetic S4 current meters in SS-C1 and SS-C2, discussed in the next subsection, are not included in Fig. 43.

From the 2004-08 program, there are 4 years of good velocity data from SS-D but only 26 months from SS-E.



**Figure 43.** Approximate periods and depths with good R (and hence velocity) time series returned from sites SS-A, SS-B and SS-C in the 2000-04 program, and sites SS-D and SS-E in the 2004-08 program. The type of measurement instrument is indicated by the colour coding of the horizontal bars representing the good-data return periods. The red dotted lines indicate the start of the different deployment periods.

### 3.3 Electromagnetic Current Meters

To investigate the vertical structure of the currents near the seafloor at site SS-C and for collaboration with Dalhousie University and GSCA investigations of sediment transport (Hill et al., 2004), separate short moorings were deployed in SS-C1 and SS-C2 with current meters within 4m of the seafloor. In SS-C1, electromagnetic InterOcean S4 meters were deployed at 2mab and 4 mab on M1413 (Table 7), with an RCM8 in between them (at 3 mab) (Table 5c). In SS-C2, an S4 was deployed at 3 mab on M1430, with an RCM8 at 2 mab. The S4s were set to burst sample for 2 minutes at one time during each hour. In each of these deployments, an extra RCM8 was deployed at 10 mab on the nearby tall mooring (M1414 and M1431 in the respective deployments).

**Table 7** Listing of InterOcean S4 electromagnetic current meters deployed at site SS-C during the 2000-04 Scotian Slope program, organized by sequential deployment #. Other columns indicate the BIO mooring #, S4 serial #, record start and end dates in the format day/month/(year-2000), water and S4 depths, and comments. An RCM8s was deployed within 1m of the S4(s) in each of these deployments (Tables 2c and 5)

Site	D #	BIO #	S4 Ser #	Start Date	End Date	Depths (m)		Comments
						Water	S4	
SS-C	1	1413	04590854	19/10/01	22/05/02	317	313	Unexpected small differences from RCM at 314m
			04590906	19/10/01	04/04/02	317	315	Slightly shortened record; unexpected small differences from RCM at 314m
	2	1430	08111786	22/05/02	23/10/02	314	311	Unexpected small differences from RCM at 312m

It appeared that good data were obtained from all of these near-bottom instruments. As an example of the measured currents, Fig. 44 shows the time series of U, V, R and D from the 3 meters on M1413 during the

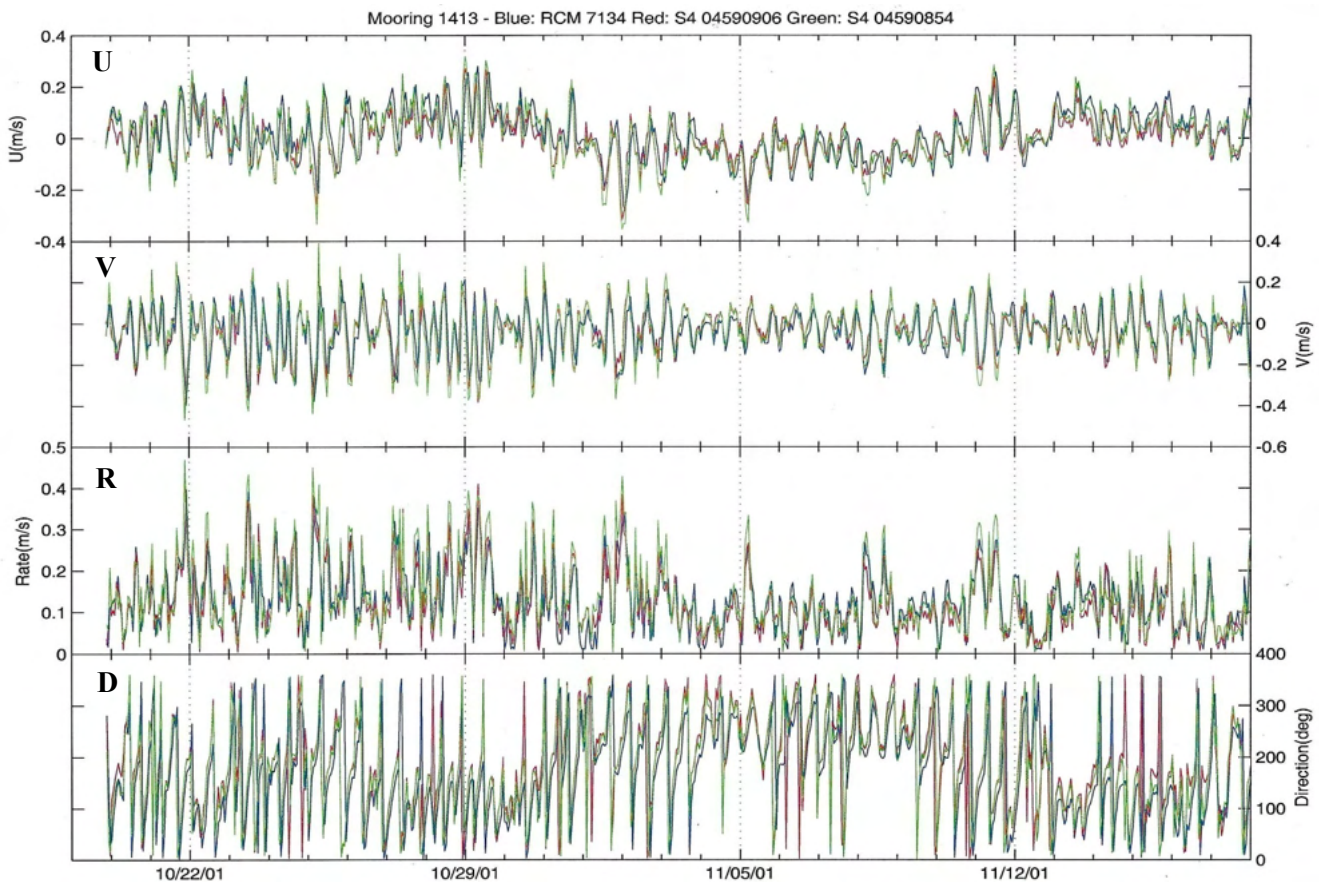


**Figure 44.** Time series of U, V, R and D from the three current meters on M1413 at SS-C1 during the first 29 days of the deployment: **S4 at 4 mab**, **RCM8 at 3 mab**, and **S4 at 2 mab**.

first 29 days of deployment SS-C1. Close agreement of the time series is apparent at the scale shown, but closer examination has indicated some unexpected vertical differences in the phase lags of the tidal currents from the S4(s) and RCM8 on both moorings (see the comments in the archived files).

Time series over the entire SS-C1 deployment of the differences between the Rates from adjacent current meters on M1413 (Fig. 45a), and scatterplots for the Rate datasets (Fig. 45b) provide further information on the differences. The most understandable differences are those between the two S4s with the R values at 4 mab higher than those at 2 mab, as expected for vertical shear in the bottom boundary layer. However, there is unexpected time variability in the difference time series for the S4s. The plots involving the RCM8 (at 3 mab) Rates indicate relatively high values - compared to the S4 ones at 2 mab, as expected in the presence of vertical shear, but again with notable time variability. On the other hand, the RCM R values (at 3 mab) are unexpectedly higher than the S4 ones at 4 mab for R values  $>0.2$  m/s, although slightly lower overall in weaker currents. Further investigation is needed to determine whether these differences and features are related to the different time sampling of the S4s and RCM8s, a clock or other instrument issue, or an actual unanticipated feature of the tidal boundary layer dynamics (perhaps related to time-varying internal waves).

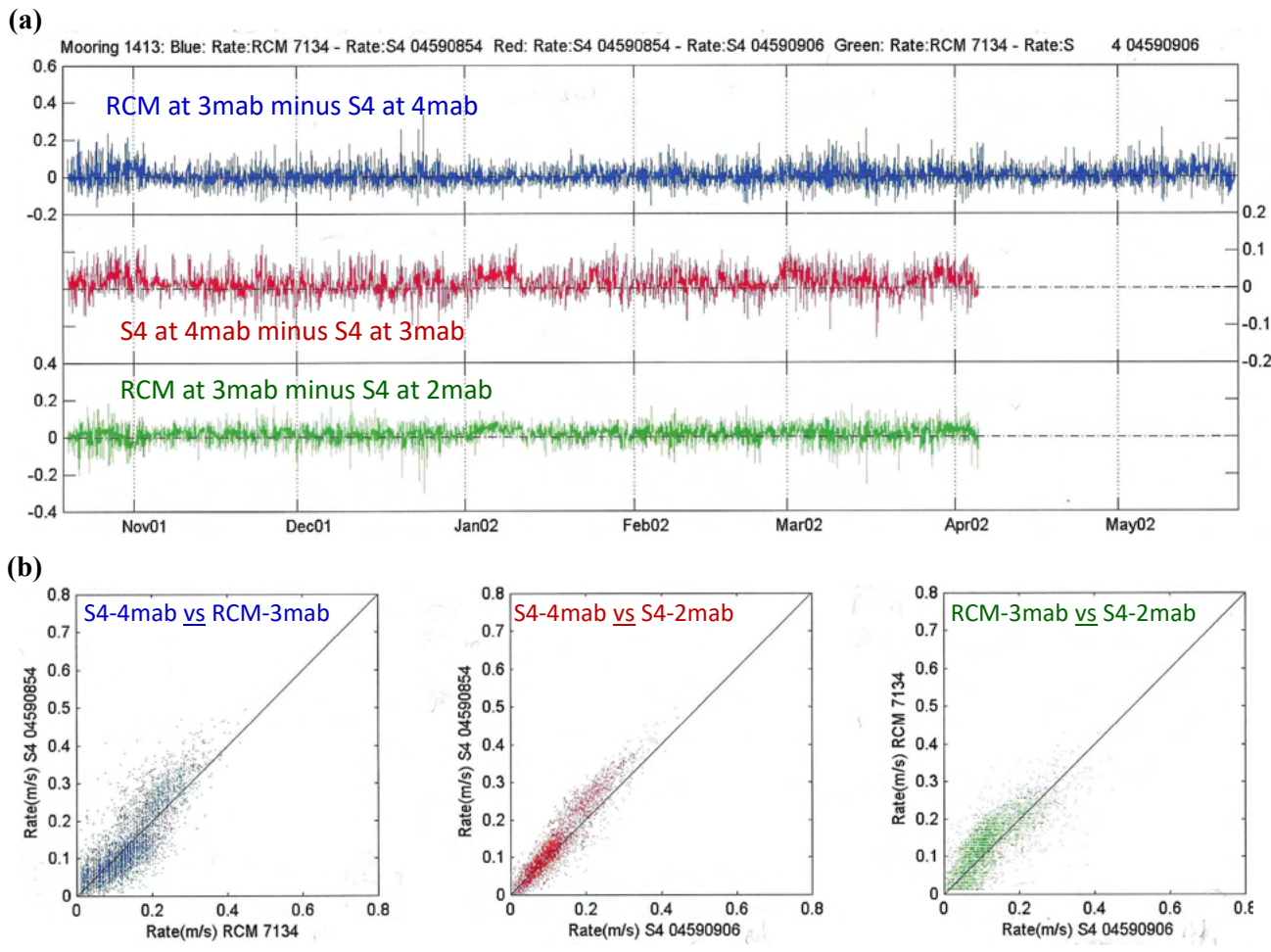


**Figure 45.** (a) Time series of the differences between the R values (m/s) measured by the 3 current meters on M1413 at SS-C1 from October 2001 to November 2002. (b) Scatterplots for the R values (m/s) from the 3 meters. The 1:1 line is included in each plot.

### 3.4 MicroCAT Temperature, Conductivity and Pressure Recorders

#### 3.4.1 Overall Summary

A total of 40 Seabird Electronics SBE37 MicroCAT (MCs) were deployed during the 2000-04 program: 17 at site SS-A, 18 at SS-B and 5 at SS-C (Table 8a,b). Fewer MCs were deployed at SS-C because of the shallower water depth and the greater S variability there such that the RCM8s (see Table 5) would hopefully provide adequate Conductivity (C) and hence Salinity measurements. For example, only one of the RCM8s deployed at SS-B (in SS-B5) had a C cell because all the other RCM8s were deployed at depths of 500 mbs or greater where the (deep-ocean) S variability had a small magnitude (requiring particular attention) and where BIO had previously experienced issues with RCM C cell performance.

**Table 8a. SS-A.** Listing of MicroCAT (MC) and Minilog (ML) deployments during the 2000-04 and 2004-08 Scotian Slope programs, organized by site (SS-A, -B, -C, -D, -E) and deployment (D) # (1 to 6, but variable with site). The other columns indicate the BIO mooring #, the instrument type (MC or ML) and serial #, the record start and end dates in the format day/month/(year-2000), the water and instrument depths, the variables sampled, the sampling interval (in minutes). Comments on data quality, especially for salinity (S), are also included.

Site	D #	BIO #	Instruments		Start Date	End Date	Depths (m)		Vari-ables	Smpl Intvl	Comments (rble =reliable, spk=spike; ΔS = S offset)
			Type	Ser #			Wter	Instr			
SS-A	1	1352	ML	2522	13/06/00	12/09/00	1119	68	T	2	
		1352	ML	2523	13/06/00	28/07/00	1119	79	T	1	
		1352	ML	2524	13/06/00	12/09/00	1119	99	T	2	
		1352	ML	2525	13/06/00	12/09/00	1119	189	T	2	
		1352	ML	2526	13/06/00	12/09/00	1119	244	T	2	
	2	1377	MC	1708	21/11/00	31/05/01	1124	148	TCP	2	Period of bad P; ΔS<0.1
		1377	MC	1601	21/11/00	31/05/01	1124	274	TC	2	Period of bad C; ΔS<0.1
		1377	MC	0863	21/11/00	31/05/01	1124	524	TCP	4	ΔS<0.02
		1377	MC	0906	21/11/00	31/05/01	1124	1024	TC	4	ΔS<0.02
	3	1387	MC	1548	31/05/01	25/09/01	1195	210	TCP	4	Mooring struck; ΔS<0.02
		1387	MC	1918	31/05/01	25/09/01	1195	335	TCP	4	Mooring struck; S<0.02
		1387	MC	1784	31/05/01	25/09/01	1195	585	TCP	4	Ditto; Period of bad C; ΔS<0.02
		1387	MC	1696	31/05/01	25/09/01	1195	1085	TCP	4	Ditto; Period of bad C, P; ΔS<0.02
	4	1419	MC	1548	21/10/01	24/06/02	1140	280	TCP	4	ΔS<0.06
		1419	MC	1696	21/10/01	24/06/02	1140	530	TCP	4	All P bad; ΔS<0.03
		1419	MC	1784	21/10/01	24/06/02	1140	1030	TCP	4	Period of bad P; ΔS<0.02
	5	1432	ML	2526	25/06/02	22/05/03	1144	152	T	10	
		1432	MC	2305	25/06/02	05/05/03	1144	284	TCP	4	Periods of bad C; ΔS<0.05
		1432	MC	2307	25/06/02	05/05/03	1144	534	TCP	4	ΔS<0.03
		1432	MC	1918	25/06/02	05/05/03	1144	1034	TCP	4	P drft 20db; ΔS<0.02 w P spcfd
6	1478	MC	1831	22/05/03	07/04/04	1125	74	TCP	4	ΔS<0.05	
	1478	MC	2292	22/05/03	07/04/04	1125	515	TCP	4	ΔS<0.05	
	1478	MC	1696	22/05/03	07/04/04	1125	1015	TCP	4	ΔS<0.05; P drft 20db	

(continued on next page)

Most of the deployed MCs had P sensors. The 3 MC records from SS-A5 ended about 2 weeks early.

**Table 8b. SS-B, SS-C.** Listing of MicroCAT (MC) and MiniLog (ML) deployments during the 2000-04 and 2004-08 Scotian Slope programs, organized by site and deployment # (see Table 8a for further details).

Site	D #	BIO #	Instruments		Start Date	End Date	Depths (m)		Variables	Sampling Intvl	Comments (rble =reliable, spk=spike; $\Delta S$ = S offset )	
			Type	Ser #			Wter	Instr				
SS-B	1	1388	MC	1708	01/06/01	20/10/01	1991	392	TCP	4	$\Delta S < 0.05$	
		1388	MC	1711	01/06/01	20/10/01	1991	991	TCP	4	$\Delta S < 0.03$	
		1388	MC	1785	01/06/01	20/10/01	1991	1592	TCP	4	Drift in P -61db; $\Delta S < 0.02$	
		1388	MC	1611	01/06/01	20/10/01	1991	1966	TC	4	$\Delta S < 0.02$	
	2	1412	MC	1708	21/10/01	24/06/02	1995	396	TCP	4	$\Delta S < 0.05$	
		1412	MC	1711	21/10/01	24/06/02	1995	995	TCP	4	Bad P; $\Delta S < 0.03$	
		1412	MC	1785	21/10/01	24/06/02	1995	1595	TCP	4	Periods of bad C; $\Delta S < 0.02$	
		1412	MC	1601	21/10/01	24/06/02	1995	1970	TC	4	$\Delta S < 0.02$	
	3	1429	MC	2304	25/06/02	20/10/02	2015	416	TCP	4	$\Delta S < 0.05$	
		1429	MC	2293	25/06/02	20/10/02	2015	1015	TCP	4	Drift in P -34db; $\Delta S < 0.04$ (specified P)	
		1429	MC	2292	25/06/02	20/10/02	2015	1990	TCP	4	$\Delta S < 0.02$	
	4	1454	MC	0862	20/10/02	14/04/03	2101	502	TCP	4	$\Delta S < 0.05$	
		1454	MC	1696	20/10/02	14/04/03	2101	1101	TCP	4	$\Delta S < 0.04$	
		1454	MC	1601	20/10/02	14/04/03	2101	2076	TCP	4	No P; Period of bad C; $\Delta S < 0.04$	
	5	1479	MC	1708	19/05/03	09/04/04	1991	92	TCP	4	$\Delta S < 0.1$	
		1479	MC	1829	19/05/03	09/04/04	1991	392	TCP	4	$\Delta S < 0.1$	
		1479	MC	2796	19/05/03	09/04/04	1991	991	TCP	4	$\Delta S < 0.05$	
		1479	MC	1601	19/05/03	09/04/04	1991	1966	TCP	4	$\Delta S < 0.05$	
	SS-C	1	1414	MC	0702	19/10/01	22/05/02	302	84	TCP	4	
			1414	MC	1916	19/10/01	22/05/02	302	291	TCP	4	
2		1431	ML	2525	22/05/02	19/10/02	305	2	T	10	On guard buoy	
		1431	ML	2522	22/05/02	19/10/02	305	85	T	10		
		1431	ML	2523	22/05/02	19/10/02	305	205	T	10		
		1431	ML	2524	22/05/02	19/10/02	305	280	T	10		
		1431	MC	2306	22/05/02	19/10/02	305	294	T	4	$\Delta S < 0.07$	
3		1455	MC	1708	19/10/02	24/12/02	305	87	TCP	4	$\Delta S < 0.2$ (probably less)	
		1455	MC	0864	19/10/02	24/12/02	305	294	TCP	4	$\Delta S < 0.05$	
4		1491	ML	2522	14/07/03	23/04/04	295	2	T	10	On guard buoy	
	1491	MC	1548	14/07/03	07/04/04	295	31	TCP	4	$\Delta S < 0.2$		

(continued on next page)

All of the MCs in the 2000-04 program were returned and provided mostly good T, C and S data. However, the 4 MCs on M1387 at SS-A3 and the 2 MCs on M1455 at SS-C3 had shortened good-data records (like other instruments on those moorings) because of the moorings having been struck by fishing vessels (Tables 2, 8). Otherwise, all of the returned T data from the MCs were of good quality.

Quality control of the P and S data from the MCs was carried out similar to QC for those variables from the RCMs. No P data, or obviously flawed data, were returned from a few of the MCs. There was a significant offset or drift in a few of the records (Table 8a,b), in which case a constant P value estimated from other information from the mooring was used in the computation of S. A similar approach was taken in the occasional occurrence of a period of bad P data. In a few of the records there were obvious periods with bad S data (related to bad C data probably resulting from interference in the C cell), in which case S was set to a NoData value.

The reliability of the remaining S time series was then assessed through comparisons with: (i) the concurrent T time series (for consistency in T-S space) from the instrument, (ii) S from other instruments on the mooring or from the previous or next MC at the same position, and (iii) the concurrent T and S data from nearby CTD profiles. In the latter comparison, the consistency of the T values provided an indication of whether consistent S values should be expected (in consideration of potential horizontal property gradients in the frontal zone). The expected reliability of each S time series based on these assessments has been noted in the archived ODF files at BIO, and is cursorily indicated in Table 8a, b.

Seven of the 8 MCs deployed (at 10 mab) in the 2004-08 program provided good T and S data, the exception being at SS-E1 (Table 8c). Two of the other MCs did not yield good P data, in which case S was computed with a specified P. Small P drifts occurred in some other cases but the measured P was still used for S. There were occasional spikes in S in various time series which were replaced using linear interpolation. The T and S data quality were assessed through comparisons with adjoining records and nearby CTD profiles, and comments added to the archived datafiles (also cursorily in Table 8c).

**Table 8c. SS-D, SS-E.** Listing of MicroCAT (MC) deployments during the 2004-08 Scotian Slope program, organized by site and deployment # (see Table 8a for further details).

Site	D #	BIO #	Instruments		Start Date	End Date	Depths (m)		Variables	Sampling Intvl	Comments (r=reliable, spk=spike; ΔS = S offset)
			Type	Ser #			Wter	Instr			
SS-D	1	1547	MC	1918	22/10/04	01/10/05	2452	2442	TCP	5	Bad P; <i>S hi 0.02-0.05</i>
	2	1585	MC	3510	23/10/05	10/10/06	2419	2409	TCP	5	<i>S low 0.02-0.05</i>
	3	1623	MC	2436	10/10/06	07/10/07	2425	2415	TCP	5	P drft -1db; ΔS 0.02-0.04
	4	1666	MC	2415	07/10/07	01/10/08	2438	2428	TCP	5	Bad P <i>S hi 0.03-0.04; Sspct S jump 0.02</i> on 23 Nov
SS-E	1	1548	MC	3300	22/10/04	23/10/05	3418	3408	TCP	5	No good data
	2	1586	MC	3309	23/10/05	20/10/06	3414	3404	TCP	5	ΔS 0.01
	3	1624	MC	1785	11/10/06	07/10/07	3395	3285	TCP	5	P drft -11db; ΔS 0.01
	4	1667	MC	1918	07/10/07	01/10/08	3414	3404	TCP	5	ΔS 0.01

### 3.4.2 Example MC Data Displays

Examples of the time series from the MCs in the 2000-04 program are shown in Fig. 46 from M1377 in SS-A2 and in Fig. 47 from M1412 in SS-B2.

Similarities in the T and S variability at the upper 3 MC positions in SS-A2 are apparent (Fig. 46) including decreases in both T and S at 148 and 247m in late March 2001, and a notable 3-week period of near-constant values in both T and S at 148m starting in late April (probably a “thermostat” and

“halostad” as result of mixing during wintertime surface convection). As expected there was less similarity between the weaker variations at the 2 deeper positions 500m apart in each of T and S, although

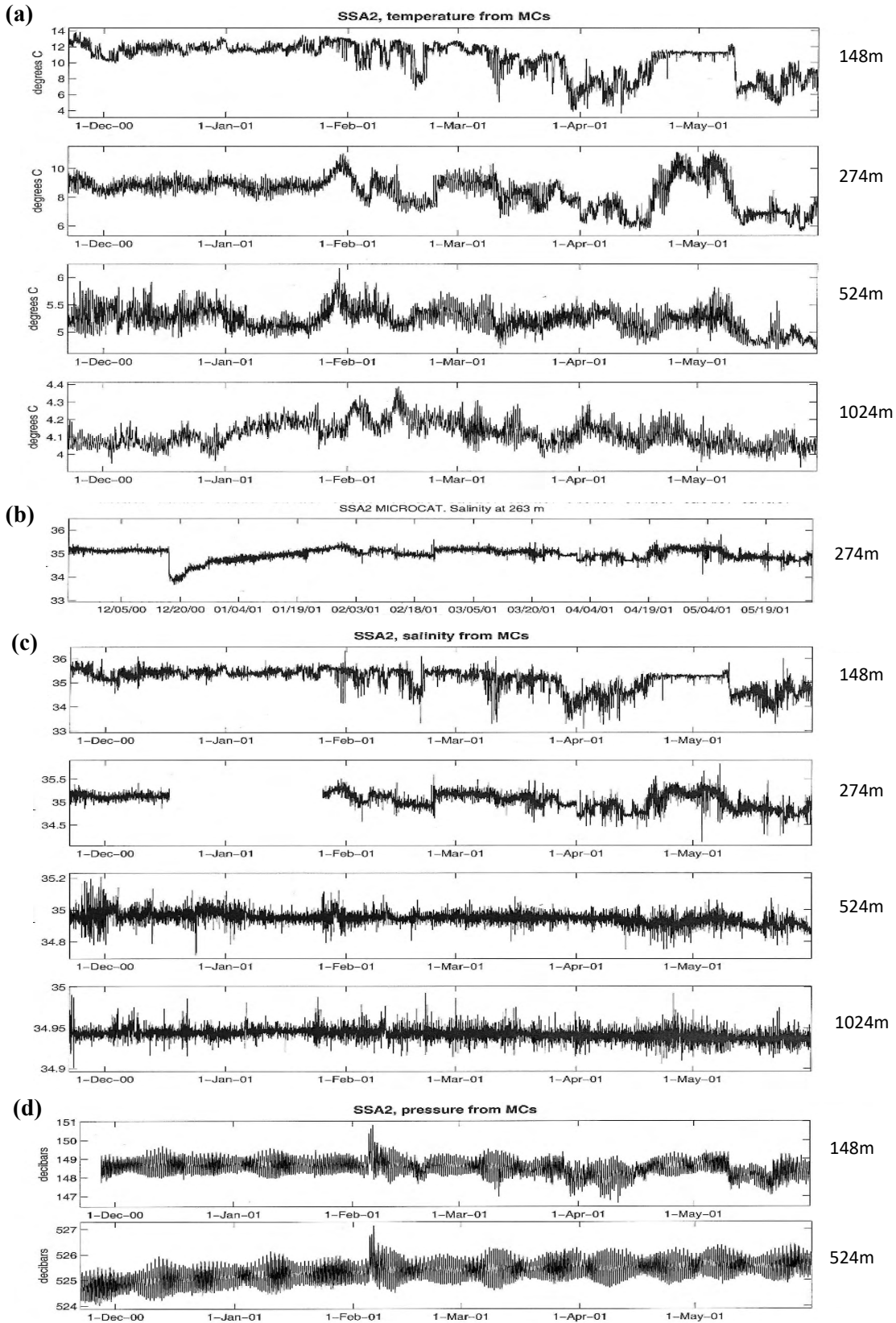


**Figure 46.** Time series of (a) T and (c) S from the 4 MCs on M1377 in SS-A2, and (d) P from 2 of the MCs. An earlier version of S from the 274m MC is shown in (b), prior to a period of bad S being set to NoData.

similarity between the T and S variations at each depth. To illustrate the occurrence of interference in an MC cell, Fig. 46b shows the S time series from 274m before the QC with an abrupt drop of about 1 unit in S in mid December 2000 followed by a gradual rebound over the following month. In the absence of a comparable feature in the T series at this position, the S values during this period were set to NoData (as in Fig. 46c). The P time series from 2 of the MCs indicates a small mooring knockdown by ~4m in February 2001, along with tidal and other (especially at the upper position) variations. The weak instrumental drift by ~1db at the 524m MC was considered insignificant to the S computation in this case.

Similarly, the MC time series from SS-B2 (Fig. 47) show notable similarities between the T and S variability at each of the upper 3 positions, especially at the upper 2 where the signals were larger, and similar variations across 2 of the upper 3 positions at times, but not at others. Of note here are some abrupt changes in S at 995m in April-May, with corresponding abrupt changes in T, such that these were actual ocean changes (in contrast to the one discussed above in SS-A2). However, portions of the S record at 1595m were set to NoData due to poor quality.

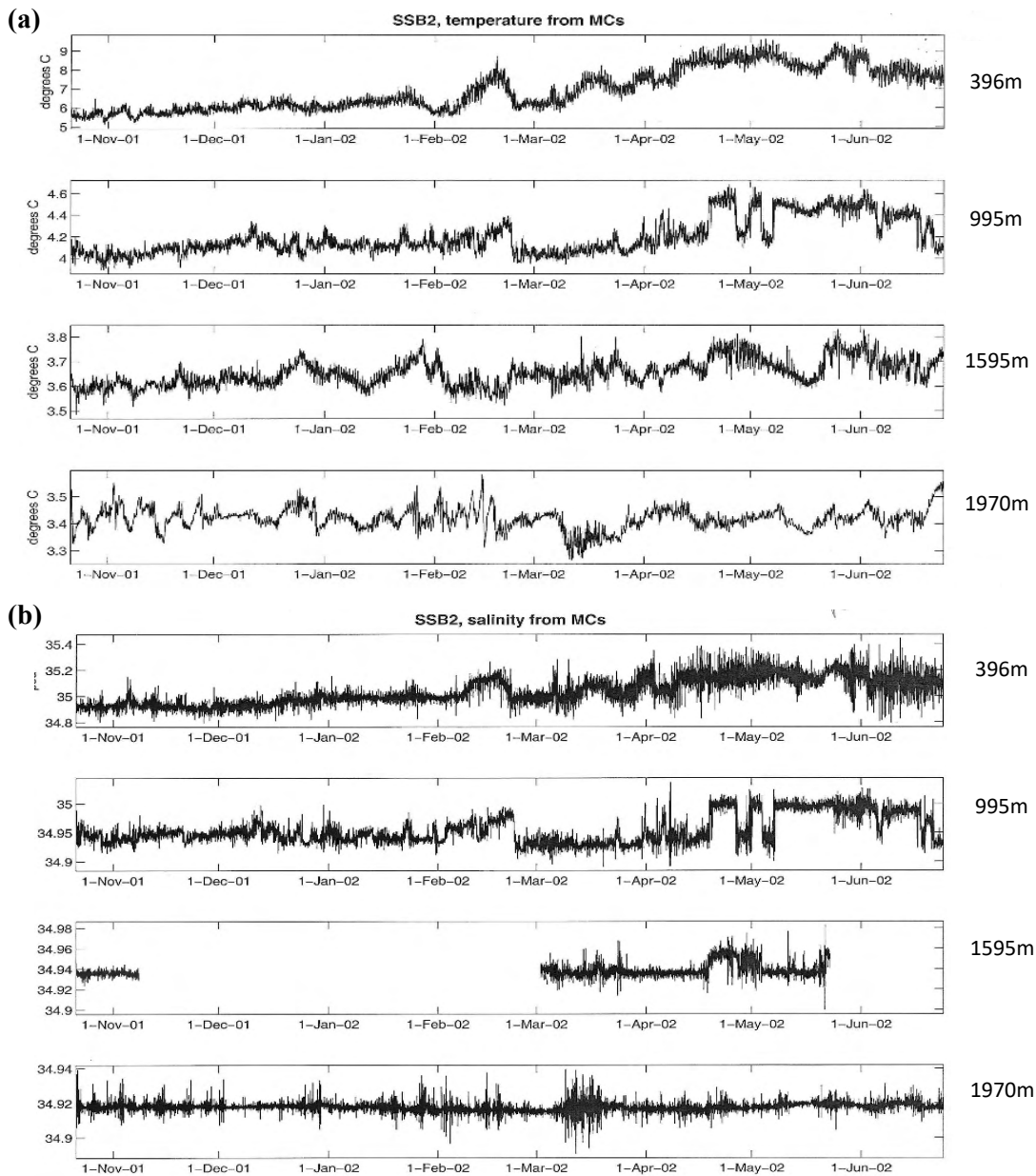


**Figure 47.** Time series of (a) T and (b) S from the 4 MCs on M1412 in SS-B2.

As an example from SS-C, time series of T, S and P from the 2 MCs in SS-C1 are shown in Fig. 48. There are similarities in the T and S variations at 84m, but less so at 291m. Note that, in this and the previous cases at SS-A and SS-B, these changes have the same sign because the instruments were deeper than 50 mbs where the major contribution to water mass variability came from horizontal advection, of either cooler and fresher water subpolar water from the shelf or east, or of warmer and saltier water from the south. In contrast, it might be expected that T and S changes in the near-surface region in the “summer” stratification season, when relatively warm and fresh water overlies cooler and saltier water, would be of opposite sign if associated with vertical displacements or vertical mixing.

The signatures of the remnant warm ring in April-May 2002 are also apparent in these records, with warmer and saltier water at both depths, and a mooring knockover by over 10m. An instrumental drift of ~2 db in the P record from 291m is apparent.

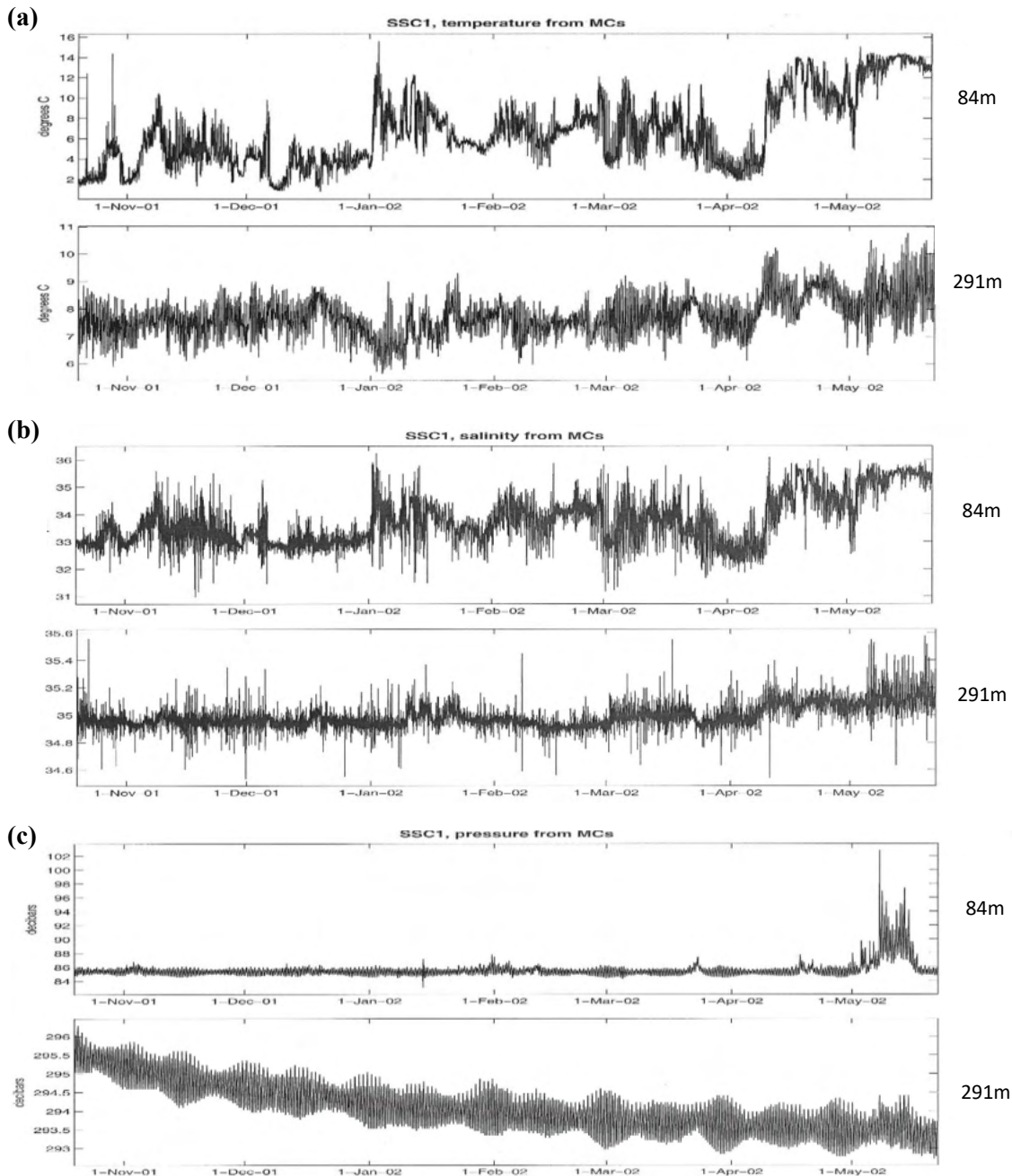


**Figure 48.** Time series of (a) T, (b) S and (c) P from the 2 MCs on M1414 in SS-C1.

Examples of the time series from the MCs in the 2004-08 program are shown in Fig. 49, specifically from the MCs at 10 mab in SS-D3 and SS-E3. The ranges of T variability at these two sites was  $\sim 0.5^{\circ}\text{C}$  and  $\sim 0.4^{\circ}\text{C}$ , and the ranges of reliable S variability  $< 0.4$ . Some spurious S spikes remain in the time series displayed in Fig. 49. P drifts are apparent, by  $\sim 1$  db at SS-D3 and  $\sim 11$  db at SS-E3. These measured Ps were used in the S computations in these cases; however, in the case of larger P drifts or offsets (as in a few other MC records from both the 2000-04 and 2004-08 programs), a specified constant value of P was used to compute S.

A few similarities in the T variations at two 2004-08 sites (approximately 40 km apart) are apparent, but the differences are more noticeable. An intriguing feature of the T variability in SS-E3 is an apparent saw-tooth pattern with a recurrence period of  $\sim 2$  months during much of the record, involving relatively abrupt decreases in T followed by much slower increases. These may be related to pulses in the DWBC moving westward around the Tail of the Grand Bank, or to cross-slope shifts in the position of the DWBC possibly related to Gulf Stream meandering events; e.g., abrupt displacements of the DWBC up the slope (with cooling at SS-E) followed by a slower relaxation to its usual position. Similar features are apparent in the 2008-14 RAPID Scotian measurements near the 3400- and 3800-m isobaths (Loder et al., 2025a).

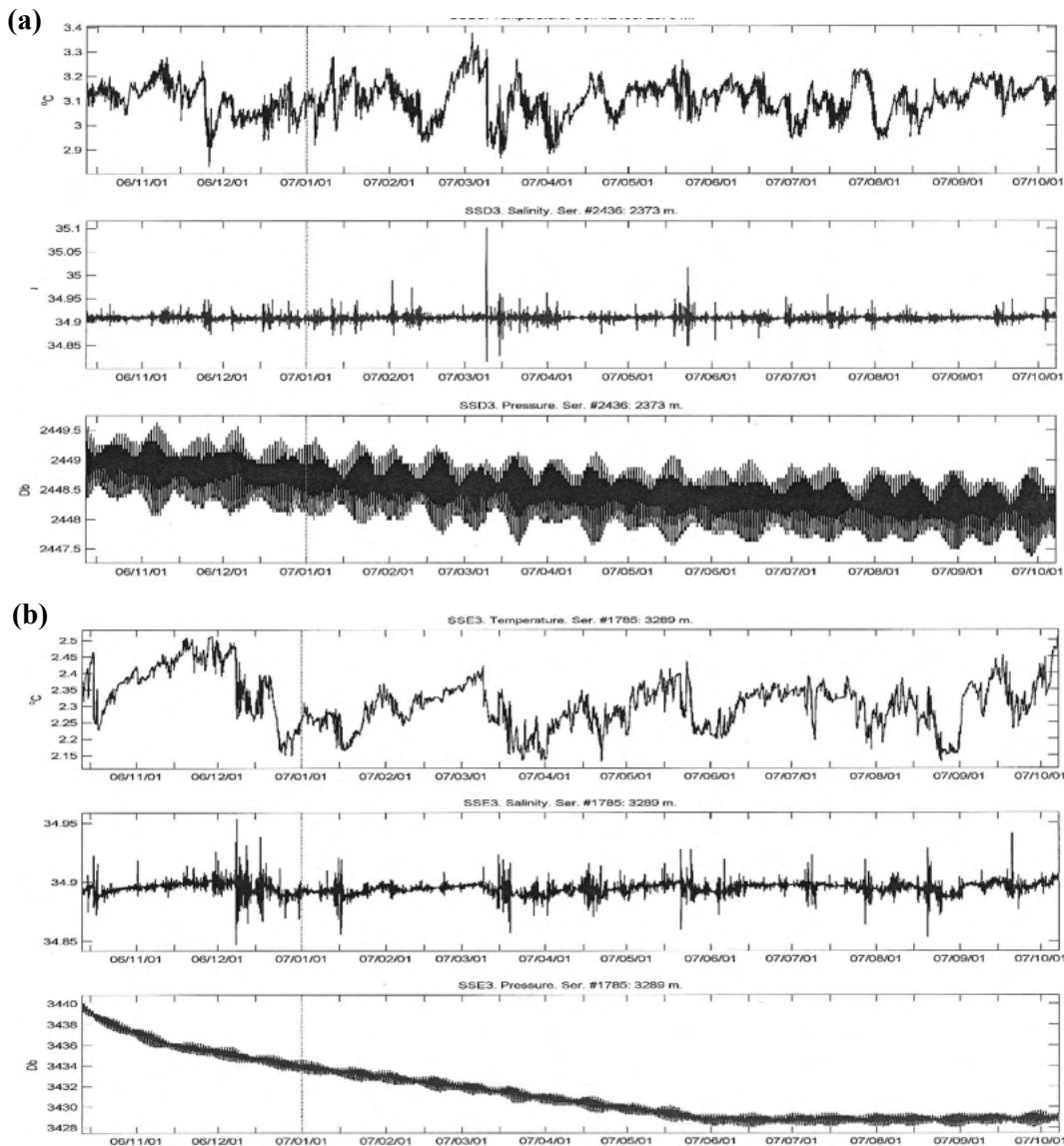


**Figure 49.** Time series of T (upper panels), S (middle) and P (lower panels) from (a) the MC at 2415mbs on M1623 in SS-D3, and (b) the MC at 3385 mbs on M1624 in SS-E3, from October 2006 to October 2007.

### 3.5 Minilog Temperature Recorders (MLs)

Additional moored measurements of T during the 2000-04 program were made using VEMCO Minilog (ML) temperature recorders ([https://www.bodc.ac.uk/data/documents/nodb/pdf/Vemco\\_minilog8.pdf](https://www.bodc.ac.uk/data/documents/nodb/pdf/Vemco_minilog8.pdf)) at sites SS-A and SS-C (Table 8). A total of 11 MLs were deployed – 6 at SS-A, mostly on SS-A1 (M1352); and 5 at SS-C, mostly on SS-C2 (M1431). The MLs were used on these particular moorings because of the unavailability of MCs. In deployments SS-C2 and SS-C4, an ML was attached to a guard buoy providing records of near-surface T at a depth of ~2 mbs. In SS-A5 which did not have an ADCP, an ML was attached to the top syntactic foam buoyancy float at 152 mbs. All of the MLs returned good data which have been archived at BIO as MTR ODF files (Table 8).

Example displays of the ML data are shown in Fig. 50, from SS-A1: the full T time series from the 5 MCs in Fig. 50a, and a 2-day zoom of T from 2 of the MLs and T from 3 nearby RCM8s on the mooring in Fig. 50b. Coherent variability on a range of time scales is apparent in the time series, from semidiurnal tidal variations to weeks and months with an apparent seasonal change (warmest in July-August at all depths). The comparison with the RCM8 records indicates that the ML measurements are reliable within a few tenths of a C°.

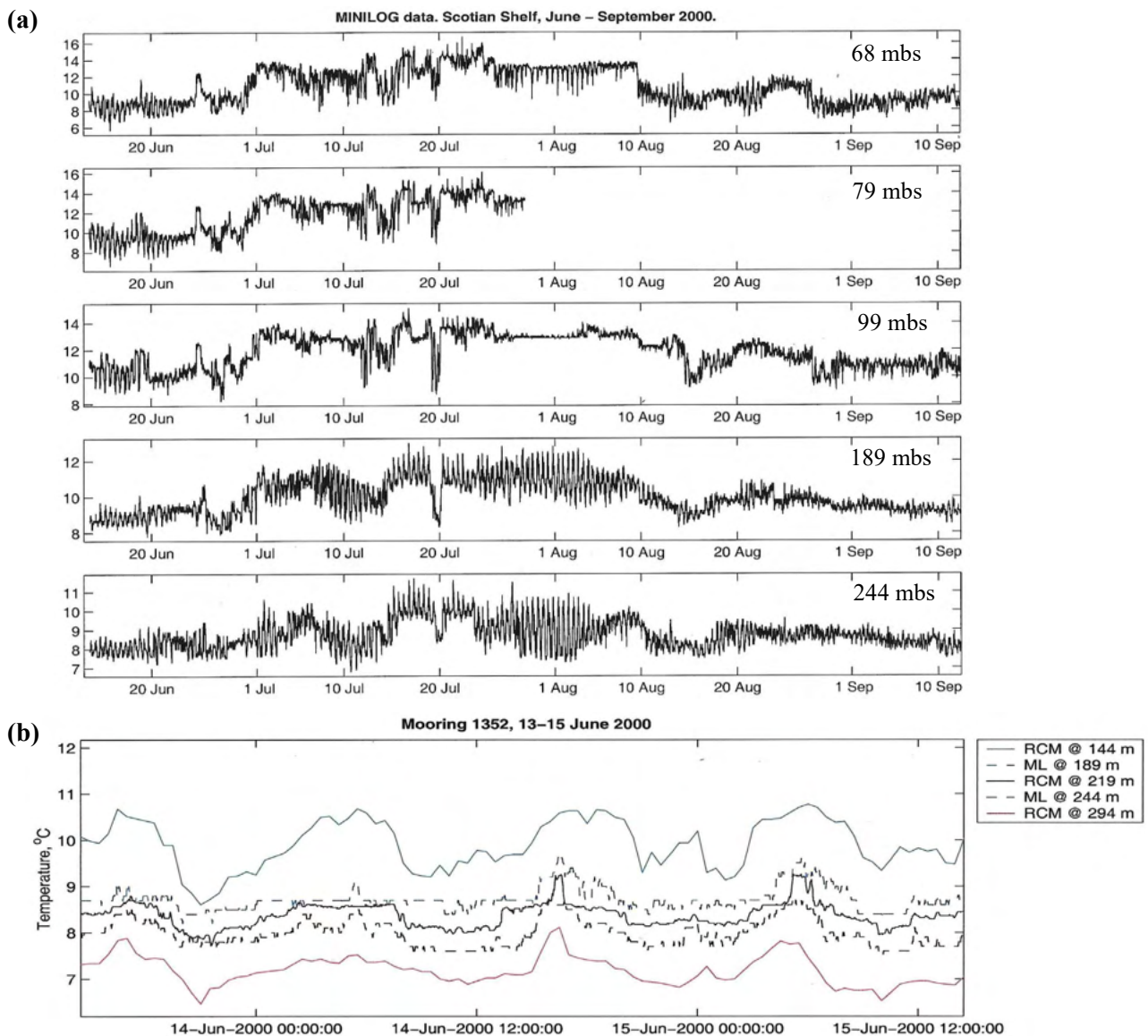


**Figure 50.** Time series of T (°C) from (a) the 5 MLs at SS-A1 over the entire deployment, and (b) two of the MLs and 3 nearby RCM8s on the moorings for ~2 days in June 2000.

### 3.6 Aanderaa Water Level Recorders

Five Aanderaa WLR8 Water Level Recorders (also commonly referred to as “bottom pressure recorders” or “tide gauges”) which measured bottom pressure and temperature were deployed during the 2000-04 program (Table 9). All were recovered and provided good datasets which are in the BIO MTR archive. The recording period was 60 minutes in all cases.

There were 3 WLRs deployed at SS-A which provided a continuous time series from October 2000 to May 2003 (31 months), and 2 deployed at SS-C which provided a continuous series from October 2001 to October 2002 (12 months). At SS-A, M1395 with a WLR was left in place for a full year, through both the SS-A3 and SS-A4 deployment periods. In all 3 of the deployments at SS-A, there was a slight P drift or transient during the first month or so of the deployment which appears to have been of instrumental (rather than oceanographic) origin.

**Table 9.** Listing of Water Level Recorders (WLRs) deployed during the 2000-04 Scotian Slope program, organized by site and sequential deployment #. Other columns indicate the BIO mooring #, WLR8 serial #, record start and end dates in format day/month/(year-2000), water and WLR depths, and comments.

Site	D #	BIO #	WLR8 Ser #	Start Date	End Date	Depths (m)		Comments
						Water	WLR	
SS-A	2	1379	1017	22/11/00	31/05/01	1115	1115	P drift +0.5db
	3/4	1395	1018	31/05/01	24/06/02	1123	1123	P drift +0.5db
	5	1433	1017	25/06/02	22/05/03	1144	1144	P drift +0.5db
SS-C	1	1413	334	19/10/01	22/05/02	317	317	
	2	1430	1271	22/05/02	19/10/02	314	314	

Example displays of the T and P time series from the WLR8 deployment on M1413 at SS-C1 are shown in Fig. 51. There are close similarities as expected between the T variations and those from the RCM8 at 3 mab on the same mooring (Fig. 27a), except during the last few days when the WLR8 T values were lower. It is unclear whether this is an actual ocean feature or indicative of a measurement flaw.

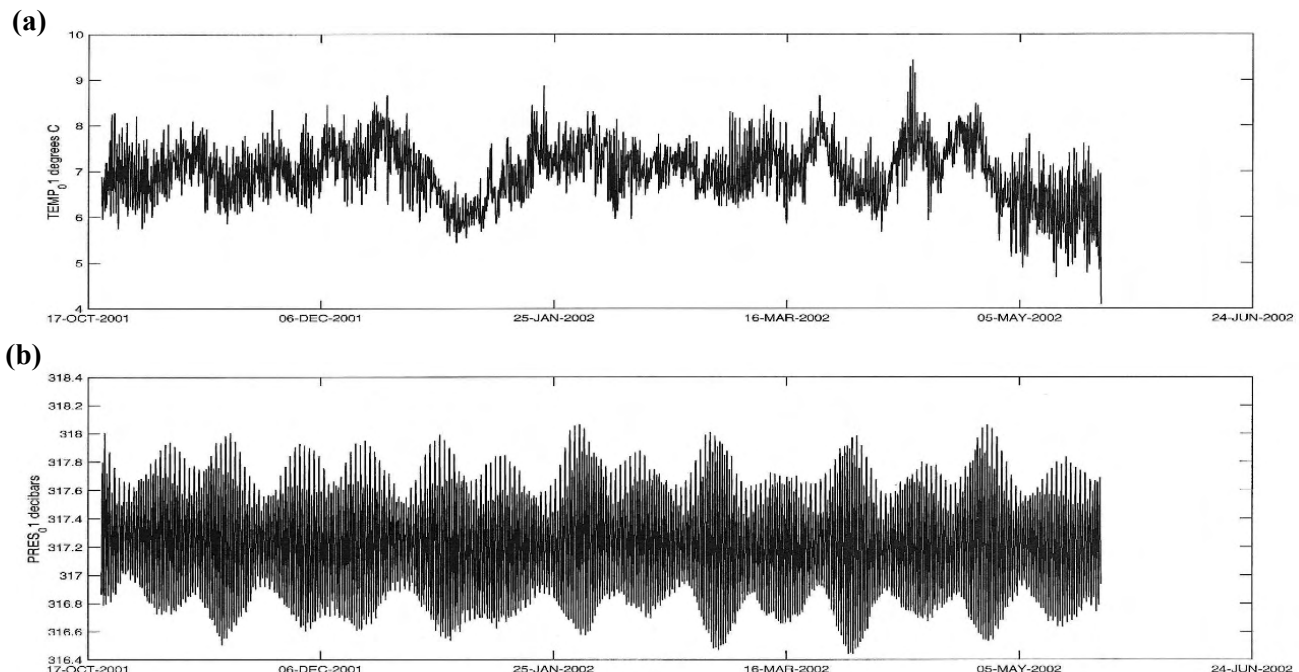


**Figure 51.** Time series of (a) T and (b) P from the WLR8 on M1413 in SS-C1 from October 2001 to May 2002.

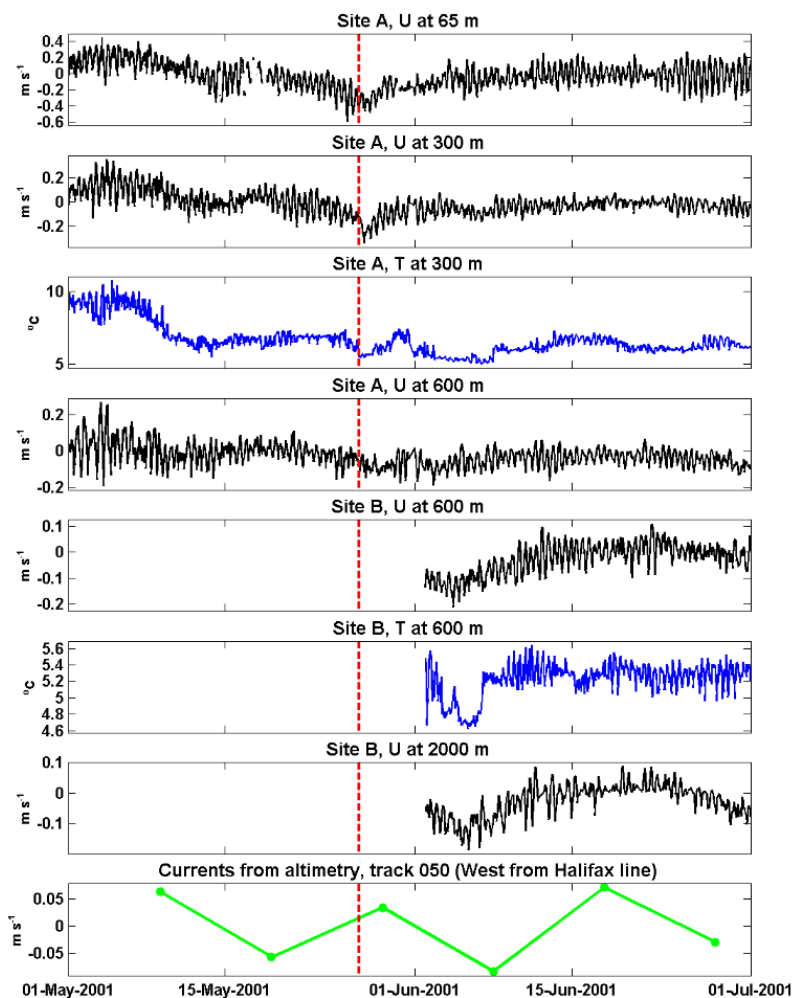
#### 4. Multi-Site and Multi-Year Time Series

In this section we present some available examples of moored time series involving multiple sites or multiple deployments. This is not intended to be a complete summary of the observational data but rather a cursory summary using available plots.

##### 4.1 Time Series involving Multiple Sites during 2000-04

Figure 52 shows time series of U and T from multiple depths at each of SS-A and SS-B, and of geostrophic surface current from altimetry for May-June 2001, using data from SS-A2, SS-A3 and SS-B1. The period is focussed on the increased westward flow at the approximate depths of 65, 300 and 600m at SS-A in late May, and an apparent similar increase in early June at the approximate depths of 600 and 2000m at SS-B (see Table 5 for the best estimates of the actual depths for the RCM8s from which these time series are taken). There is similarity in the low-frequency U variability at the 3 depths at SS-A, with a T reduction associated with the peak westward flow, and similarity in the low-frequency U variability at 600m at SS-A and SS-B and also at 2000m at SS-B, with reduced T associated with the peak westward flow at 2000m. There is also variability on an apparently similar time scale in the flow normal to the satellite track (also, see Figs. 16 and 18), but there may be aliasing of higher-frequency variability into the sawtooth pattern in the current time series from altimetry. Further investigation is needed.

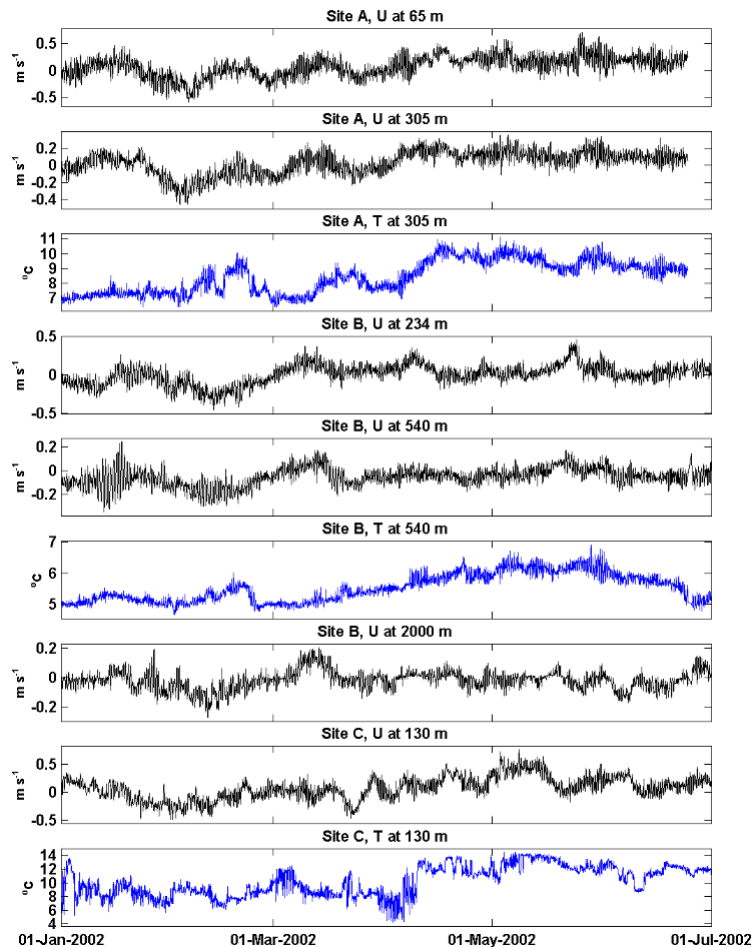
**Figure 52.** Time series of U from 3 depths at SS-A and 2 depths at SS-B, T from one depth at each of SS-A and SS-B, and the estimated geostrophic surface flow normal to the satellite altimetry track to the west of the mooring line for the 2-month period of May-June 2001. The subsurface U and V time series are from RCMs on M1378, M1387 and M1388, and the altimetric current estimates from Han (2007). The depths indicated on the plots are only approximate ones (see Tables 2 and 5 for the best-estimates of the depths of the RCMs involved).



Another example of concurrent time series from multiple depths and sites (in this case all 3 sites) is shown in Fig. 53 with U and T from January to June 2002, during which time the remnant warm-core eddy affected the oceanography at the mooring sites. The low-frequency flow at all 3 sites swung between eastward and westward at all 3 sites in January-March with different phasing from site to site, followed by

a series of eastward flow periods at SS-B and SS-A in March to June. There was associated warming at all positions during the latter period. Again, further investigation using all of the available data from the moored measurement program and AZMP (SST, HL sections, altimetry) should be instructive in untangling the complex variability associated with the eddy intrusion. The various observations from this period provide a unique dataset for describing and understanding the variability associated an eddy intrusion into the area of the primary Maritimes AZMP sampling line.

**Figure 53.** Time series of  $\underline{U}$  (in black) from 2 depths ( $\sim 65\text{m}$  from the ADCP and  $\sim 305\text{m}$  from an RCM8) at SS-A, 3 depths at SS-B ( $\sim 234\text{m}$  from the ADCP and  $\sim 540$  and  $2000\text{m}$  from RCMs), and 1 depth at SS-C (an RCM at  $\sim 130\text{m}$ ), and of  $\underline{T}$  (in blue) from 1 depth at each of SS-A, SS-B and SS-C (from RCMs) during the period January-July 2002. The time series from SS-A are from M1419, those from SS-B from M1412 and M1419, and those at SS-C from M1413 and M1431. The depths indicated above and on the plots are only approximate ones (see Tables 2, 5 and 6 for the best-estimates of the depths of the ADCPs and RCMs involved).



#### 4.2 Concatenated (Merged) Time Series from the 2000-04 Program

We start with time series of  $T$  from the first 4 deployments at SS-A, covering the period June 2000 to June 2002 (Fig. 54), drawing on RCM, MC and AVHRR data. The strong seasonal variation in SST is apparent, with annual maxima in late summer. There is also an indication of a seasonal variation at  $300\text{m}$  and below with seasonal maxima in winter, as might be expected with some combination of the gradual downward penetration of the upper-ocean summer maxima associated with vertical mixing and advection from upstream (e.g., Petrie et al., 1991; Umoh and Thompson 1994). However, it is unclear from these 2 years of data whether this was a recurring seasonal variation associated with summer surface warming or the result of more episodic variability associated with GS meanders and eddies.

Based on visual inspection, the  $T$  time series from the moored instruments in the 6 deployments at SS-A (Fig. 55a) are inconclusive with respect to a significant seasonal variation at depths of  $\sim 100\text{m}$  and below at this site. The same applies to the  $S$  series from the  $\sim 100\text{-}300$  mbs interval (Fig. 55b). Strong variability in  $T$  and  $S$  at various time scales days to months is apparent, and an additional complication is the different depths (by up to  $70\text{m}$ ) of the instruments in the different deployments because of the different water depths of the moorings. This is then also an issue for the multi-year density time series (Fig. 55c).

**Figure 54.** Time series of subsurface T at 5 approximate depths in the SS-A1 to SS-A4 deployments between June 2000 and June 2002 (lower 5 panels), and of SST from AVHRR from the BIO Remote Sensing Group (*SST time series provided by Dr. Brian Petrie*).

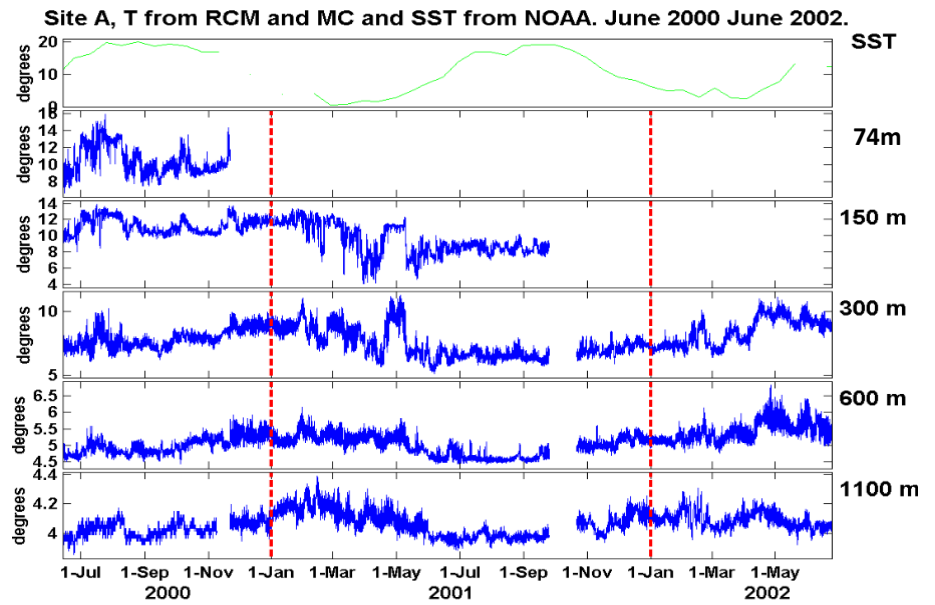
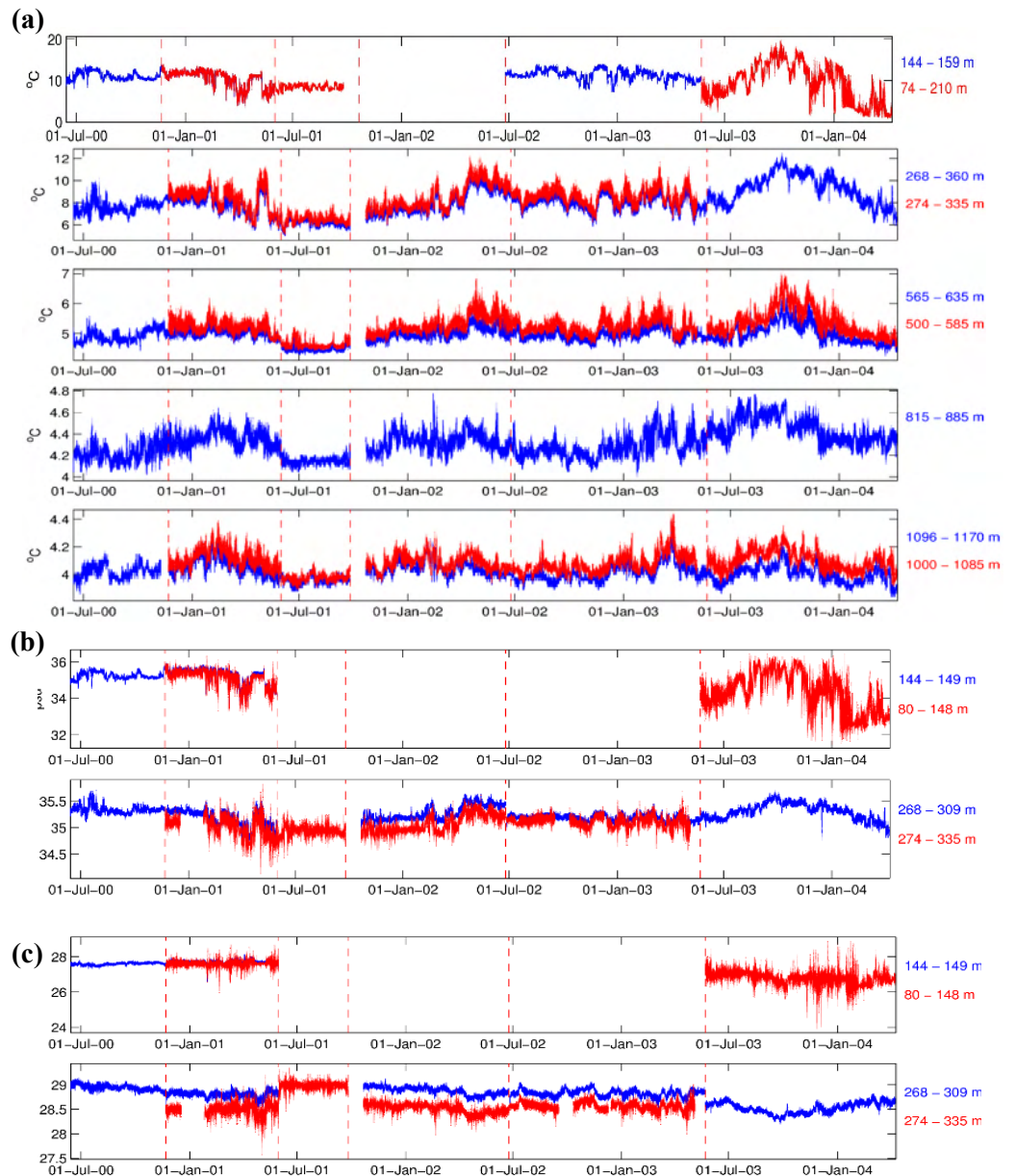


**Figure 55.** Time series of (a) subsurface T at 5 approximate depths in the SS-A1 to SS-A6 deployments between June 2000 and April 2004, and (b) S and (c) density (in  $\sigma_t$  units) at 2 of these approximate depths. The blue curves denote data from the RCMs, and the red curves data from the MCs. The depth ranges of these instruments in the different deployments are indicated to the right of each panel. T data from the MLs are not included.



The Rate time series at 6 approximate depths during the ~4-yr SS-A program are shown in Fig. 56, and the PVDs for 4 depths during the first 3 deployments in Fig. 57. The larger current speeds in the upper ocean are apparent, with a peak value of ~1 m/s at 45-49 mbs in October 2003, actually ~2 weeks after Hurricane Juan (which passed to the west) rather than during it. Peak values were <0.5 m/s at depths of ~600m and below, and <0.3 m/s at ~850m and below (see later). Gaps in the record associated with no ADCP coverage of the upper ocean in SS-A1 and SS-A2, and rotor stalling in SS-A4, are apparent.

The low-frequency current direction was primarily southwestward during deployments SSA1-SSA3 (Fig. 57) with the exception of the disruption in the upper 300m in January-April 2001 which was described earlier in relation to Fig. 35.

**Figure 56.** Time series of Rate from 6 different approximate depths in the SS-A1 to SS-A6 deployments between June 2000 and April 2004. The blue curves denote data from the RCMs, and the green curves data from the ADCPs. The depth ranges over the different deployments are indicated to the right of each panel. The start of each new deployment is indicated by the dashed red vertical lines. A common ordinate scale is used to emphasize the large vertical variation in current speed.

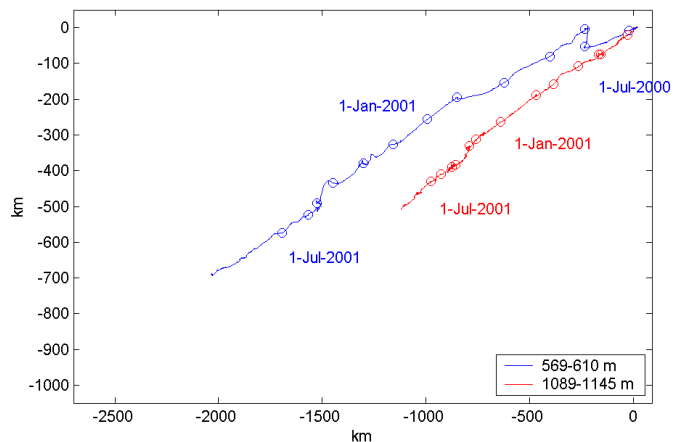
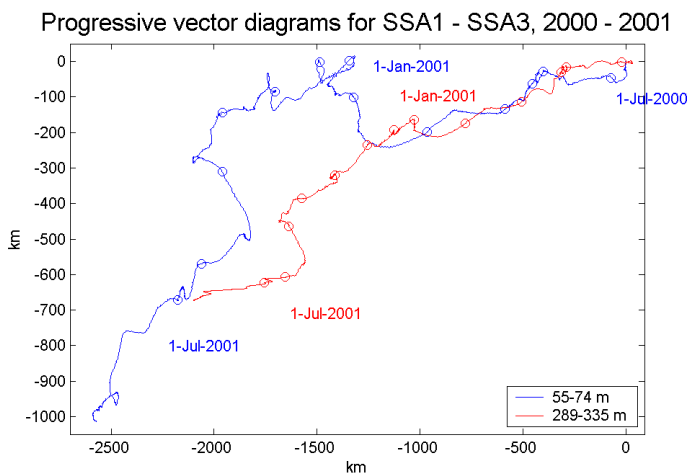
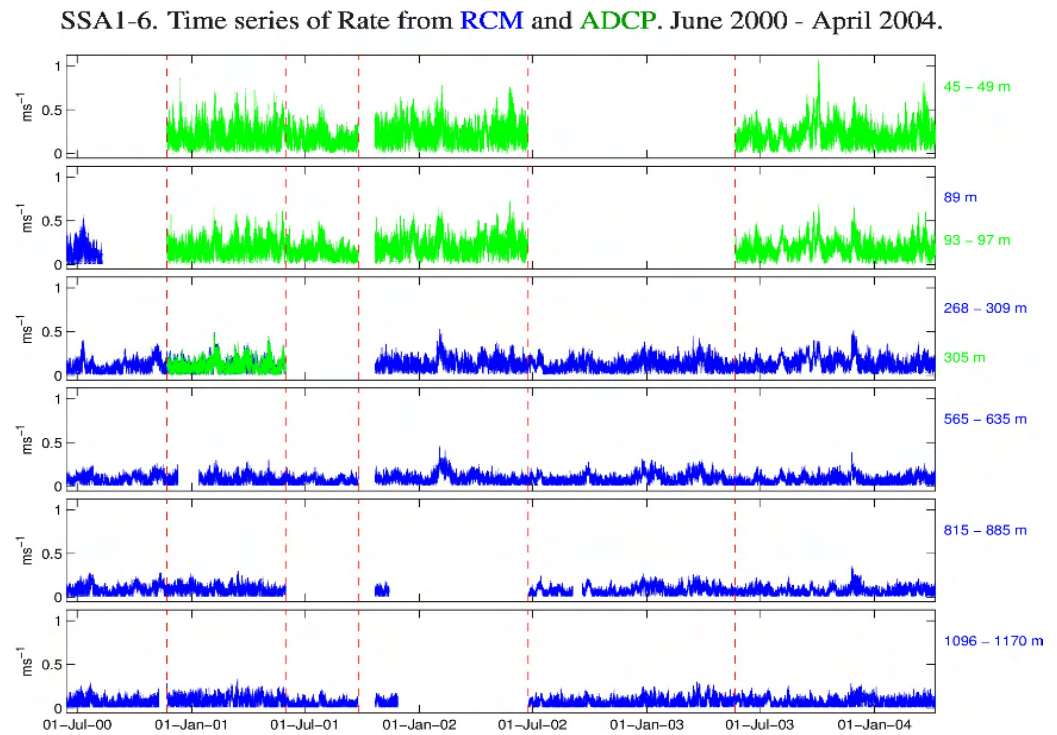
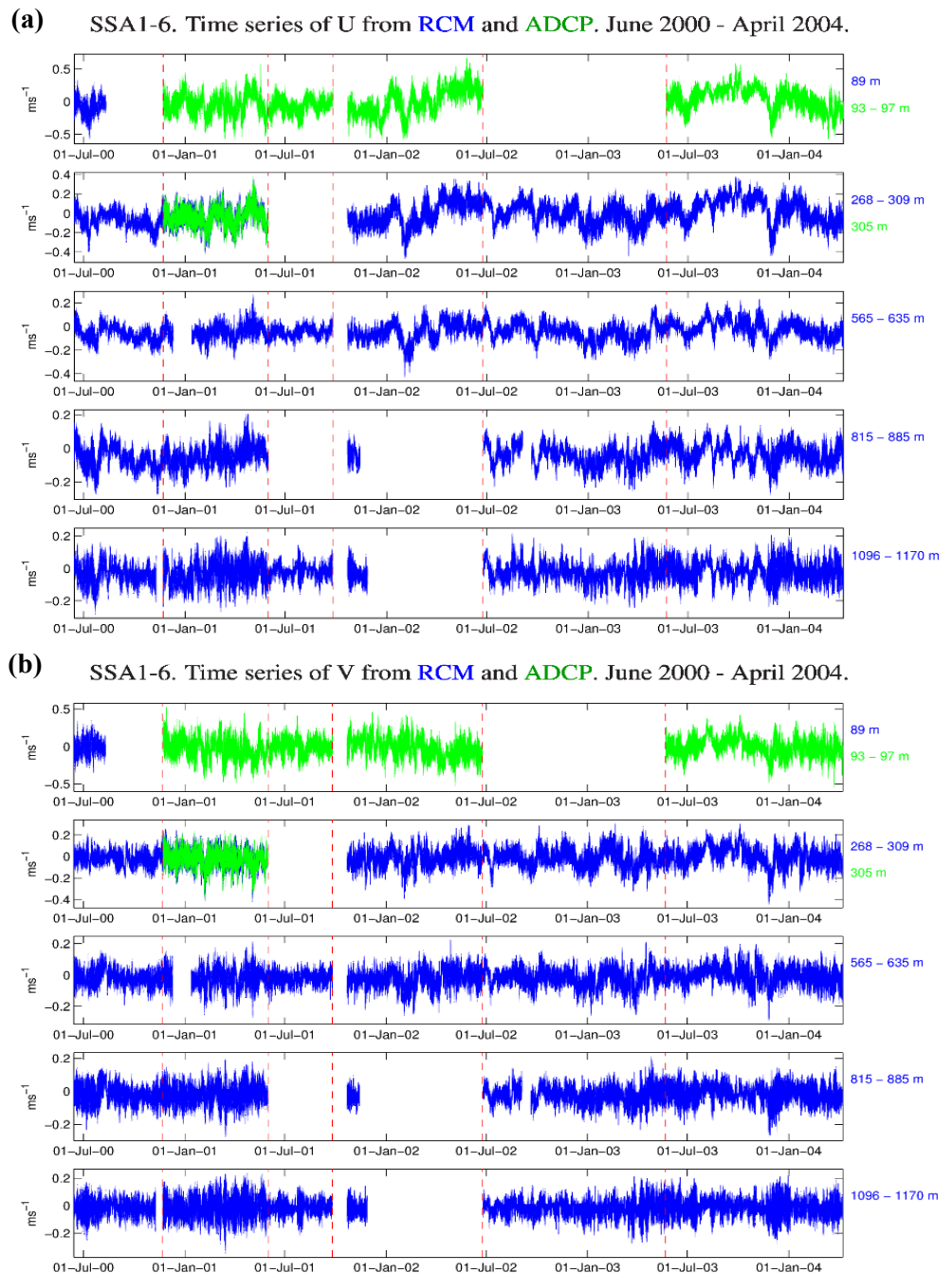


**Figure 57.** PVDs for the velocity in 4 different vertical intervals during deployments SS-A1 to SS-A3, from June 2000 to September 2001. The approximate vertical intervals are indicated in the legend boxes (note that some of the depths indicated may not be the final depths after small adjustments based on all available information). The velocity data for the shallowest interval is from a combination of RCMs and ADCPs, and for the other intervals from RCMs. The circles on the curves indicate 1-month intervals.

The time series of U and V at the same 5 approximate depths (as in Fig. 56) at SS-A are shown in Fig. 58. The magnitude of the east-west current fluctuations is slightly less than that of the north-south ones at all depths. A notable period of prolonged east-northeastward flow in early fall 2003, especially in the upper 300m is apparent during the period of warmer and saltier water there (Fig. 55). As described by Loder and Geshelin (2009) in relation to these observations, SST composites from satellite imagery, and the fall 2003 AZMP survey on the HL, this event was also associated with the incursion of a remnant warm-core eddy into the region.

There were also two notable short periods with increased flow in a generally southwestward direction during the 4-year mooring period at SS-A. One was for a 2-week period in later fall 2003 with the peak westward flow magnitude  $>0.5$  m/s at  $\sim 100$  mbs, the increased westward flow extending to at least 850 mbs, and associated cooling and freshening in the upper 300m. The other was in the upper 600m in February but without a distinct T and S signature.

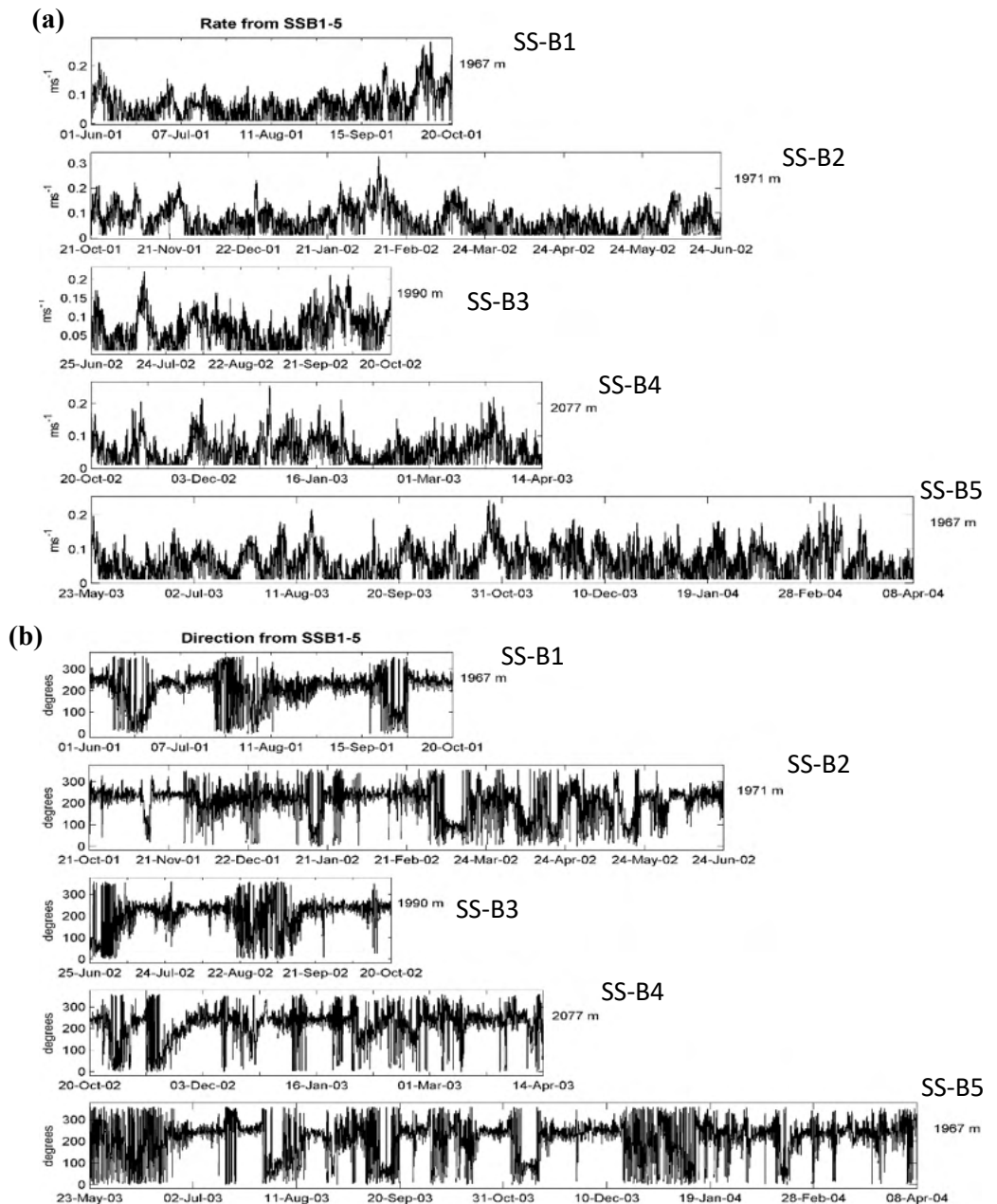
**Figure 58.** Time series of (a) U and (b) V from 5 different approximate depths in the SS-A1 to SS-A6 deployments between June 2000 and April 2004. The blue curves denote data from the RCMs, and the green curves data from the ADCPs. The depth ranges across the different deployments are indicated to the right of each panel.



Moving to the multi-deployment time series from site SS-B, Fig. 59 shows the records of R, D, U and V from the deepest RCM8 (at 25 mab) in the 5 deployments there. Differences in the length of the records are apparent, associated with the variable timing of opportunistic vessel availability for the mooring deployments and recoveries. The occurrence of substantial rotor stalling in all of the deployments is apparent (Fig. 59a), similar to that discussed in §3.1 in relation to SS-B2 (Fig. 22a). Interestingly, all of the 25-mab rotors re-started after periods no longer than 27 hours (Table 5), and thus no R values were set to NoData. The consistent re-starts indicate some sluggishness in the rotors in low currents and a threshold speed of at least few cm/s for their normal performance. However, the measurement of peak speeds of over 0.2 m/s in all of the deployments, including in the latter portion of 4 of them, indicates reliable performance other than during weak currents.

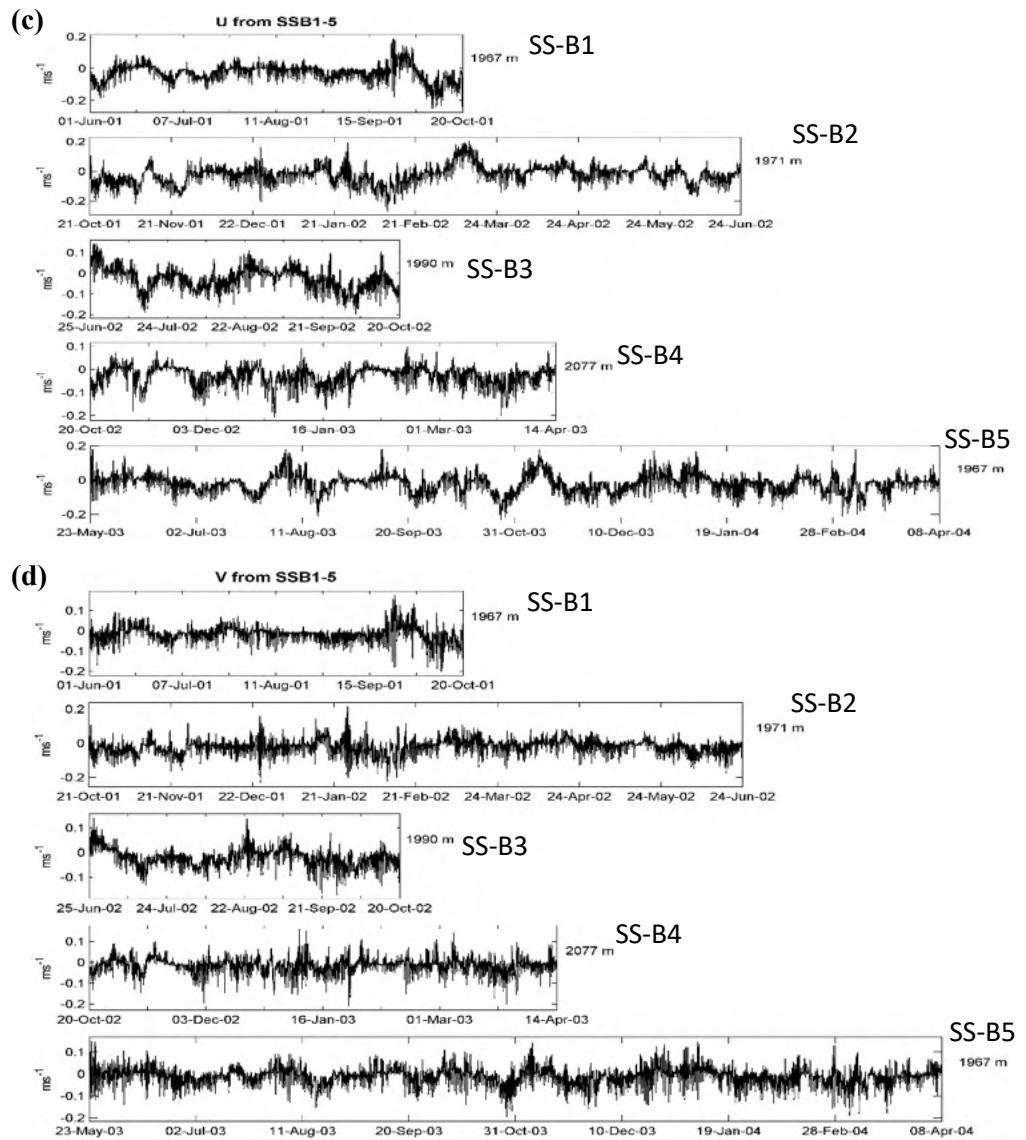
Flow was persistently in a generally southwestward direction most of the time in all the deployments, although there were multiple week-long periods of eastward flow in all of the deployments and also periods of variable flow direction (generally during weak currents) (Fig. 59b).

**Figure 59a,b.** Time series of (a) Rate and (b) Directions from the deepest RCM (at 25 mab) in the 5 deployments at SS-B, proceeding from SS-B1 (top panels) to SS-B5 (bottom panels). The time axis has the same scale in all the panels.



The occurrence of variability on a wide range of time scales in both U and V at 25 mab at SS-B (Fig. 59c,d), without any apparent prolonged periods of essentially no flow, is encouraging for the reliability of the RCM8 data from this position. Slight biases towards westward and southward flow are apparent in the respective flow components, but there are also periods of significant flow in other directions.

**Figure 59c,d.** Time series of (c) U and (d) V (m/s) from the deepest RCM (at 25 mab) in the 5 deployments at SS-B, proceeding from SS-B1 (top panels) to SS-B5 (bottom panels).



Time series of R from 7 approximate depths (actually vertical intervals) during the 5 deployments at SS-B are shown in Fig. 60. The gradual decrease in the current magnitude with depth is apparent, similar to that at SS-A (Fig. 56). However, the most striking feature of the time series is the occurrence of greatly enhanced current magnitudes in the upper 275m in the fall of 2003, during SS-B5. Peak magnitudes repeatedly exceeded 1.1 m/s in the upper 100m during a month-long period in September-October 2003, and the duration, depth and magnitude of the enhanced speeds were greater than at site SS-A (Fig. 56).

An important clue to at least part of the origin of the high current speeds at SS-B during this period comes from the combination of the T time series measured in SS-B5 and SST from AVHRR imagery. T at depths to 1100m was substantially enhanced in September 2003 (Fig. 61), and also somewhat at all depths (to ~2000m). As described by Loder and Geshelin (2009), this warming was related to a remnant warm-core eddy feature. Further examination of the multiple peak current events in the upper ocean at SS-B in September 2003 indicates that one of those peaks occurred on 23 September 2003 when Hurricane Juan

was moving northward over the Scotian Slope towards Nova Scotia. Further investigation is needed but it seems likely that two major episodic factors contributed to the greatly-enhanced current magnitudes at SS-B in that month. It is noteworthy that the 3<sup>rd</sup> year of upper-ocean current measurements at SS-B resulted in the measured peak speed during the program being twice as large as from the first 2 years. This points to the difficult issue of the appropriate probability distribution function for episodic factors in extremal analyses, and also the value of good observational datasets for describing and understanding complex difficult-to-measure events like those described here so that they can be understood and predicted better.

**Figure 60.** Time series of R from 7 approximate depth levels during the 5 deployments at SS-B, proceeding from ADCP data (green) for the upper ocean in the upper panels, to RCM8 data (blue) for the greater depths in the lowest 4 panels. Both ADCP and RCM data are included for the ~250m depth from SS-B5. The vertical intervals across the different deployments are indicated on the right.

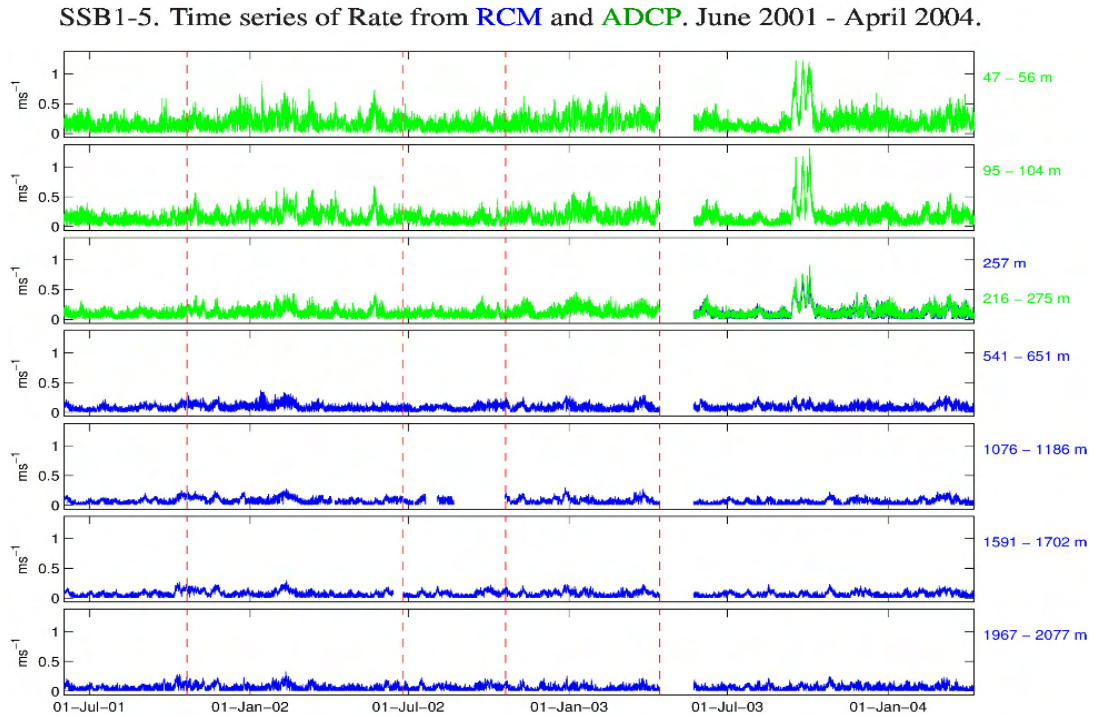
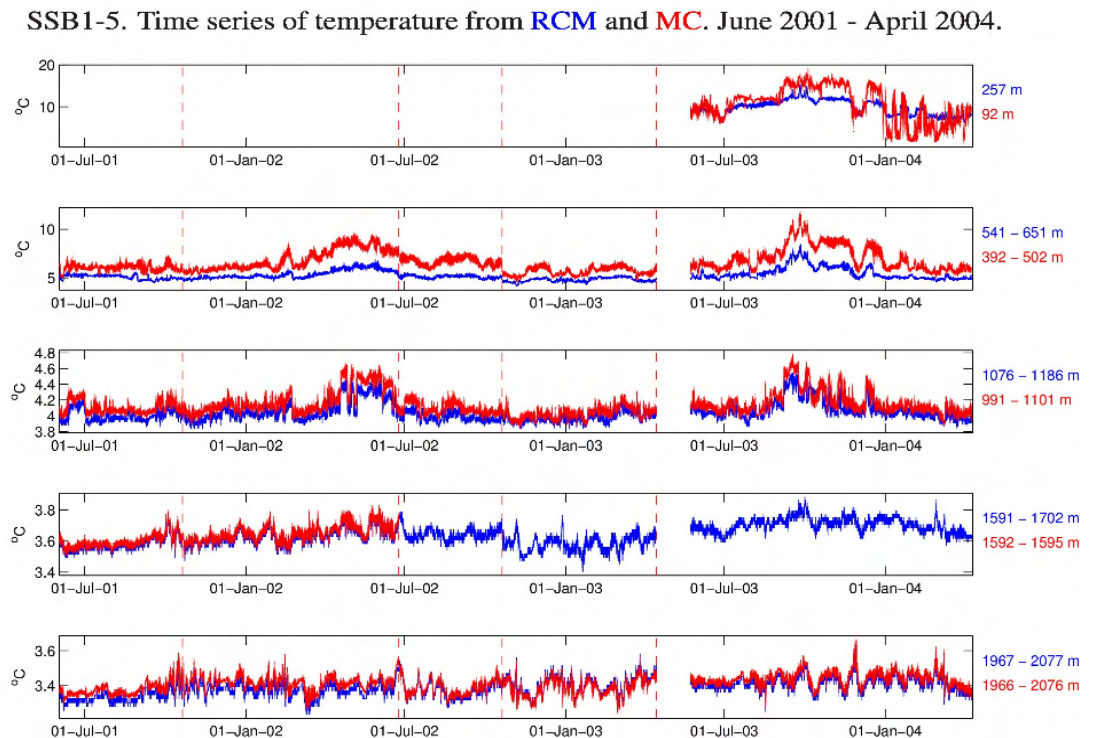


**Figure 61.** Time series of T from 5 approximate depth intervals during the 5 deployments at SS-B. Data from both the MCs (red) and RCM8s (blue) are included. The vertical range of the depths in the different deployments is indicated to the right of each panel. Note the wide range of these depths in the upper 2 panels which is the reason for the discrepancies in the T time series in those panels.



Moving to the merged time series from SS-C, Fig. 62 shows R from 6 approximate depths, and Fig. 63 shows T for 3 depths. There were enhanced current speeds at all the depths down to 25 mab during the May-June 2002 and September 2003 eddy events, but not by much at 25 mab and 22 mbs for the former event. The peak speeds were  $\sim 1$  m/s at 22 mbs and 0.6-0.7 m/s between 50 and 200 mbs.

There was only a limited return of the T series, except near the bottom, at SS-C (Fig. 63); however, note that T time series from the ADCPs and MLs are not included in the present plot. There was nevertheless notable warmer water in the available records during the late spring 2002 and early fall 2003 events, consistent with the other evidence discussed earlier for remnant warm-eddy influences.

**Figure 62.** Time series of R from 6 approximate depth levels during the 4 deployments at SS-C, proceeding from **ADCP** data (**green**) for the upper ocean in the upper panels, to **RCM8** data (**blue**) for the greater depths in the lowest 5 panels. The vertical intervals across the different deployments are indicated on the right. The premature loss of the tall SS-C3 mooring in December 2002 resulted in a data gap of over 6 months.

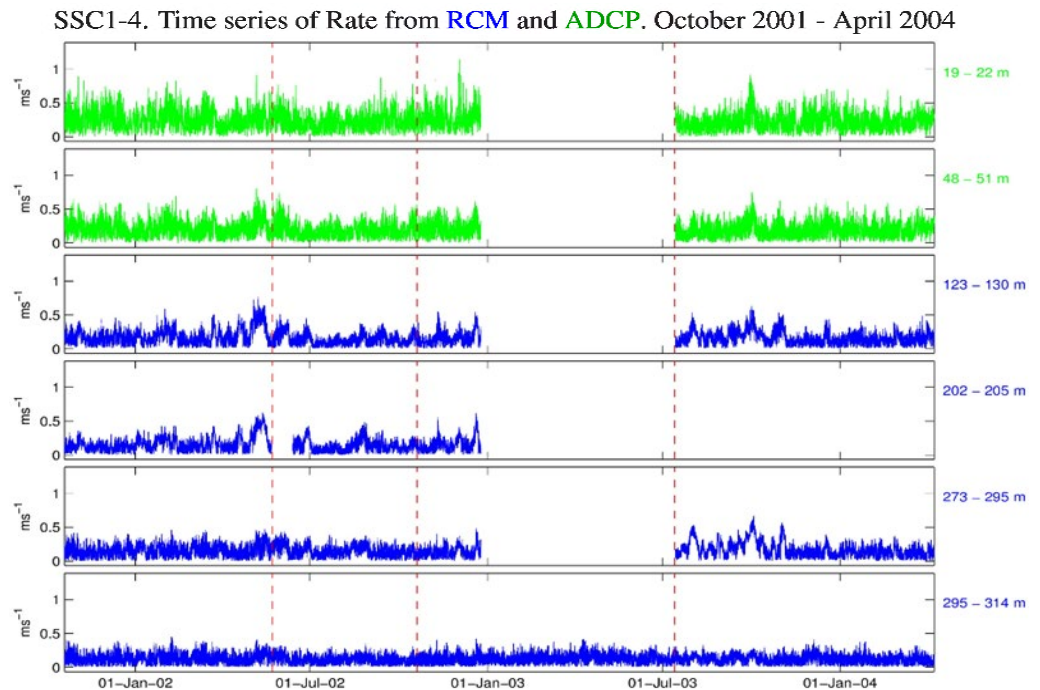
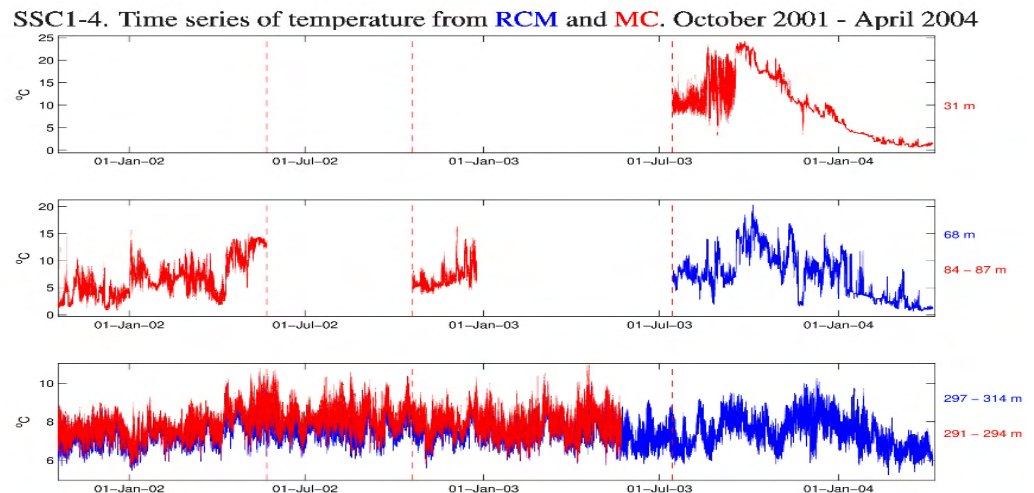


**Figure 63.** Time series of T from 3 approximate depth intervals during the 3 deployments at SS-C. Data from both the **MCs** (**red**) and **RCM8s** (**blue**) are included. The vertical range of the depths in the different deployments is indicated to the right of each panel.

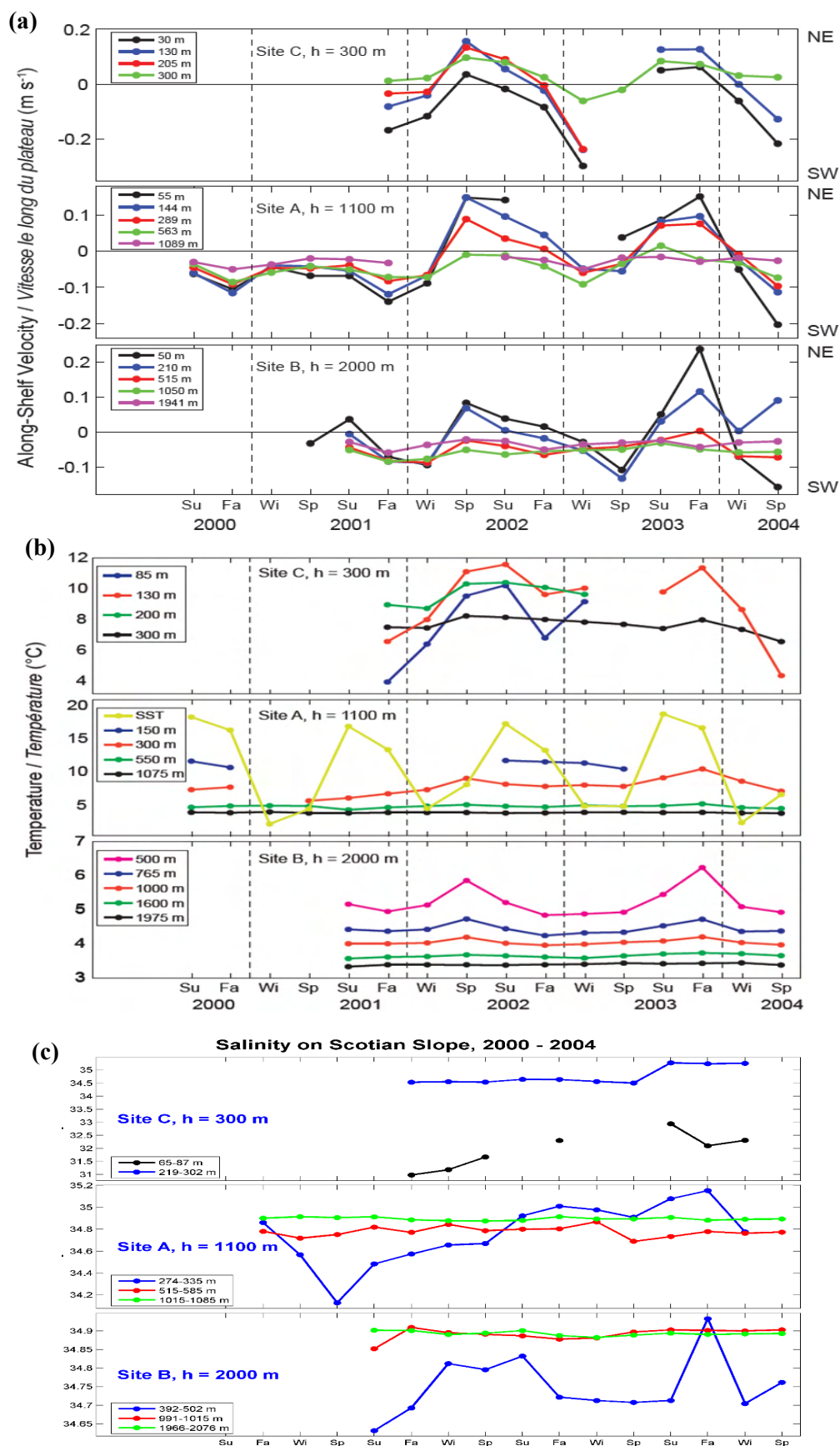


### 4.3 Time Series of Seasonal Means, 2000-04

The discussion of the seasonal means of along-slope velocity and T in Loder and Geshelin (2009) was instructive, so it will be highlighted here in relation to the time series of these variables for different depths at each of the mooring sites (Fig. 64a,b). The influence of the two warm-eddy events dominates in both subsurface T and along-slope velocity over the seasonal variation associated with surface heating

(see the SST seasonal means in the SS-A panel of Fig. 64b). The associated warming extended over most of the water column at SS-C and SS-A, and to at least 1600 mbs at SS-B. The usual southwestward

**Figure 64.** Time series of the seasonal means of (a) the along-shelf component of velocity (positive northeastward), (b) Temperature and (c) Salinity at representative approximate depths in the moored measurements during the 2000-04 Scotian Slope program. The series for site SS-C are in the upper panels, for site SS-A in the middle panels, and for site SS-B in the lower panels for each variable. The approximate depths are indicated in the legend boxes with different colours for the different depths for the the different variables, but with the same sequencing of colours according to depth for each variable. Seasonal means of SST from AVHRR data are included (provided by Dr. Brian Petrie and the BIO Remote Sensing Group of AZMP).



seasonal-mean flow was disrupted (reversed) over the entire water column at SS-C and at depths down to ~500m at SS-A and SS-B, and reduced through the entire water column (2000m) at SS-B in spring 2002. It is uncertain of the extent to which the southwestward flow in shallower depths along the shelf edge was affected, but it seems highly likely that the total southwestward transport was substantially reduced.

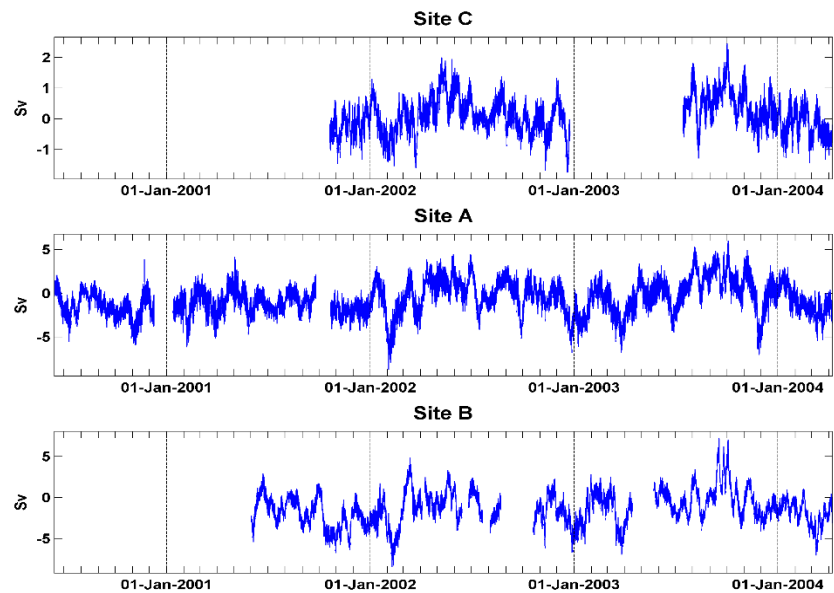
The seasonal S time series show more variability with site depth and year (than those of T), in part related to the more complex cross-slope and vertical structure of S in the region (e.g., Fig. 16). Higher S at 200-500m (the depth of WSW) is apparent at all 3 sites in fall 2003, and at SS-B in spring 2002 (but not at SS-C and SS-A). The reason for this is uncertain. The S time series for SS-C are notably limited.

#### 4.4 Transport Variability, 2000-04

The moored time series of along-slope velocity can be used to estimate the along-slope transport between the shelf edge (say at water depth 150m) and the lower slope beyond SS-B (say at 2300m water depth) if the measured velocities are assumed to be representative of specific vertical intervals and cross-slope distance intervals.

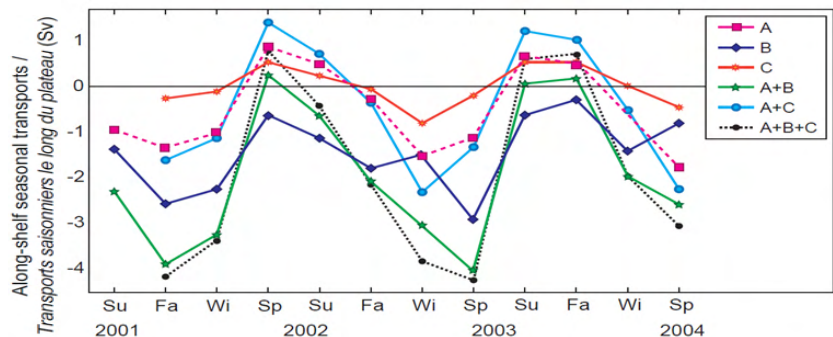
Hourly transport time series for each site are shown in Fig. 65. Note the variability at each site on a range of time scales, from weeks to multiple months. There is a clear indication that the LCE along the upper Scotian Slope and Shelf edge is not a slowly-varying stream as depicted in the seasonal numerical model results displayed in Fig. 9. Coherent pulses of increased southwestward flow at all 3 sites in early January 2002 and late December 2002 are apparent, but some other features differ from site to site.

**Figure 65.** Time series of estimates of along-slope transport (positive northeastward) for each mooring site assuming that its velocities are representative of specified vertical intervals and cross-slope distances consistent with the separation of the instruments and sites.



The seasonal-mean transport time series are shown in Fig. 66, showing the contribution from each site and from combinations of the sites. There is an apparent seasonal variation but it is actually a longer-

**Figure 66.** Time series of seasonal-mean along-slope transport (positive northeastward) from the moored measurements, for individual mooring “sections” and combinations thereof. The units are Sverdrups with  $1 \text{ Sv} = 10^6 \text{ m}^3/\text{s}$ .



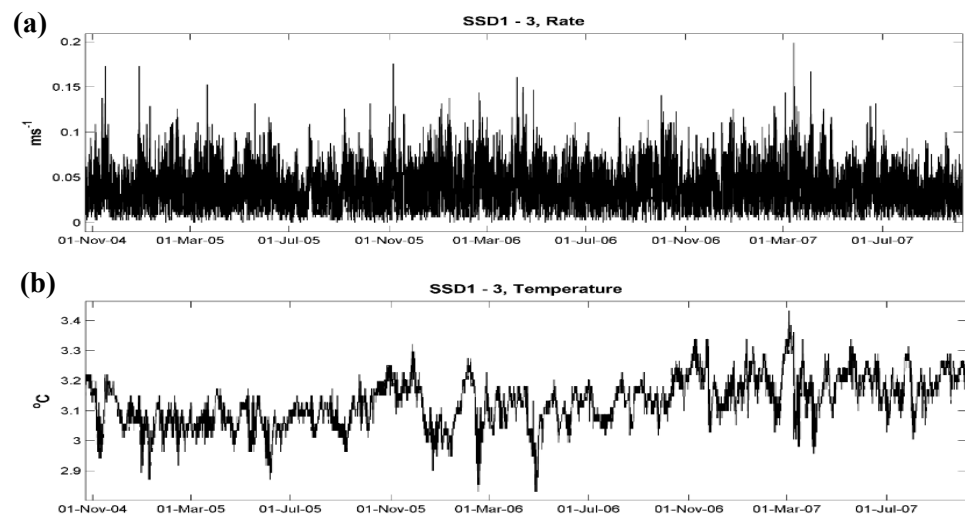
period variation dominated by the transport disruptions in spring 2002 and fall 2003. The overall mean transport is 1.5 Sv with a minimum in summer ( $\sim 1$  Sv) and maximum in winter (1.9 Sv), similar to the values in the Hannah et al. (2001) model solutions. But the details and origin of the variation during 2000-04 are different than in the model (and than in the climatological density fields forcing the model), dominated by the warm eddy incursions rather than a robust seasonality.

#### 4.5 Merged Time Series from the 2004-08 Program

As examples of the multi-year time series from the 2004-08 Scotian Slope program, Fig. 67 shows R and T from the first 3 deployments at site SS-D, from October 2004 to October 2007. As discussed earlier, RCM11s were used in these deployments such that there is no reason to believe that the predominant occurrence of very weak currents is not real. R values were less than 0.1 m/s for a large fraction of the 3-year period, and less than 0.05 m/s most of the time, indicating very weak currents at depth in this portion of the lower Scotian Slope and Rise (Fig. 67a). This is consistent with the results from the 2008-14 RAPID Scotian moored measurement program (Loder et al., 2025a) which found that the near-bottom current speeds in the vicinity of the 2300- and 2800-m isobaths were generally lower than those in the vicinity of the 1100-, 1700-, 3400- and 3900-m isobaths. It appears that this cross-slope variation is a result of the shallower sites being affected by the LCE and the deeper sites by the DWBC, and GS-related influences not having a strong influence on the near-bottom currents at SS-D (and at SS-E). Note, however, the finding above (e.g., §4.2 and §4.3) that remnant warm-core GS eddies can reduce the southwestward mean flow at all depths at site SS-B on the 2000-m isobath.

The origin of the strongest current speeds, in the 0.15-0.2 m/s, at this position is uncertain at this time. Some of these, e.g., those in November 2004, December 2005 and March 2007, appear to be associated with higher T values (Fig. 67b; raising the possibility of warm-eddy influences), while others don't. It may be that some are related to GS ring impingements (with warming) and others to DWBC pulses (with cooling) or shifts. Further investigation is again needed.

**Figure 67.** Concatenated (merged) time series of **(a)** Rate (m/s) and **(b)** Temperature ( $^{\circ}$ C) from the RCM11 at 50 mab in deployments SS-D1, -D2 and -D3, extending from October 2004 to October 2007.

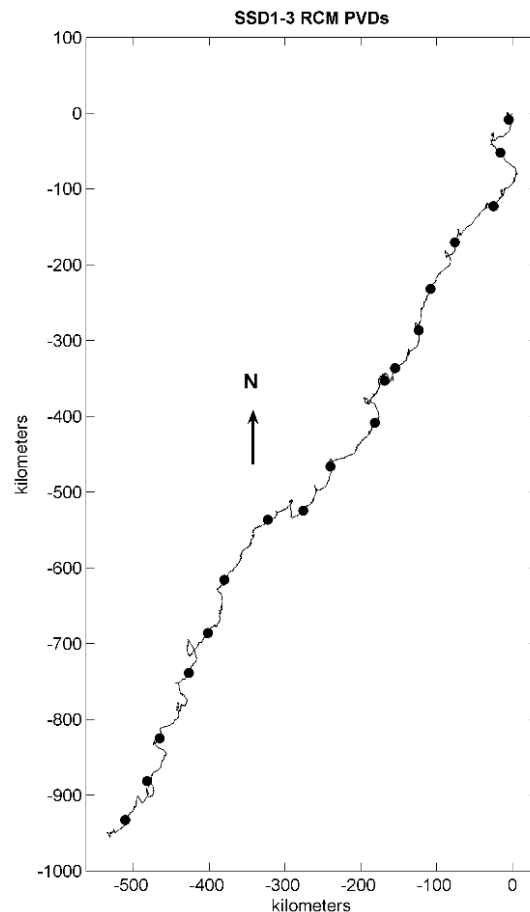


Loder et al. (2015a,b; 2025a) use moored measurements in the vicinity of the HL/XHL between 2000 and 2014, including those from the 2000-04 and 2004-08 program, to show an overall warming of the near-bottom waters over the Scotian Slope between the 1100- and 2700-m isobaths (i.e., from SS-A to SS-D) during this period. It appears that this is related to anthropogenic global warming of the Northwest Atlantic, although it must be cautioned that there is pronounced multi-decadal variability related to the North Atlantic Oscillation and variable deep convection in the Labrador Sea that is also occurring (e.g., Yashayaev and Loder 2016). For example, the Petrie and

Smith (1982) moored measurements from the 1970s and analyses of historical and recent (AZOMP) hydrographic survey data from the XHL indicate cooling in the 1990s which needs to be considered in long-term trends interpretations (Loder et al., 2015a,b). Further, while a 3-year warming trend is apparent in Fig. 67b, the T time series from SS-D4 (not shown in Fig. 67b) show cooling, indicating that multi-year T variability on a range of time scales is occurring at depth on the HL.

The PVD for the velocity from SS-D1, -D2 and -D3 (Fig. 68) shows persistent seasonal-mean flow in a generally southwestward direction, but with variations of a factor of 3 in the magnitude of the bi-monthly mean velocity and occasional episodes of flow reversal or direction shifting lasting for days to weeks.

**Figure 68.** PVD for the hourly velocity data from the RCM11 at 50 mab on M1547, M1585 and M1623 at SS-D1, -D2 and -D3, covering the period October 2004 to October 2007. The solid circles are at intervals of 2 months.



## 7. Concluding Remarks

This report, together with the comments in the final datafiles and the supplementary documents in the BIO Archive (see References), provide a fairly thorough outline of the multiple types of moored data collected during the 2000-04 BIO-PERD-industry moored measurement program on the HL, and in the 2004-08 BIO-PERD program (which complemented moored measurements on the RAPID B Line and elsewhere). Meta information on all of the moored measurements, and discussions of the data processing and quality, have been provided here, together with example displays of the data and discussion of some key features. The supplementary documents are in the ArchivedDataProjects directory of the BIO, and include selected cruise reports and bridge logs, and pdf files of selected workshop and conference presentations on the collected data. Other cruise reports and bridge are listed in the References.

The more extensive 2000-04 measurement program was jointly funded by DFO, PERD and industry, with the PERD and industry funding motivated by strong industry interest in deep-water oil and gas exploration along the entire Scotian Slope between Laurentian and Northeast Channels. It was facilitated by exceptional cooperation by the Chief Scientists and staff of multiple DFO AZMP and AZOMP cruises which included physical (e.g., CTD, vessel-mounted ADCP), chemical (e.g., DO, nutrients, tracers) and biological (nanoplankton, phytoplankton, zooplankton) sampling at standard stations along the XHL, including the central mooring site (SS-A near HL6). In turn, the choice of a central mooring line across the Scotian Slope, specifically along the HL, has the potential to be of immense benefit to a detailed description, modelling and understanding of the interlinked physical, chemical and biological processes that result in the observed variability in the tri-seasonal monitoring surveys, especially if used in conjunction with the AZMP SST composites (e.g., Loder and Geshelin 2006, 2009) and altimetric indices (Han 2007).

If nothing else, the example displays shown in this report from the 2000-04 mooring program together with the AZMP section data and SST composites confirm that the Scotian Slope frontal region is complex and that its subsurface variability is severely undersampled with seasonal surveys. A degree of undersampling will probably always be the case in such a complex and variable region, even with new measurement techniques and platforms. A helpful and cost-effective approach to improved and more efficient monitoring and understanding of the complex physical-chemical-biological interactions in the region on various time scales would be to take advantage of the 2000-04 moored datasets (which have continuous high-frequency sampling) in descriptive and interpretative investigations of the variability seen in the AZMP and all available data (see Loder and Geshelin (2009) for examples). Coupled physical-chemical-biological models, validated by or assimilating observations, should be helpful in this. Moored measurements by industry at other positions (e.g., Fig. 2) over the Scotian Slope (available from the BIO Archive) could also be helpful in these investigations.

The more limited 2004-08 moored datasets, including those collected by POL at other sites between the 1800- and 4000-m isobaths on the RAPID B Line (e.g., Elipot et al., 2013; Fig. 1), provide a 4-year continuation of the near-bottom 2001-04 measurements at site SS-B (discussed above), and a bridge to the 2008-2018 RAPID WAVE Scotian moored measurements at 6 sites between the 1100- and 3900-m isobaths on the HL/XHL (Hughes et al., 2013; Loder et al., 2025a; Xing et al., 2025b). They are also complementary to more extensive moored measurements on Line W south of Cape Cod during 2004-08 (Toole et al., 2011) and earlier. All of these time series are highly relevant to important deep-ocean climate questions such as the downstream influences (via the LCE and DWBC) of the observed decadal-scale variability in deep convection in the Labrador and Nordic Seas (e.g., Le Bras et al., 2017), and variability in the AMOC “conveyor-like belt” such as the potential (Collins et al., 2013), and now apparent (e.g., Bilo et al., 2024; Xing et al., 2025a,b), decline in the AMOC which would have a major influence on anthropogenic global climate change (Gulev and Thorne 2021).

While it is unfortunate that a multitude of circumstances, including giving priority to additional moored measurements on the Atlantic Canadian slope while funding was available (e.g., Loder et al., 2025a,b,c) and unexpected challenges with data quality (RCM8 rotor stalling, intermittent ADCP range, MC calibrations), organizational changes (e.g., downsizing) and personal situations (e.g., health, pandemic, retirement), have led to a delay in publications, the potential value of these moored datasets remains. It is hoped that others will be able to make good use of this and other delayed reports, and the continued strong data archival capability at BIO, in leading further investigations and publications using the unique datasets described in this report.

## 8. Acknowledgements

Primary funding for the 2000-04 and 2004-08 Scotian Slope moored measurement programs was provided by DFO and the PERD Offshore Environmental Factors program. Substantial funding for the 2000-04 program was also provided by several oil and gas companies: ChevronTexaco, EnCana, ExxonMobil, Kerr-McGee, Marathon and Shell. The managers and representatives (especially the industry meteorological-oceanographic liaisons) of these organizations are thanked for their input and support.

Major support was provided by DFO through vessel time, equipment usage and acquisition, salaries for scientific, technical and at-sea personnel, and other supporting activities at BIO and the Canadian Coast Guard. The management, administrative and technical personnel in these organizations are thanked for their substantial and diligent support.

The successful field activities would not have been possible without the extensive cooperation and support of the personnel involved in DFO's AZMP and AZOMP cruises on which the field operations were conducted, and the personnel in BIO's Technical Operations (TO) group which led the mooring activities. In particular, Gary Bugden, Allyn Clarke, Glen Harrison, Erica Head, Ed Horne, Michel Mitchell and Murray Scotney for their cooperative leadership and support as the Chief Scientists of the cruises, and Rick Boyce, Jay Barthelotte, Adam Hartling, Bert Hartling, Bob Ryan and Murray Scotney for their dedication and lead roles within the TO group and at sea. The important contributions of the many other personnel at DFO and BIO, including the officers and crew of the CCGS Hudson, Parizeau and Sir William Alexander, who made the execution of the field program successful, are also gratefully acknowledged. The personnel associated with the industry supply vessel Bonavista are thanked for the recovery of a drifting mooring.

Drs. Igor Yashayaev of BIO and Guoqi Han of DFO NAFC are thanked for the provision of some figures (see figure captions), and helpful discussions. The personnel of the Remote Sensing Group at BIO are gratefully acknowledged for their contributions to the invaluable SST composites available through AZMP, Dr. Brian Petrie of BIO for the SST time series for the study site, and Inna Yashayaev of BIO for the hydrographic section displays.

Finally, the personnel of the Data Services group at BIO are thanked for the maintenance of the data archives where the source data, processed data files and supporting documentation are held.

## 9. References

(\* indicates that a pdf is available in the BIO Archive at:

[\BIODataSvc\ARC\ArchivedDataProjects\Loder\SlopeCurrents\ScotSR\\_RAPID2008-18](#),

with the filename indicated in *[green italicized square brackets]*. A copy can be requested from [DFO.BIODataServices-BIOServicesdeDonnees.MPO@dfo-mpo.gc.ca](mailto:DFO.BIODataServices-BIOServicesdeDonnees.MPO@dfo-mpo.gc.ca) )

AZMP, 2002. Atlantic Zone Monitoring Program Bulletin, No. 2, edited by J.-C. Therriault and L. Devine, 36 p. <https://waves-vagues.dfo-mpo.gc.ca/Library/365695.pdf>

AZMP, 2010. Atlantic Zone Monitoring Program Bulletin No. 9. Fisheries and Ocean Canada, 36 p. <https://waves-vagues.dfo-mpo.gc.ca/library-bibliotheque/365688.pdf>

Campbell, D.C., D.J.W. Piper, D.C. Mosher and K.A. Jenner. 2008. Sun-illuminated seafloor topography, Mohican Channel, Scotian Slope. "A" Series Map 2124A, Geological Survey of Canada.

\*Clarke, R.A. 2002. Cruise Report, Hudson 2002-032, Labrador Sea, 23 Jun – 19 Jul 2002. 81 p. *[cr2002032.pdf]*

- \*Clarke, R.A. 2003. Cruise Report, Hudson 2003-038, Labrador Sea, 13 Jul – 4 Aug 2003. 62 p. [\[cr2003038.pdf\]](#)
- Collins, M., et al. 2013. Long-term climate change: Projections, commitments and irreversibility, in *Climate Change 2013: The Physical Science Basis. Contribution of Working Group I to the Fifth Assessment Report of the Intergovernmental Panel on Climate Change*, edited by T. F. Stocker et al., p. 1029–1136, Cambridge Univ. Press, Cambridge, U. K.
- de la Ronde, M.S. 1972. Temperature, salinity and density distributions of the Scotian Shelf 1965–1971. *BIO Data Series/B1-D-72-6*, 51 p, Bedford Inst. of Oceanogr., Dartmouth, N. S., Canada.
- Drinkwater, K.F., and G. Taylor. 1982. Monthly means of the temperature, salinity and density along the Halifax section, *Can. Tech. Rep. Fish. Aquat. Sci.* 1093, 67 p.
- Drozdowski, A., and B.J.W. Greenan. 2012. An intercomparison of acoustic current meters deployed on the Scotian Slope. *Can. Tech. Rep. Hydrogr. Ocean Sci.* 279, Fisheries and Oceans Canada, 44 p.
- Drozdowski, A., and B.J.W. Greenan. 2013. An intercomparison of acoustic current meter measurements in low to moderate flow regions. *J. Atmos. Oceanic Tech.* 30, 1924-1938. [doi:10.1175/JTECH-D-12-00198.1](#)
- Drozdowski, A., B.J.W. Greenan, M.D. Scotney, J.W. Loder, and Y. Geshelin. 2010. An intercomparison of acoustic current meters deployed on the Scotian Shelf. *Can. Tech. Rep. Hydrogr. Ocean Sci.* 264, Fisheries and Oceans Canada, vi + 53 p.
- Fuglister, F.C. 1963. Gulf Stream'60. *Prog. Oceanogr.* 1, 265-373.
- Gatien, M.G. 1976. A study in the Slope water region south of Halifax. *J. Fish. Res. Board Can.* 33, 2213-2217.
- Grant, A.B., and R.F. Reiniger. 1970. Current meter and thermograph observations on the Scotian Shelf - 1967. *Bedford Inst. Rep., AOL Data Ser.* 1970-9-D:237 p.
- Grant, A.B., and R.F. Reiniger. 1971. Current meter and thermograph observations on the Scotian Shelf - 1968. *Bedford Inst. Rep., AOL Data Ser.* 1971-6-D; 395 p.
- Gulev, S.K., and P.W. Thorne. 2021. Changing state of the climate system. *In: Climate Change 2021: The Physical Science Basis. Contribution of Working Group I to the Sixth Assessment Report of the Intergovernmental Panel on Climate Change.* Cambridge University Press, p 287-422. [doi:10.1017/9781009157896.004](#)
- Han, G. 2004. Scotian Slope circulation and eddy variability from TOPEX/Poseidon and frontal analysis data. *J. Geophys. Res.*, 109, C03028. [doi:10.1029/2003JC002046](#).
- Han, G. 2007. Satellite observations of seasonal and interannual changes of sea level and currents over the Scotian Slope. *J. Phys. Oceanogr.* 37, 1051-1065. [doi 10.1175/JPO3036.1](#)
- Han, G., C.G. Hannah, J.W. Loder, and P.C. Smith, 1997: Seasonal variation of the three-dimensional mean circulation over the Scotian Shelf. *J. Geophys. Res.* 102, 1011–1025.
- Han, G., J. Loder and B. Petrie. 2010. Tidal and non-tidal sea level variability along the coastal Nova Scotia from satellite altimetry. *Int. J. Remote Sens.* 31(17), 4791-4806. [doi:01431161.2010.485152](#)
- Hannah, C.G., J.A. Shore, J.W. Loder and C.E. Naimie. 2001. Seasonal circulation on the western and central Scotian Shelf. *J. Phys. Oceanogr.* 31, 591-615.

- Heffler, D.E. 1984. Ralph: an instrument to monitor seabed sediments. Geological Survey of Canada, Paper, 84-1B, 47-52. <https://doi.org/10.4095/119606>
- Herman, A. and K. Denman. 1979. Intrusions and vertical mixing at Shelf/Slope Water front south of Nova Scotia. J. Fish. Res. Bd. Can. 36, 1445-1453.
- Hill, P., A. Hay, A. Bowen and D. Piper. 2004. Progress report: hoaling iInternal waves and sediment transport on the Scotian Slope. Unpublished report, 9 p.
- \*Hudson 2008. Bridge Log Book, Hud 2008-037, 28 Sep – 21 Oct 2008. 39 p. DFO-BIO Archive. [\[HUD2008037\\_BridgeLogBook.pdf\]](#)
- Hughes, C., M.A.M. Maqueda et al. 2007. Rapid evaluation report – WAVE (Western Atlantic Variability Experiment). Unpublished document, 12 p, May 2007.
- Lee, A.H. 1970. The T-S structure, circulation and mixing in the Slope Water region east of the Scotian Shelf. Ph.D. Thesis, Dalhousie Univ., H alifax, N.S.191 p.
- Lively, R.R. 1979a,b. Current meter and meteorological observations on the Scotian Shelf, December 1975 to January 1978, Vol 1, 2. Bedford Institute of Oceanography Report Series BI-D-79-1.
- \*Loder, J.W. and Y. Geshelin. 2006. Circulation and hydrographic variability from moored measurements across the Scotian Slope in 2000-2004. Canadian Meteorological and Oceanographic Society Annual Congress, Toronto, 29 May – 1 Jun, , 22 p. [\[CMOS2006\\_PERD-SS.pdf\]](#)
- Loder, J.W. and Y. Geshelin. 2009. Currents and temperature variability from moored measurements on the outer Halifax Line 2000-2004. p. 44-50 *In*: Atlantic Zone Monitoring Program Bulletin No. 8. <https://waves-vagues.dfo-mpo.gc.ca/library-bibliotheque/365689.pdf>
- \*Loder, J., Y. Geshelin, D. Gregory, B. Petrie, C. Hannah, F. Dupont, G. Han, E. Colbourne and D. Senciall. 2004b. PERD OEF: Currents and circulation in the Atlantic offshore. PERD Currents Meeting, 11-12 Feb 2004, Dartmouth, NS. [\[PERD-Currents-SS&FP-12Feb2004.pdf\]](#)
- Loder, J.W., Y. Geshelin, M.A.M. Maqueda, I. Yashayaev, S. Elipot and C.W. Hughes. 2025a. Moored current and hydrographic measurements from the RAPID WAVE Scotian Line, 2008 to 2018. Can. Tech.. Rep. Hydrogr. Ocean. Sci. 398: viii + 74 p.
- Loder, J.W., Y. Geshelin and I. Yashayaev. 2025b. Moored current and hydrographic measurements in Flemish Pass, 2002 to 2005. Can. Tech.. Rep. Hydrogr. Ocean. Sci. 396: x + 101 p.
- Loder, J.W., Y. Geshelin and I. Yashayaev. 2025c. Moored current and hydrographic measurements in Orphan Basin, 2004 to 2010. Can. Data Rep. Hydrogr. Ocean Sci. 226: xii + 99 p.
- Loder, J.W., C.G. Hannah, B.D. Petrie and E.A. Gonzalez. 2003. Hydrographic and transport variability on the Halifax section. J. Geophys. Res. 108 (C11), 8003, 1-18.
- Loder, J., K. Lee, G. Sonnichsen, P. Macnab and D. McAlpine. 2005. Towards safe and environmentally-sound petroleum exploration, development and regulation. p. 21-25 *In*: BIO 2004 in Review, Bedford Institute of Oceanography.
- Loder, J.W., B. Petrie and G. Gawarkiewicz. 1998. Ch.5: The coastal ocean off northeastern North America: a large-scale view. p. 105-133 *In*: The Global Coastal Ocean: Regional Studies and Synthesis. The Sea, Vol. 11, A.R. Robinson and K.H. Brink (Eds.), John Wiley & Sons, Inc.

- Loder, J.W., R.G. Pettipas and D.J. Belliveau. 1990. Intercomparison of current measurements from the Georges Bank Frontal Study. *Can. Tech. Rep. Hydrogr. Ocean Sci.* 127: vi + 75 p.
- Loder, J.W., J.A. Shore, C.G. Hannah and B.D. Petrie. 2001. Decadal-scale hydrographic and circulation variability in the Scotia-Maine region. *Deep-Sea Res. II* 48, 3-35.
- Loder, J., I. Yashayaev, Y. Geshelin, M.M. Maqueda and C. Hughes. 2015a. Recent oceanographic variability on the Scotian Slope and Rise, and upstream linkages. *Canadian Meteorological and Oceanographic Annual Congress (7850)*, Whistler, B.C., 2 June 2015. 19 p. [[CMOS2015\\_RAPID-XHL.pdf](#)]
- Loder, J., I. Yashayaev and M.A.M. Maqueda. 2015b. Recent variability in water mass properties in the Labrador Sea and Scotian Rise regions. *US AMOC International Science Meeting*, Bristol, UK. 21 July 2015. 23 p. [[RAPID-AMOC2015\\_LS-SR.pdf](#)]
- MacLellan, H.J. 1957. On the distinctness and origin of the Slope Water off the Scotian Shelf and its easterly flow south of the Grand Banks. *J. Fish. Res. Board Can.* 10, 155-176.
- Mann, C R., and G.T. Needler. 1967. Effect of aliasing on studies of long-term variability off Canada's coasts, *J. Fish. Res. Board Can.*, 24, 1827–1831, 1967.
- Petrie, B. 2007. Does the North Atlantic Oscillation affect hydrographic properties on the Canadian Atlantic continental shelf? *Atmos.-Ocean* 45(3), 141-151.
- Petrie, B.D., and K. Drinkwater. 1993. Temperature and salinity variability on the Scotian Shelf and in the Gulf of Maine 1945–1990, *J. Geophys. Res.*, 98, 20,079–20,089.
- Petrie, B., J.W. Loder, S. Akenhead and J. Lazier. 1991. Temperature and salinity variability on the eastern Newfoundland shelf: the annual harmonic. *Atmos.-Ocean* 29, 14-36.
- Philibert, B.J. Todd, D.C. Campbell, E.L. King, A. Normandeau, S.E. Hayward, E.R. Patton and L. Campbell. 2022. Updated surficial geology compilation of the Scotian Shelf bioregion, offshore Nova Scotia and New Brunswick, Canada. Geological Survey of Canada, Open File 8911, [https://publications.gc.ca/collections/collection\\_2022/rncan-nrcan/m183-2/M183-2-8911-eng.pdf](https://publications.gc.ca/collections/collection_2022/rncan-nrcan/m183-2/M183-2-8911-eng.pdf)
- Piper, D.J.W., and R. Sparkes. 1987. Proglacial sediment instability features on the Scotian Slope at 63W. *Mar Geol* 76, 15-31.
- Piper, D.J.W., J.W. Farre and A. Shor. 1985. Late Quaternary slumps and debris flows on the Scotian Slope. *Geol. Soc. America Bull.* 96, 1508-1517.
- Sandstrom, H., and J. A. Elliott. 1984. Internal tide and solitons on the Scotian Shelf: A nutrient pump at work, *J. Geophys. Res.*, 89, 6415-6426, 1984.
- Smeed, D.A., S. Josey, C. Beaulieu, W. Johns, B. Moat, E. Frajka-Williams, D. Rayner, C.S. Meinen, M.O Baringer, H.L. Bryden, et al. (2018): The North Atlantic Ocean is in a state of reduced overturning. *Geophys. Res. Lett.* 45(3), 1527–153. [doi.org/10.1002/2017GL076350](https://doi.org/10.1002/2017GL076350)
- Smith, P.C. 1983. The mean and seasonal circulation off southwest Nova Scotia. *J. Phys. Oceanogr.*, 13, 1034–1054.
- Smith, P.C. 1989. Seasonal and interannual variability of current, temperature and salinity off southwest Nova Scotia. *Can. J. Fish. Aquat. Sci.*, 46, 4–20.
- Smith, P.C., R.W. Houghton, R.G. Fairbanks and D.G. Mountain. 2001. Interannual variability of boundary fluxes and water mass properties in the Gulf of Maine and Georges Bank: 1993-1997. *Deep-Sea Res. II* 48, 37-70.

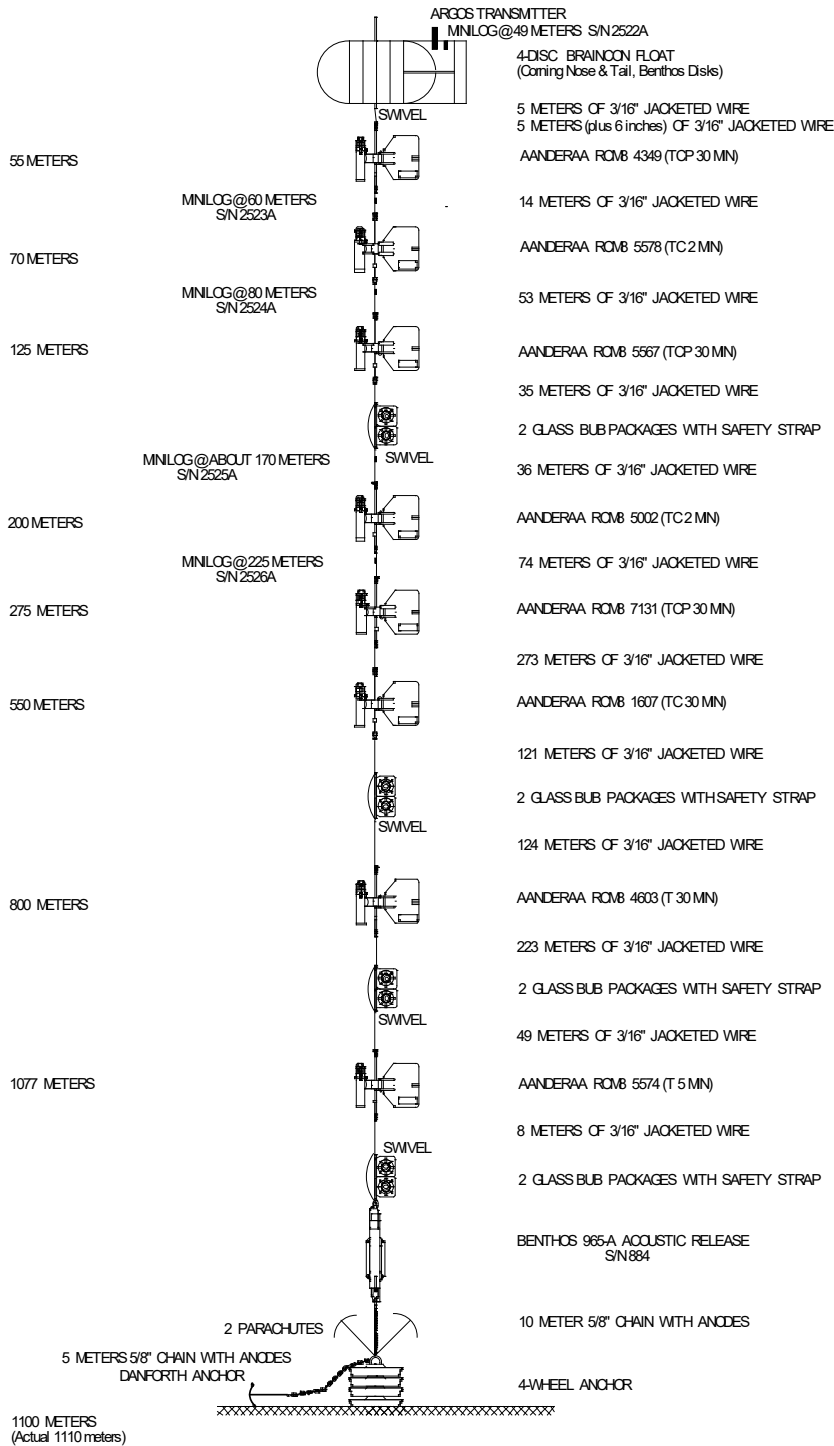
- Smith, P.C., and B.D. Petrie. 1982. Low-frequency circulation on the edge of the Scotian Shelf. *J. Phys. Oceanogr.* 12, 28–46.
- Smith, P.C., B.D. Petrie and C.R. Mann. 1978. Circulation, variability, and dynamics of the Scotian Shelf and slope. *J. Fish. Res. Board Can.* 35, 1067–1083.
- Toole, J.M., M. Andres, I.A. Le Bras, T.M. Joyce, M.S. McCartney. 2017. Moored observations of the Deep Western Boundary Current in the NW Atlantic: 2004–2014. *J. Geophys. Res. Oceans* 122 (9), 7488–7505. [doi.org/10.1002/2017JC012984](https://doi.org/10.1002/2017JC012984)
- Umoh, J.U., and K.R. Thompson. 1994. Surface heat flux, horizontal advection and the seasonal evolution of water temperature on the Scotian Shelf. *J. Geophys. Res.* 99, 20,403–20,416.
- Xing, Q., S. Elipot, W.E. Johns, D.A. Smeed, B.I. Moat, M. Lankhorst and J.W. Loder. 2025a. Significant and widespread decline of the observed Atlantic Meridional Overturning Circulation. (Abstract only). European Geophysical Union Assembly, Vienna, 27 April – 2 May.
- Xing, Q., S. Elipot, W.E. Johns, D.A. Smeed, B.I. Moat and J.W. Loder. 2025b. Widespread decline in the observed western boundary contribution to the Atlantic Meridional Overturning Circulation. *Nature* (to be submitted)
- Yashayaev, I. 2007. Hydrographic changes in the Labrador Sea, 1960–2005. *Prog. Oceanogr.* 73 (3–4), 242–276.
- Yashayaev, I., and J.W. Loder. 2016. Recurrent replenishment of Labrador Sea Water and associated decadal-scale variability. *J. Geophys. Res. Oceans* 121, 8095–8114. [doi:10.1002/2016JC012046](https://doi.org/10.1002/2016JC012046)

## APPENDIX - Mooring Diagrams

*Note: Water and instrument depths are nominal. See Tables 5-9 for instrument serial numbers and actual depths.*

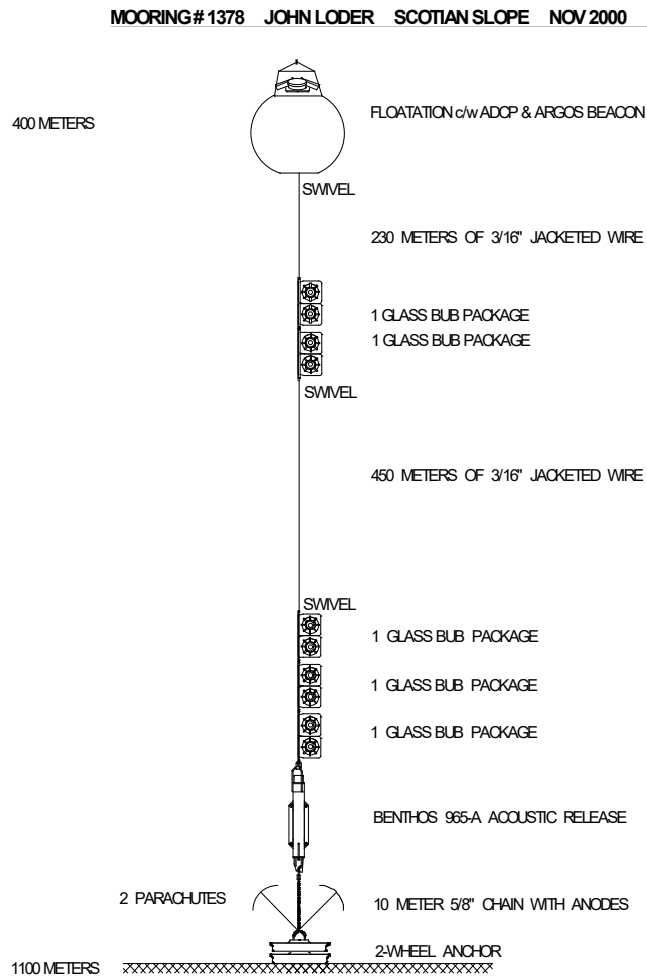
### SS-A1: Deployment 1 at Site SS-A (June to November 2000)

#### MOORING # 1352 JOHN LODER SCOTIAN SLOPE JUNE 2000



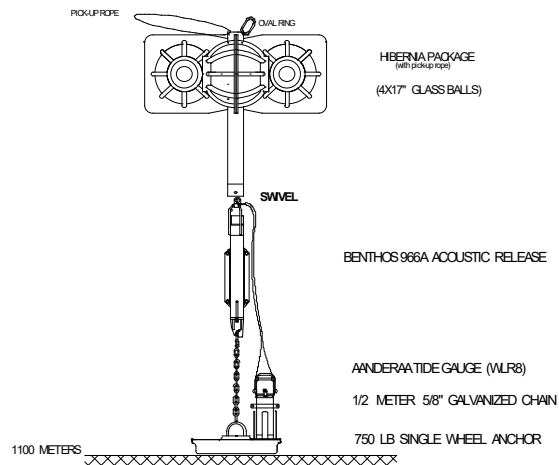
## SS-A2: Deployment 2 at Site A (November 2000 to May 2001)

LR ADCP  
Mooring:



Tide Gauge  
Mooring:

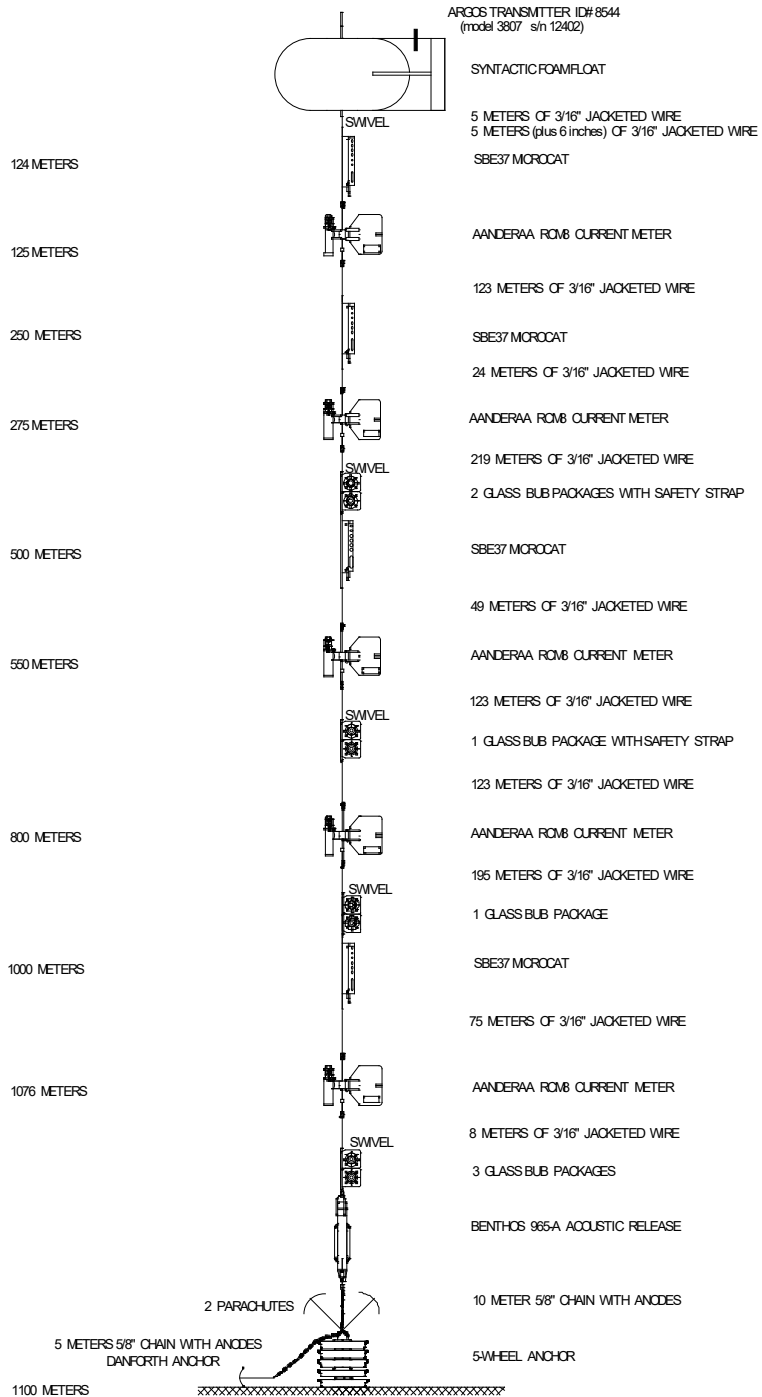
MOORING # 1379 JOHN LODER SCOTIAN SLOPE NOV 2000



SS-A2 (continued)

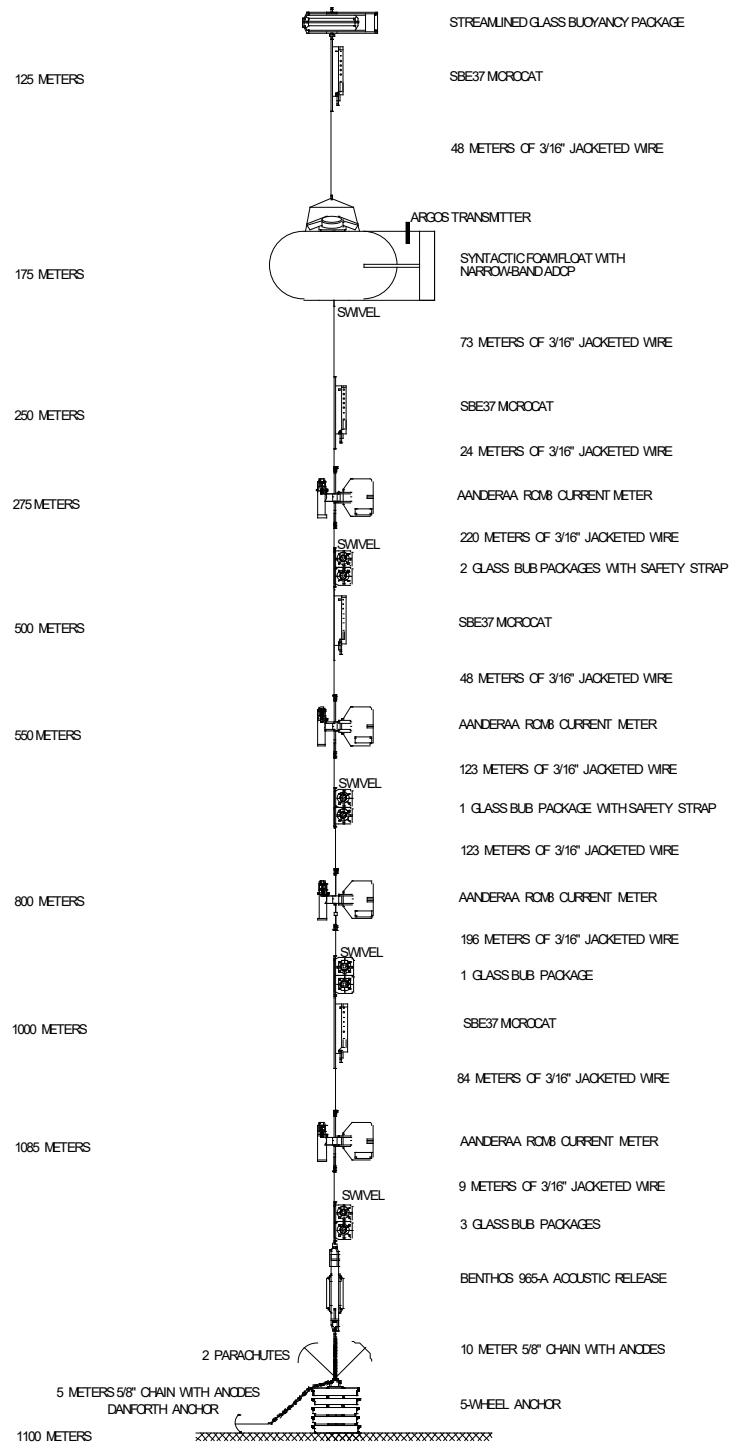
RCM Mooring:

MOORING # 1377 JOHN LODER SCOTIAN SLOPE NOV 2000



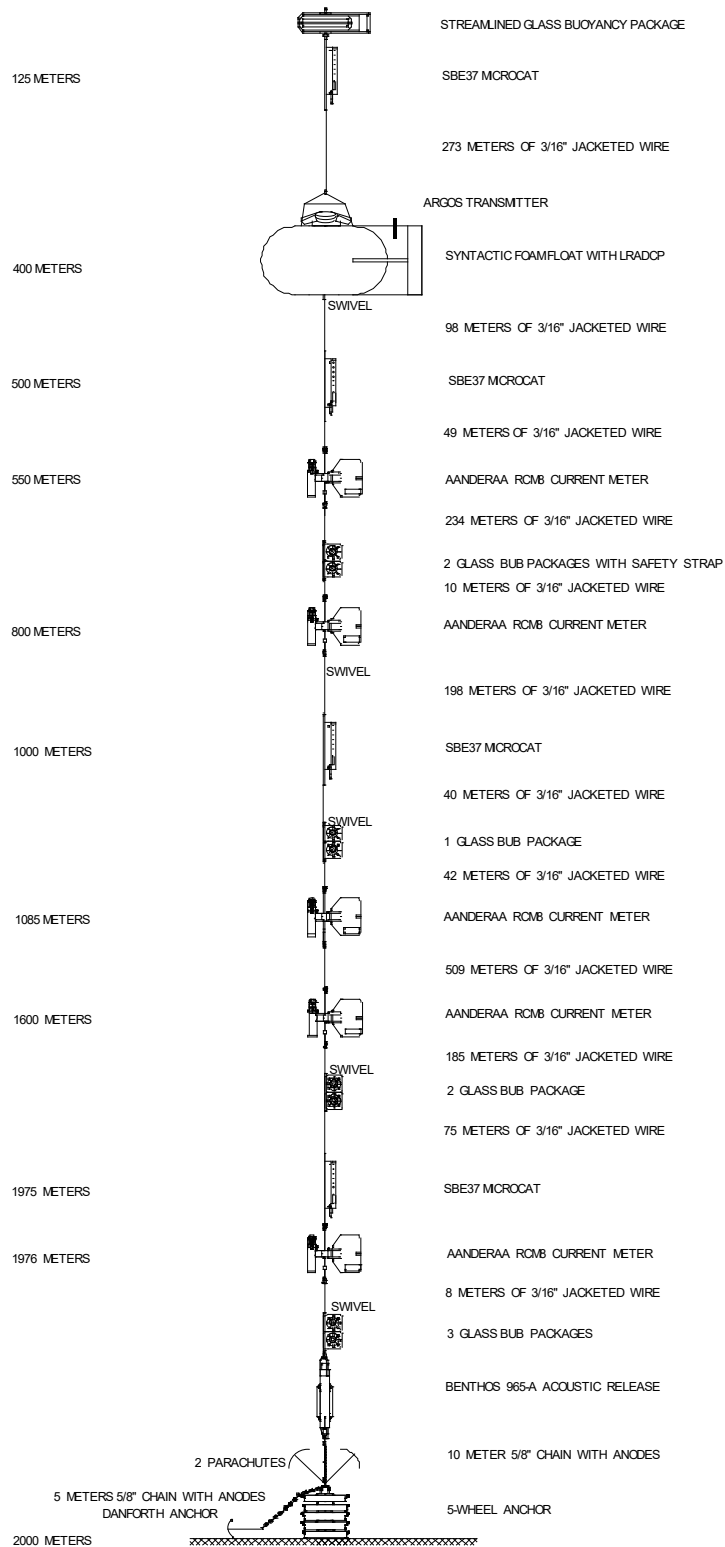
# SS-A3: Deployment 3 at Site A (May – October 2001)

MOORING# 1387 JOHN LODER SCOTIAN SLOPE JUNE 2001



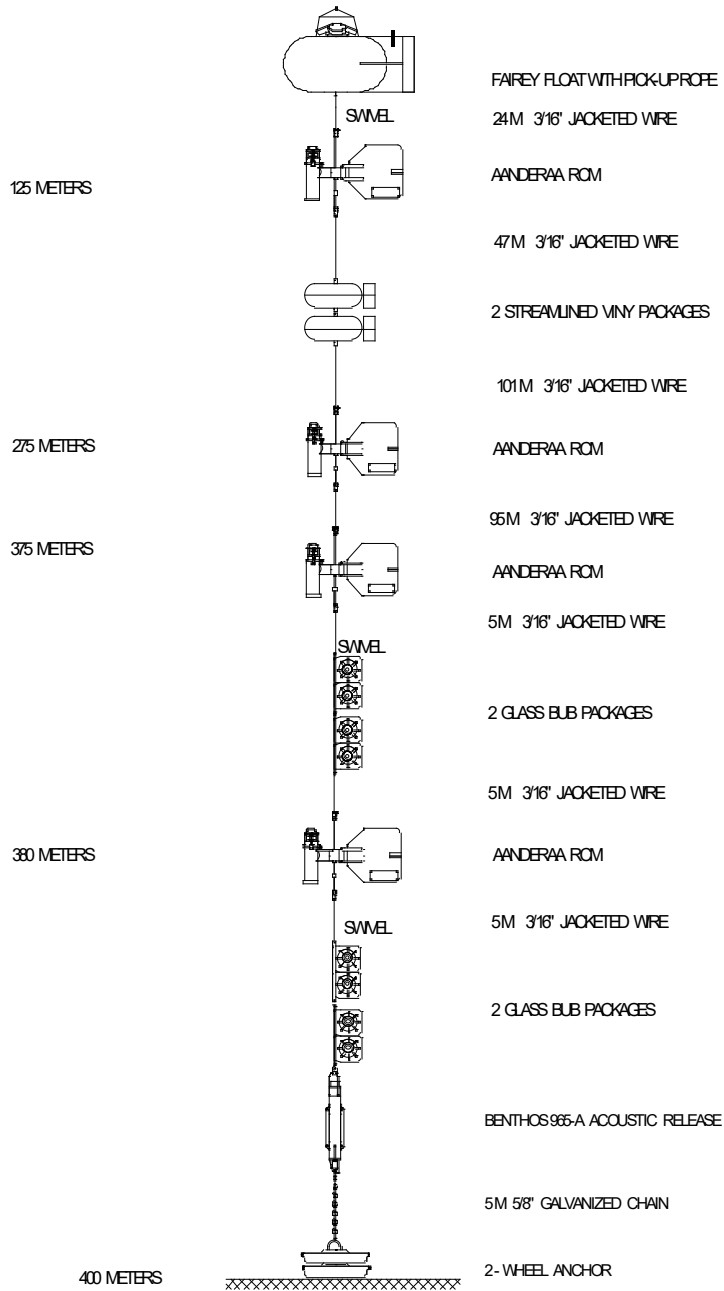
# SS-B1: Deployment 1 at Site B (June -October 2001)

## MOORING # 1388 JOHN LODER SCOTIAN SLOPE JUNE 2001



SS-C1: Deployment 1 at Site C (October 2001 – May 2002)

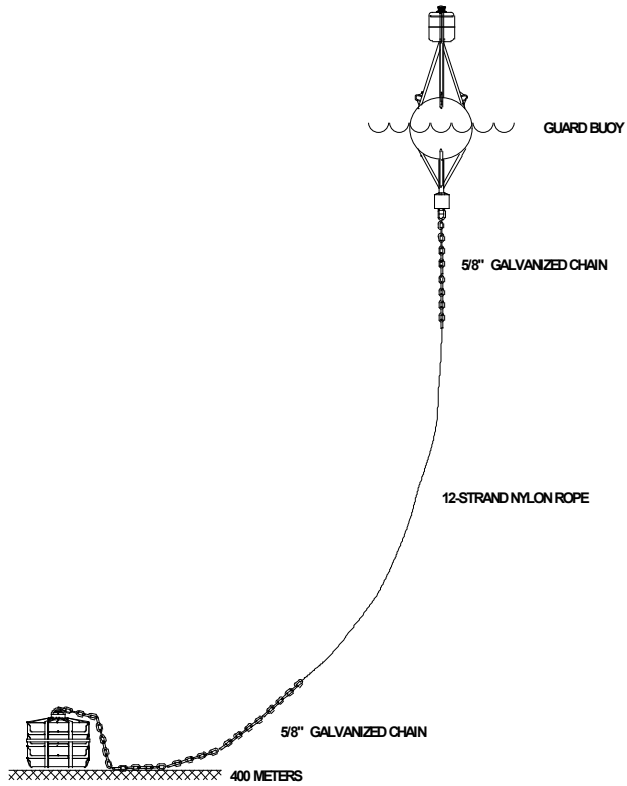
RCM MOORING SS-C-1 LODER SCOTIAN SHELF NOV 2001



SS-C1 (continued)

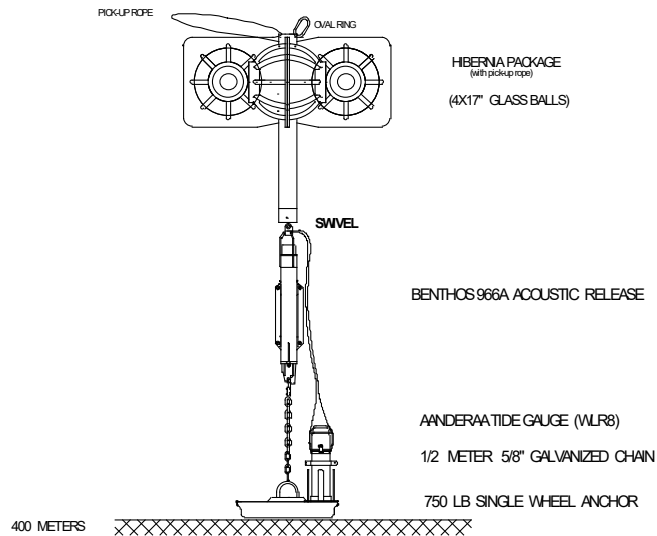
Guard Buoy  
Mooring  
(One of Three)

GUARD BUOY FOR SS-C-1 LODER SCOTIAN SHELF NOV 2001



Tide Gauge  
Mooring

TIDE GAUGE MOORING SS-C-1 LODER SCOTIAN SLOPE NOV 2001



# SS-C4: Deployment 4 at SS-C (July 2003 – April 2004)

## MOORING # 1491 SITE "C" JOHN LODER SCOTIAN SLOPE JULY 2003

